

Table of Contents

Experimental part	2
1) General informations	2
2) Synthetic methods.....	3
3) X-ray diffraction crystallography	15
4) EPR spectroscopy.....	31
5) UV-visible spectra	35
6) Cyclic voltammetry	42
7) Reactivity test of catalytic oxidation cleavage of PNPG.....	47
8) Computational Studies.....	52
9) NMR spectra.....	62
10) References	71

Experimental part

1) General information

All commercial reagents and solvents were used as purchased without further purification unless otherwise stated.

Dry solvents were obtained by standard procedures according to D. D. Perrin and D. R. Perrin, Purification of Laboratory Chemicals. Tetrahydrofuran and diethylether were purified by distillation from benzophenone ketyl radical. Dichloromethane, toluene, trimethylamine and trimethylsilyl chloride were purified by distillation from calcium hydride. Technical grade ethyl acetate and petroleum ether (40 to 65 °C fraction) were evaporated under reduced pressure.

Analytical thin layer chromatography (TLC) was carried out on Merck Millipore F254 silica gel 60 plates (210-270 µm thickness, aluminium supported). The plates were visualized using ultra-violet light (254 nm).

Flash column chromatography was carried out on ROCC silica gel 60Å (230-400 Mesh).

Proton nuclear magnetic resonance (^1H NMR) spectra were recorded using Bruker Avance II-300 (300 MHz) spectrometers. Carbon nuclear magnetic resonance (^{13}C NMR) spectra were recorded using Bruker Avance II-300 (75 MHz) spectrometers. Chemical shifts (δ) are reported in parts per million (ppm) relative to residual solvent peaks: ^1H (CDCl_3 $\delta_{\text{ppm}} = 7.26$, $d_6\text{-DMSO}$ $\delta_{\text{ppm}} = 2.50$, D_2O $\delta_{\text{ppm}} = 4.79$, ^{13}C ($d_6\text{-DMSO}$ $\delta_{\text{ppm}} = 39.5$). Coupling constants are reported in Hertz (Hz). Splitting patterns are designed as: s (singlet), d (doublet), t (triplet), q (quartet), and m (multiplet).

Mass spectra were recorded by the Mass Spectrometry Service of the “asm” platform from the Institute of Condensed Matter and Nanosciences (IMCN) at UCLouvain, using Q-ToF Waters Synapt XS spectrometers with a Thermo Orbitrap Exactive device. The values are given in Dalton..

All diffraction data were recorded on a MAR345 image plate using Mo-K α radiation generated by an Incoatec I μ S microfocus source (Montel Mirrors). All crystals were stable and measured at ambient conditions. Data integration and reduction was carried out using the CrysAlis^{PRO} software package, and the implemented absorption correction was applied. The structures were solved by dual space direct methods (SHELXT) and refined against F^2 by SHELXL-2018/3 or 2019/3. All non-hydrogen bonds were refined anisotropically, hydrogen atoms were added in

calculated positions and refined in riding mode, with temperature factors 1.2 times higher than their parent atoms (1.5 for methyl hydrogens).

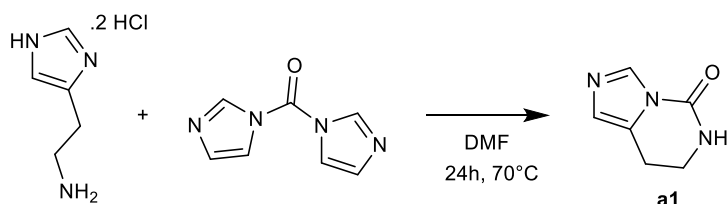
UV/Visible experiments were performed on a VWR UV-1600PC Scanning Spectrophotometer equipped with Deuterium/Tungsten Halogen Lamp.

CW-EPR spectra were recorded at 100 K (frozen solutions), on a Bruker Magnetech ESR5000 EPR spectrometer operating at ~9.5 GHz (X-band). Unless otherwise stated, 10–3 M solutions of copper complexes were prepared in methanol. Samples were contained in 3 mm OD quartz tubes closed with PE caps. The EPR spectra were obtained with the following spectrometer settings: microwave power: 20 mW; modulation amplitude: 0.7 mT and modulation frequency: 100 kHz. The number of scans was 4. Data handling was performed on the Bruker ESR Studio version 1.90.0 software. All spectra are shown after baseline correction. The Spin Count software module (Bruker) was used for quantitative measurements. Results of the quantification were confirmed using a copper disodium ethylenediaminetetraacetate solution (Cu(II)EDTA(Na)2) and acquisition of a spectrum in the same conditions before and after the spectra of the samples. The simulations of CW EPR spectra were run with Easyspin 6.0.61 using the ‘pepper’ function with one electron spin $S=1/2$ (Cu unpaired electron). All parameters were optimized using ‘esfit’ function.

Elemental Analysis (CHNS) was done with ThermoTM FlashSmartTM Elemental Analyzer.

Only crystalline material of the copper cocomplexes was used for all the analysis and reactivity studies.

2) Synthetic methods

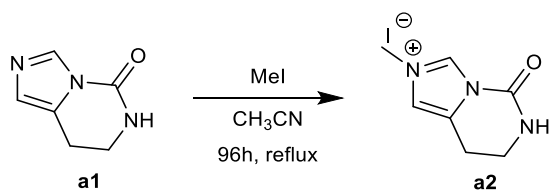


Scheme S1: Synthesis of **a1**. Adapted from²

A solution of histamine dihydrochloride (3.002 g, 16.3 mmol, 1 eq.) and carbonyldiimidazole (2.683 g, 16.5 mmol, 1 eq.) in DMF (15 ml) was stirred at 70°C for 24h. The solvent was then removed under vacuum. The oily product was redissolved in a saturated solution of NaHSO₄

(50 mL) and, the solution was extracted with DCM (10 x 60 mL). The organic layers were combined, dried over Na_2SO_4 and evaporated under vacuum. The crude was resuspended in acetonitrile (4 mL), filtered and dried to afford the product **a1** as a white powder (1.162 g, **50%**).

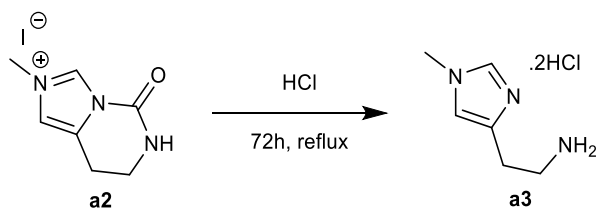
¹H NMR (300 MHz, *d*₆-DMSO) δ (ppm): 8.20 (s, 1H), 8.05 (d, *J* = 0.9 Hz, 1H), 6.80 (m, 1H), 3.40 – 3.33 (m, 2H), 2.88 (td, *J* = 6.5, 1.2 Hz, 2H).



Scheme S2: Synthesis of **a2**. Adapted from³

Iodomethane (7 mL, 112.4 mmol, 3 eq.) was added to a suspension of **a1** (5 g, 36.9 mmol, 1 eq.) in acetonitrile (200 mL) and the reaction mixture was refluxed for 4 days covered from light. The solvent was then removed under vacuum and the orange powder was suspended in acetone, filtered and dried under vacuum to afford the product **a2** as a beige shiny powder (9.979 g, 97%).

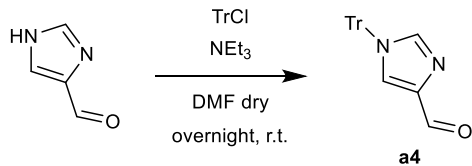
¹H NMR (300 MHz, *d*₆-DMSO) δ (ppm): 9.67 (dd, *J* = 1.4, 0.8 Hz, 1H), 9.01 (s, 1H), 7.61 (d, *J* = 1.3 Hz, 1H), 3.90 (s, 3H), 3.47 (td, *J* = 6.5, 2.8 Hz, 2H), 3.03 (dd, *J* = 9.5, 3.6 Hz, 2H).



Scheme S3: Synthesis of **a3**. Adapted from³

A suspension of **a2** (2,008 g, 7.17 mmol, 1 eq.) in HCl 6 M (30 mL) was refluxed for 3 days covered from light. The solvent was then removed under vacuum, and residual iodine impurities were removed by azeotroping with toluene several times. The crude was stirred overnight in acetonitrile then filtered to afford the methylated histamine **a3** as a white powder (1.235 g, 87%).

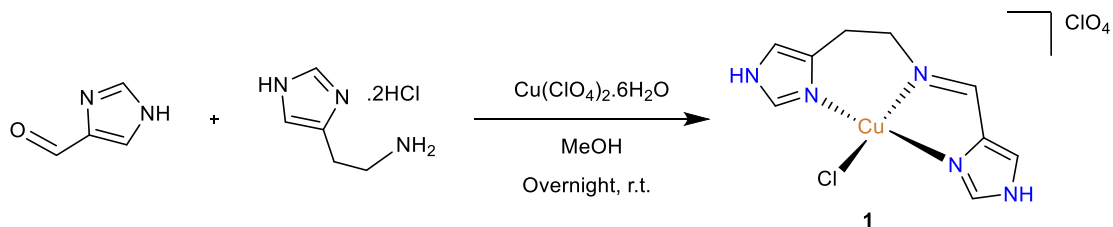
¹H NMR (300 MHz, *d*₆-DMSO) δ (ppm): 9.08 (d, *J* = 0.8 Hz, 1H), 8.41 (s, 3H), 7.56 (d, *J* = 0.9 Hz, 1H), 3.81 (s, 3H), 3.20 – 3.07 (m, 2H), 3.03 (t, *J* = 6.6 Hz, 2H).



Scheme S4: Synthesis of **a4**. Adapted from⁴

To a solution of 1*H*-imidazole-4-carbaldehyde (5 g, 52.07 mmol, 1 eq.) and dry triethylamine (10.5 g, 14.5 mL, 104.13 mmol, 2 eq.) in dry DMF (60 mL) under argon was added drop by drop a 80 mL solution of trityl chloride (14.5 g, 52.07 mmol, 1 eq.) in dry DMF. The resulting solution was stirred at room temperature overnight. Water (250 mL) was then added, the resulting precipitate was filtered washed with water and ether and dried under vacuum to afford the product **a4** as a fluffy pale pink powder (15.6 g, **89%**).

¹H NMR (300 MHz, DMSO) δ 9.72 (s, 1H), 7.80 (d, *J* = 1.3 Hz, 1H), 7.67 (d, *J* = 1.0 Hz, 1H), 7.51 – 7.37 (m, 9H), 7.16 – 7.05 (m, 6H).

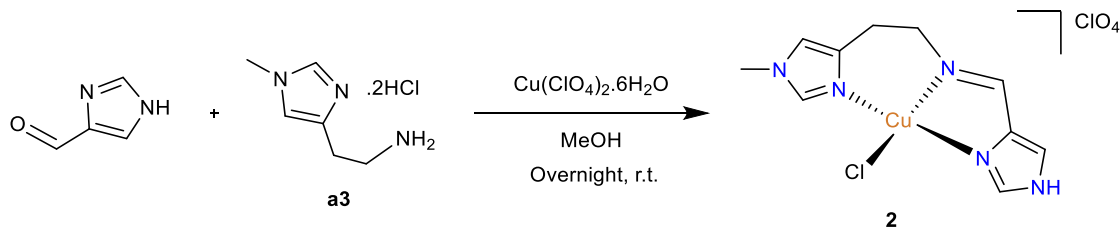


Scheme S5: Synthesis of **1**. Adapted from⁵

1*H*-imidazole-4-carbaldehyde (0.097 g, 1.1 mmol, 1 eq.), histamine dihydrochloride (0.186 g, 1.1 mmol, 1 eq.) and copper perchlorate hexahydrate (0.374 g, 1.1 mmol, 1 eq.) were dissolved in MeOH (6 mL). The mixture was stirred at room temperature overnight. The resulting suspension was cooled down to 0°C and filtered. The solid was collected, triturated in diethyl ether, filtered and dried under vacuum. Slow diffusion of ether in a methanol solution of the complex yielded the pure compound **1** as deep blue crystals (0.141 g, **33%**).

HRMS (ESI) m/z calculated for C₉H₁₁ClCuN₅ [M + Cl]⁺ 286.99990, found 286.99924

Elemental analysis: Calculated for $C_9H_{11}N_5Cl_2CuO_4$, C, 27.88; H, 2.86; N, 18.07. Found C, 27.96; H, 2.84; N, 18.02

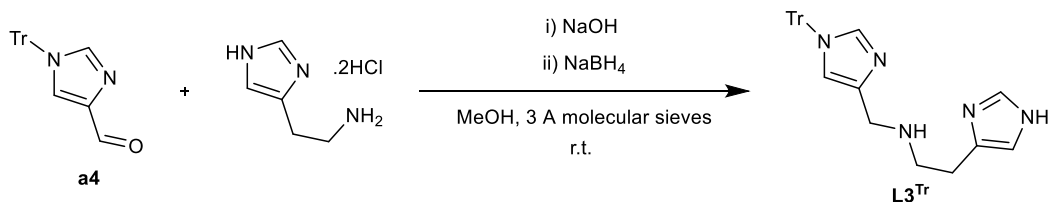


Scheme S6: Synthesis of **2**. Adapted from⁵

1H-imidazole-4-carbaldehyde (0.097 g, 1.1 mmol, 1 eq.), **a3** (0.2 g, 1.1 mmol, 1 eq.) and copper perchlorate hexahydrate (0.374 g, 1.1 mmol, 1 eq.) were dissolved in MeOH (6 mL). The mixture was stirred at room temperature overnight. The resulting suspension was cooled down to 0°C and filtered. The solid was collected, triturated in diethyl ether, filtered and dried under vacuum. Slow diffusion of ether in a methanol solution of the complex yielded the pure compound **1** as deep blue crystals (0.159 g, **36%**).

HRMS (ESI) m/z calculated for $C_{10}H_{13}ClCuN_5$ [M+Cl]⁺ 301.01555, found 301.01495, m/z calculated for $C_{11}H_{14}CuN_5O_2$ [M+Formiate]⁺ 311.04435, found 311.04378

Elemental analysis: Calculated for $C_{10}H_{13}N_5Cl_2CuO_4$, C, 29.9; H, 3.26; N, 17.44. Found C, 29.9; H, 3.25; N, 17.17



Scheme S7: Synthesis of **L3^{Tr}**. Adapted from⁶

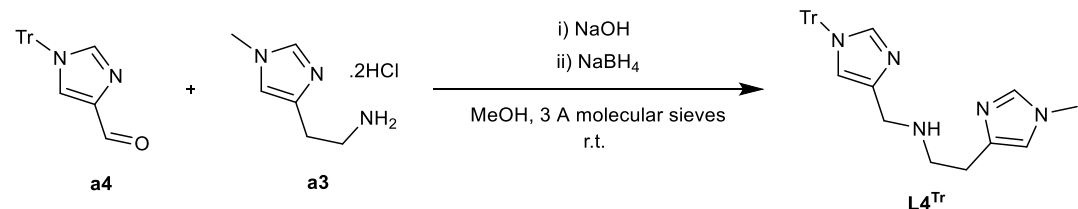
To a solution of **a4** (2.5 g, 7.39 mmol, 1 eq.) and histamine dihydrochloride (1.36 g, 7.39 mmol, 1 eq.) in dry methanol (75 mL, dried on 3 Å molecular sieves) under argon were added 3 Å activated molecular sieves and sodium hydroxide (0.56 g, 14.04 mmol, 1.9 eq.). The solution was stirred 3h at room temperature and NaBH₄ (0.56 g, 14.78 mmol, 2 eq.) was added. After 1h at room temperature the mixture was filtered and evaporated under vacuum. The resulting

solid was extracted with water (100 mL) and dichloromethane (3 x 75 mL), the organic phases were gathered dried on Na₂SO₄ and evaporated under vacuum to afford the product **L3^{Tr}** as an off-white solid (2.448 g, **76%**).

¹H NMR (300 MHz, *d*₆-DMSO) δ (ppm): 7.53 – 7.23 (m, 11H), 7.15 – 6.97 (m, 6H), 6.70 (d, *J* = 6.9 Hz, 2H), 3.56 (s, 2H), 2.78 – 2.65 (m, 2H), 2.59 (t, *J* = 6.7 Hz, 2H).

¹³C NMR (75 MHz, *d*₆-DMSO) δ (ppm): 142.80, 140.92, 138.09, 134.82, 129.65, 128.63, 128.40, 118.61, 74.85, 49.34, 49.05, 47.25.

HRMS (ESI) : m/z calculated for C₁₁H₁₇N₅ [M+H]⁺ 434.23392, found 434.23404



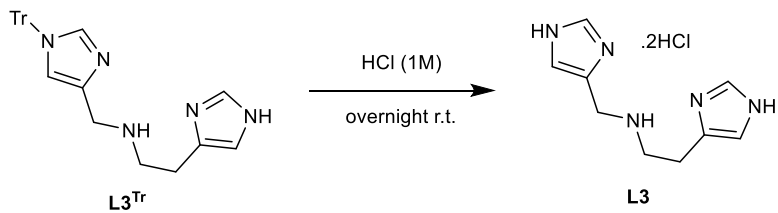
Scheme S8: Synthesis of **L4^{Tr}**. Adapted from⁶

To a solution of **a4** (1.53 g, 4.54 mmol, 1 eq.) and **a3** (0.9 g, 4.54 mmol, 1 eq.) in dry methanol (75 mL, dried on 3 Å molecular sieves) under argon were added 3 Å activated molecular sieves and sodium hydroxide (0.364 g, 8.63 mmol, 1.9 eq.). The solution was stirred 3h at room temperature and NaBH₄ (0.364 g, 9.09 mmol, 2 eq.) was added. After 1h at room temperature the mixture was filtered and evaporated under vacuum. The resulting solid was extracted with water (100 mL) and dichloromethane (3 x 75 mL), the organic phases were gathered dried on Na₂SO₄ and evaporated under vacuum to afford the product **L4^{Tr}** as an off-white solid (1.448 g, **65%**).

¹H NMR (300 MHz, *d*₆-DMSO) δ (ppm): 7.46 – 7.27 (m, 12H), 7.09 (dd, *J* = 7.8, 1.9 Hz, 5H), 6.78 (s, 1H), 6.73 (s, 1H), 3.58 (s, 2H), 3.55 (s, *J* = 3.5 Hz, 3H), 2.72 (t, *J* = 7.0 Hz, 2H), 2.58 – 2.53 (m, 2H).

¹³C NMR (75 MHz, *d*₆-DMSO) δ (ppm): 142.80, 140.80, 138.08, 137.48, 129.65, 128.64, 128.41, 118.63, 117.07, 74.87, 49.42, 47.28, 33.11, 31.14, 28.80.

HRMS (ESI) : m/z calculated for C₉H₁₄N₅ [M+H]⁺ 192.12437, found 192.12410

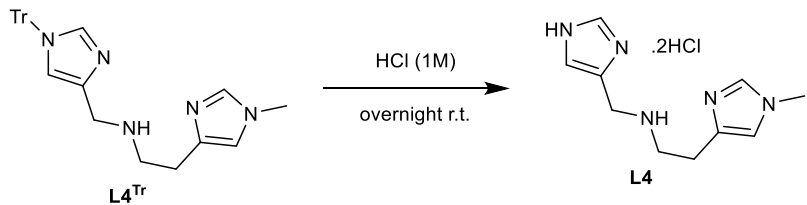


Scheme S9: Synthesis of L3

The suspension of **L3^{Tr}** (1 g, 2.31 mmol, 1 eq.) in aqueous HCl (40 mL, 1M) was stirred at room temperature overnight. The resulting suspension was filtered and the filtrate was evaporated under vacuum to afford **L3** the product as a white powder (0.566 g, 93%).

¹H NMR (300 MHz, *d*₆-DMSO) δ (ppm): 9.16 (d, *J* = 1.2 Hz, 1H), 9.07 (d, *J* = 1.3 Hz, 1H), 7.88 (s, 1H), 7.58 (s, 1H), 4.34 (s, 2H), 3.35 – 3.28 (m, 2H), 3.22 – 3.14 (m, 3H).

^{13}C NMR (75 MHz, d_6 -DMSO) δ (ppm): 134.90, 134.41, 128.99, 124.54, 121.01, 117.39, 44.72, 21.36.

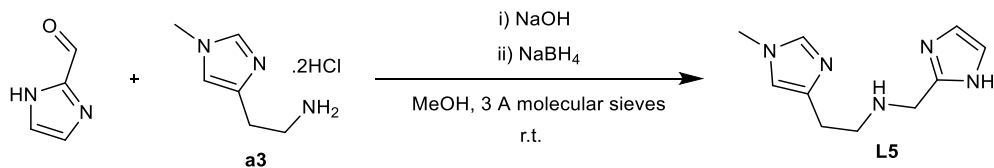


Scheme S10: Synthesis of L4

The suspension of **L4^{Tr}** (0.75 g, 1.67 mmol, 1 eq.) in aqueous HCl (40 mL, 1M) was stirred at room temperature overnight. The resulting suspension was filtered and the filtrate was evaporated under vacuum to afford the product as a white powder (0.401 g, **86%**).

^1H NMR (300 MHz, d_6 -DMSO) δ (ppm): 9.14 (d, J = 1.2 Hz, 1H), 9.05 (d, J = 0.7 Hz, 1H), 7.88 (d, J = 1.0 Hz, 1H), 7.60 (d, J = 1.0 Hz, 1H), 4.33 (s, 2H), 3.82 (s, 3H), 3.29 (t, J = 7.3 Hz, 2H), 3.20 – 3.14 (t, J = 7.3 Hz, 2H).

^{13}C NMR (75 MHz, d_6 -DMSO) δ (ppm): 136.00, 134.95, 129.34, 124.53, 121.51, 121.06, 44.80, 35.96, 21.39.



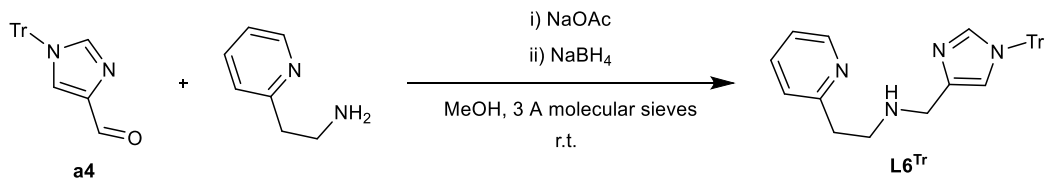
Scheme S11: Synthesis of **L5**. Adapted from⁶

To a solution of 1H-imidazole-2-carbaldehyde (1 g, 10.19 mmol, 1 eq.) and **a3** (2.02 g, 10.19 mmol, 1 eq.) in dry methanol (50 mL, dried on 3 Å molecular sieves) under argon were added 3 Å activated molecular sieves and sodium hydroxide (0.774 g, 19.36 mmol, 1.9 eq.). The solution was stirred 2h at room temperature and NaBH4 (0.771 g, 20.39 mmol, 2 eq.) was added. After 3h at room temperature the mixture was filtered and evaporated under vacuum. The resulting solid was suspended in water (100 mL) and extracted with dichloromethane (3 x 75 mL) and followed with a solution of isopropanol (25%) in chloroform (3 x 100 mL). The isopropanol phases were gathered, dried on Na2SO4 and evaporated under vacuum to afford the product **L5** as a white solid (1.129 g, **55%**).

1H NMR (300 MHz, d₆-DMSO) δ (ppm): 7.42 (d, J = 0.7 Hz, 1H), 6.87 (s, 1H), 6.80 (s, 1H), 3.69 (s, 2H), 3.57 (s, 3H), 2.70 (t, J = 6.9 Hz, 2H), 2.55 (t, J = 7.1 Hz, 2H).

13C NMR (75 MHz, d₆-DMSO) δ (ppm): 147.59, 140.47, 137.54, 117.19, 49.48, 46.95, 33.12, 28.81.

HRMS (ESI) : m/z calculated for C₁₀H₁₆N₅ [M+H]⁺ 206.14002, found 206.13987



Scheme S12: Synthesis of **L6^{Tr}**. Adapted from⁶

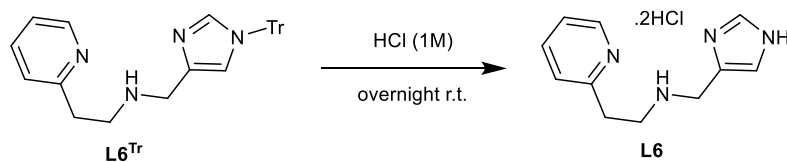
To a solution of **a4** (0.554 g, 1.637 mmol, 1 eq.) and 2-Pyridylethylamine (0.2 g, 1.637 mmol, 1 eq.) in dry methanol (25 mL, dried on 3 Å molecular sieves) under argon were added 3 Å activated molecular sieves and sodium acetate (0.134 g, 1.637 mmol, 1 eq.). The solution was stirred 4h at room temperature and NaBH4 (0.124 g, 3.274 mmol, 2 eq.) was added. After 2h at room temperature the mixture was filtered and evaporated under vacuum. The resulting solid was suspended in water (75 mL) and extracted with dichloromethane (3 x 75 mL), the organic

phases were gathered, dried on Na_2SO_4 and evaporated under vacuum. The crude product was purified over flash silica gel chromatography (Methanol- NH_3 (7N)/DCM, 3:97) to afford the product **L6^{Tr}** as a white solid (0.314 g, **43%**).

$^1\text{H NMR}$ (300 MHz, d_6 -DMSO) δ (ppm): 8.42 (ddd, J = 4.9, 1.8, 0.9 Hz, 1H), 7.64 (td, J = 7.6, 1.9 Hz, 1H), 7.45 – 7.35 (m, 9H), 7.27 (d, J = 1.4 Hz, 1H), 7.17 (ddd, J = 8.4, 6.0, 4.5 Hz, 2H), 7.12 – 7.04 (m, 6H), 6.69 (d, J = 1.1 Hz, 1H), 3.56 (s, 2H), 2.82 (s, 4H).

$^{13}\text{C NMR}$ (75 MHz, d_6 -DMSO) δ (ppm): 160.78, 149.39, 142.86, 140.65, 138.19, 136.80, 129.72, 128.72, 128.49, 123.55, 121.73, 118.85, 74.92, 49.06, 47.18, 38.28.

HRMS (ESI) : m/z calculated for $\text{C}_{30}\text{H}_{29}\text{N}_4$ [$\text{M}+\text{H}$]⁺ 445.2392, found 445.2394



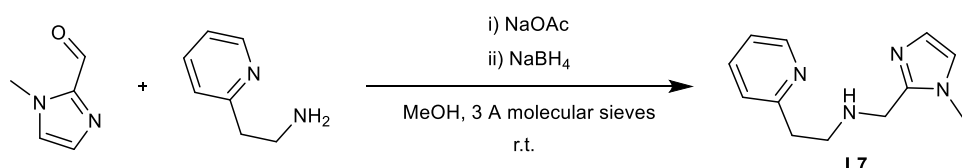
Scheme S13: Synthesis of **L6**

The suspension of **L6^{Tr}** (0.314 g, 0.706 mmol, 1 eq.) in aqueous HCl (15 mL, 1M) was stirred at room temperature overnight. The resulting suspension was filtered and the filtrate was evaporated under vacuum to afford the product **L6** as a white powder (0.194 g, **quantitative**).

$^1\text{H NMR}$ (300 MHz, d_6 -DMSO) δ (ppm): 10.27 (s, 2H), 9.16 (d, J = 1.3 Hz, 1H), 8.76 (dd, J = 5.5, 0.9 Hz, 1H), 8.35 (td, J = 7.8, 1.3 Hz, 1H), 7.95 – 7.84 (m, 2H), 7.79 (d, J = 6.5 Hz, 1H), 4.36 (s, 2H), 3.53 – 3.41 (m, 4H).

$^{13}\text{C NMR}$ (75 MHz, d_6 -DMSO) δ (ppm): 152.92, 145.64, 143.12, 134.98, 127.79, 125.74, 124.54, 121.05, 44.91, 39.57, 31.24.

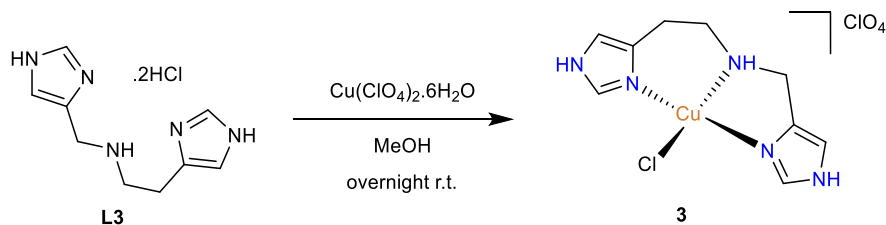
HRMS (ESI) : m/z calculated for $\text{C}_{11}\text{H}_{15}\text{N}_4$ [$\text{M}+\text{H}$]⁺ 203.1297, found 203.1296



Scheme S14: Synthesis of **L7**. Adapted from⁶

To a solution of 1-methyl-2-imidazolecarboxaldehyde (0.1 g, 0.908 mmol, 1 eq.) and 2-pyridylethylamine (0.111 g, 0.108 mL, 0.908 mmol, 1 eq.) in dry methanol (10 mL, dried on 3 Å molecular sieves) under argon were added 3 Å activated molecular sieves and sodium acetate (0.075 g, 0.908 mmol, 1 eq.). The solution was stirred 3h at room temperature and NaBH₄ (0.069 g, 1.816 mmol, 2 eq.) was added. After 2h at room temperature the mixture was filtered and evaporated under vacuum. The resulting solid was suspended in a saturated bicarbonate aqueous solution (50 mL) and extracted with dichloromethane (3 x 50 mL). The organic phases were gathered, dried on Na₂SO₄ and evaporated under vacuum. The crude was purified over flash silica gel chromatography (Methanol/Net₃/DCM, 5:1:94) to afford the product **L7** as a white solid (0.097 g, **50%**).

¹H NMR (300 MHz, CDCl₃) δ (ppm): 8.55 – 8.48 (m, 1H), 7.58 (td, *J* = 7.7, 1.8 Hz, 1H), 7.19 – 7.06 (m, 2H), 6.90 (d, *J* = 1.1 Hz, 1H), 6.79 (d, *J* = 1.0 Hz, 1H), 3.87 (s, 2H), 3.61 (s, 3H), 3.10 – 3.01 (m, 2H), 3.02 – 2.92 (m, 2H).

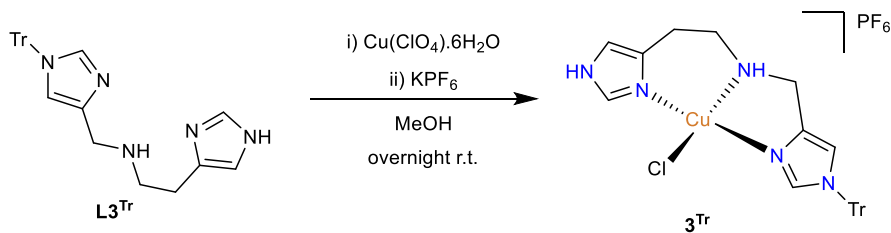


Scheme S15: Synthesis of **3**

L1 (0.136 g, 0.711 mmol, 1 eq.) and copper perchlorate hexahydrate (0.263 g, 0.711 mmol, 1 eq) were dissolved in MeOH (4 mL). The mixture was stirred overnight at room temperature, diethylether was then added to the crude and a blue powder was filtered. Slow evaporation of a methanol solution of the complex yielded the pure compound **3** as deep blue crystals (0.55 g, **20%**)

HRMS (ESI): m/z calculated for C₉H₁₃N₅ClCu[M+Cl]⁺ 289.01555, found 289.01485

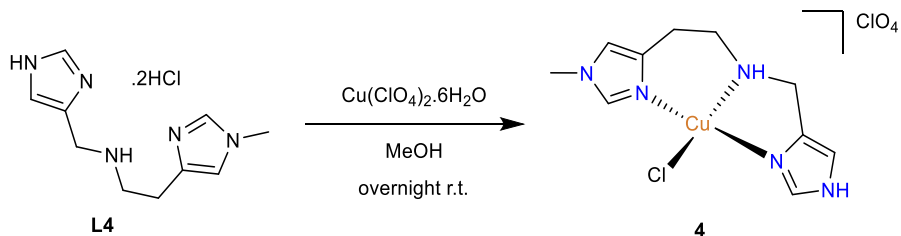
Elemental analysis: Calculated for C₉H₁₃N₅Cl₂CuO₄·H₂O, C, 26.51; H, 3.71; N, 17.18. Found C, 26.33; H, 3.36; N, 16.38



Scheme S16: Synthesis of 3^{Tr}

L3^{Tr} (0.1 g, 0.231 mmol, 1 eq.) and copper chloride anhydrous (0.031 g, 0.231 mmol, 1 eq) were dissolved in 3 mL of a acetonitrile/MeOH mixture (5:1 v/v). The mixture was stirred at room temperature, after 5 minutes KPF_6 (0.085 g, 0.462 mmol, 2 eq.) was added and the resulting suspension was stirred at room temperature for 5 minutes. The precipitate was filtered and ether (100 mL) was added to the filtrate. The resulting suspension was filtered and washed with ether to yield the complex 3^{Tr} as a blue powder (0.154 g, **98%**).

HRMS (ESI): m/z calculated for $\text{C}_{28}\text{H}_{27}\text{N}_5\text{CuCl} [\text{M}+\text{Cl}]^+$ 531.12455, found 531.12472

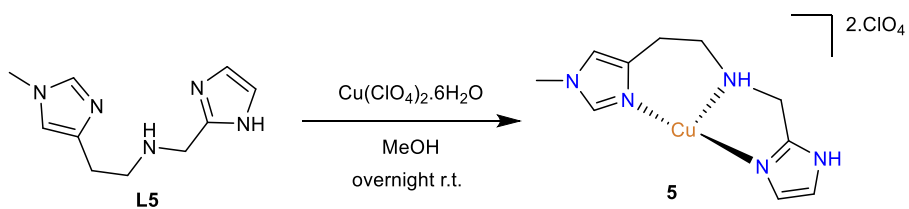


Scheme S17: Synthesis of **4**

L4 (0.2 g, 0.447 mmol, 1 eq.) and copper perchlorate hexahydrate (0.16 g, 0.447 mmol, 1 eq.) were dissolved in MeOH (2 mL). The mixture was stirred at room temperature, after 2h triethylamine (0.09 g, 0.894 mmol, 2 eq.) was added and the suspension filtered. The solid was resuspended in methanol and trifluoracetic acid was added (0.102 g, 0.894 mmol, 2 eq.), the resulting solution was stirred 2h at room temperature then evaporated under vacuum. Slow diffusion of ether in a methanol solution of the complex yielded the pure compound **4** as deep blue crystals (0.255 g, **37%**).

HRMS (ESI): m/z calculated for $\text{C}_{10}\text{H}_{15}\text{N}_5\text{CuCl} [\text{M}+\text{Cl}]^+$ 303.03120, found 303.03073

Elemental analysis: Calculated for $\text{C}_{10}\text{H}_{15}\text{N}_5\text{Cl}_2\text{CuO}_4$, C, 29.75; H, 3.75; N, 17.35. Found C, 29.86; H, 3.72; N, 17.05

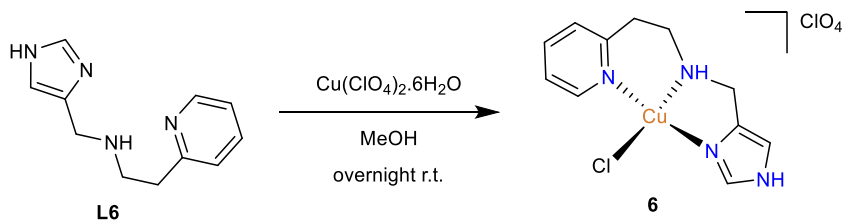


Scheme S18: Synthesis of **5**

L5 (0.1 g, 0.487 mmol, 1 eq.) and copper perchlorate hexahydrate (0.181 g, 0.487 mmol, 1 eq.) were dissolved in MeOH (2 mL). The mixture was stirred 4h at 60°C then room temperature overnight. Diethylether was then added to the crude and the solution was filtered to afford the complex **5** as deep blue crystals (0.120 g, **48%**).

HRMS (ESI): m/z calculated for $C_{10}H_{15}N_5Cu$ $[M-H]^{+}$ 267.05397, found 267.05389

Elemental analysis: Calculated for $C_{10}H_{15}N_5Cl_2CuO_8.2H_2O$, C, 23.83; H, 3.80; N, 13.90. Found C, 23.43; H, 3.84; N, 13.34

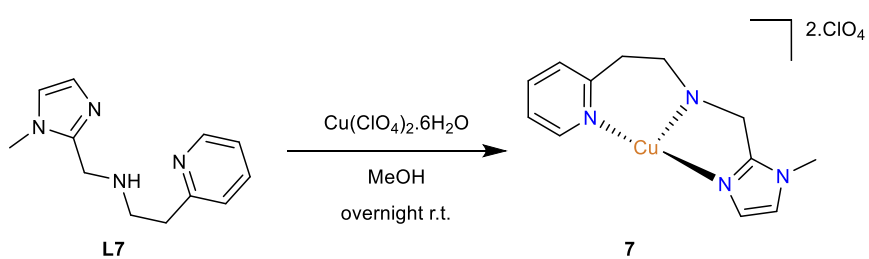


Scheme S19: Synthesis of **6**

L6 (0.2 g, 0.727 mmol, 1 eq.) and copper perchlorate hexahydrate (0.269 g, 0.727 mmol, 1 eq.) were dissolved in MeOH (10 mL). The mixture was stirred overnight at room temperature, diethylether was then added to the crude and a blue powder was filtered. Slow diffusion of ether in a methanol solution of the complex yielded the pure compound **6** as deep blue crystals (0.0845 g, **28%**).

HRMS (ESI): m/z calculated for $C_{11}H_{14}N_4Cu$ $[M-H]^{+}$ 300.02030, found 300.01959

Elemental analysis: Calculated for $C_{11}H_{14}N_4Cl_2CuO_4$, C, 32.97; H, 3.52; N, 13.98. Found C 32.34; H 3.33; N, 13.81



Scheme S20: Synthesis of 7

L7 (0.0972 g, 0.449 mmol, 1 eq.) and copper perchlorate hexahydrate (0.166 g, 0.449 mmol, 1 eq.) were dissolved in MeOH (3 mL). The mixture was stirred overnight at room temperature, diethylether was then added to the crude and a blue powder was filtered. Slow diffusion of ether in a methanol solution of the complex yielded the pure compound **7** as deep blue crystals (0.162 g, **71%**).

Elemental analysis: Calculated for $\text{C}_{13}\text{H}_{20}\text{N}_4\text{Cl}_2\text{CuO}_9$, C, 30.57; H, 3.95; N, 10.97. Found C, 30.31; H, 3.87; N, 10.75

3) X-ray diffraction crystallography

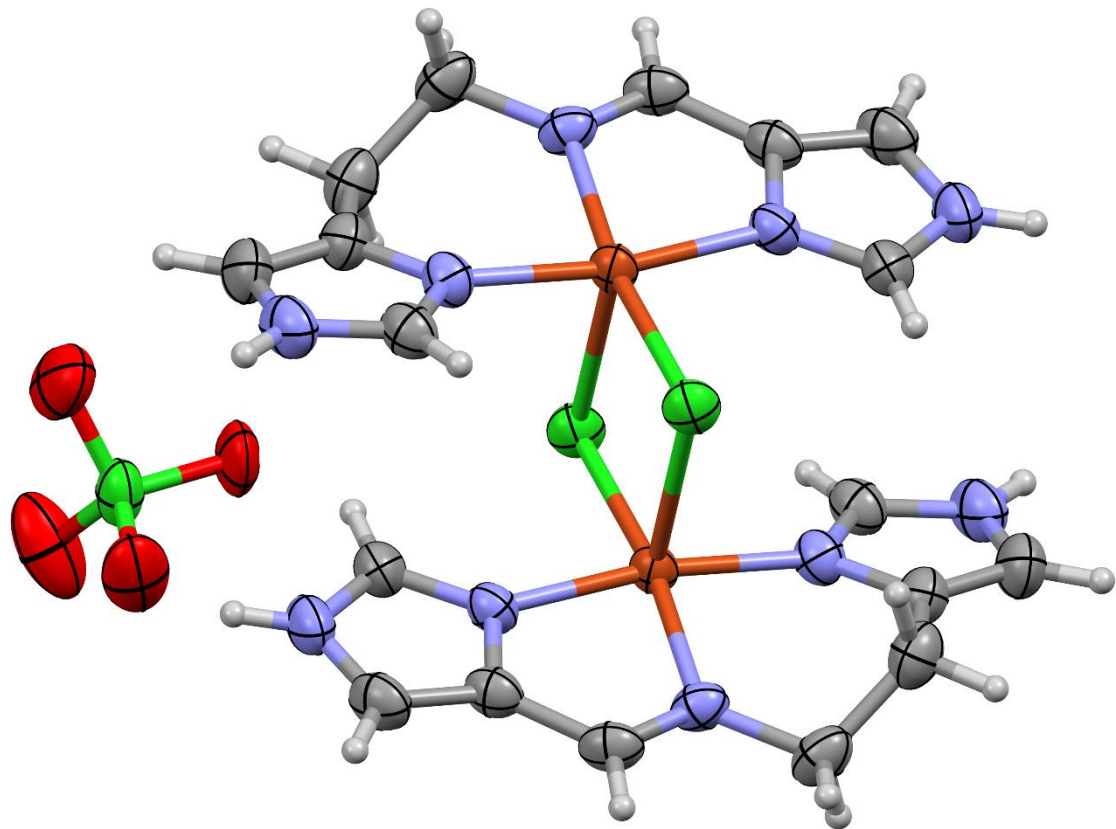


Figure S1: Ortep representation of **1** with displacement ellipsoids drawn at the 50% probability level. The minor part of the disordered perchlorate anion was omitted for clarity.

Table S1: Crystal data and structure refinement for **1**

Identification code	Complex 1
CCDC Deposition Number	2369751
Empirical formula	C18 H22 Cl4 Cu2 N10 O8
Formula weight	775.33
Temperature	293(2) K
Wavelength	0.71073 Å
Crystal system	Triclinic
Space group	P-1
Unit cell dimensions	$a = 7.2149(9)$ Å $b = 8.6311(15)$ Å $c = 12.702(2)$ Å $\alpha = 98.960(15)^\circ$ $\beta = 101.239(14)^\circ$ $\gamma = 112.587(15)^\circ$
Volume	692.7(2) Å ³
Z	1
Density (calculated)	1.859 Mg/m ³
Absorption coefficient	1.985 mm ⁻¹
F(000)	390
Crystal size	0.40 x 0.20 x 0.03 mm ³
Theta range for data collection	3.151 to 26.145°
Reflections collected	9837
Independent reflections	2735 [$R_{(int)} = 0.0301$]
Completeness to theta = 25.242°	99.7 %
Absorption correction	Semi-empirical from equivalents
Max. and min. transmission	1.00000 and 0.70219
Refinement method	Full-matrix least-squares on F ²
Data / restraints / parameters	2735 / 30 / 227
Goodness-of-fit on F ²	1.050
Final R indices [I>2sigma(I)]	$R_1 = 0.0273$, $wR_2 = 0.0736$
R indices (all data)	$R_1 = 0.0295$, $wR_2 = 0.0747$
Largest diff. peak and hole	0.303 and -0.332 e.Å ⁻³

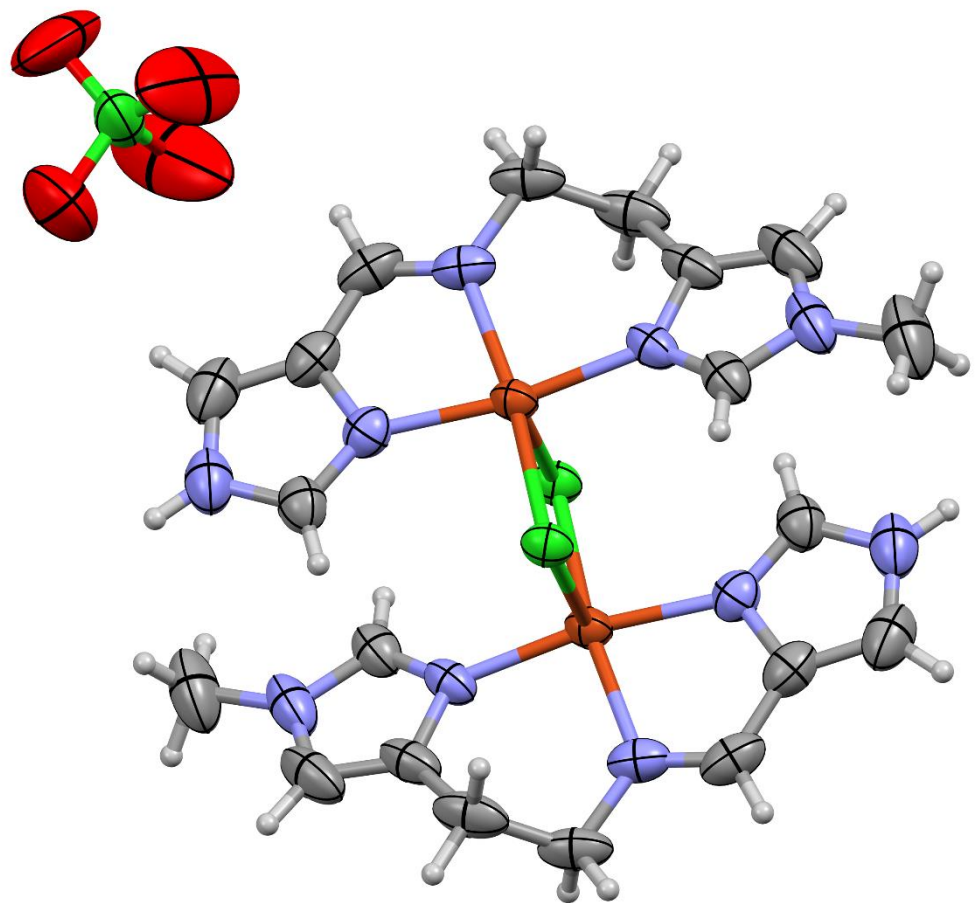


Figure S2: Ortep representation of **2** with displacement ellipsoids drawn at the 50% probability level. The minor part of the disordered perchlorate anion was omitted for clarity.

Table S2 : Crystal data and structure refinement for **2**

Identification code	Complex 2
CCDC Deposition Number	2369752
Empirical formula	C ₂₀ H ₂₆ Cl ₄ Cu ₂ N ₁₀ O ₈
Formula weight	803.39
Temperature	293(2) K
Wavelength	0.71073 Å
Crystal system	Triclinic
Space group	P-1
Unit cell dimensions	$a = 7.3349(9)$ Å $b = 8.8634(12)$ Å $c = 12.9399(12)$ Å $\alpha = 106.261(10)^\circ$. $\beta = 90.179(8)^\circ$. $\gamma = 109.045(12)^\circ$.
Volume	759.25(16) Å ³
Z	1
Density (calculated)	1.757 Mg/m ³
Absorption coefficient	1.814 mm ⁻¹
F(000)	406
Crystal size	0.22 x 0.07 x 0.03 mm ³
Theta range for data collection	2.954 to 26.117°.
Reflections collected	9645
Independent reflections	2986 [$R_{(int)} = 0.0476$]
Completeness to theta = 25.242°	99.7 %
Absorption correction	Semi-empirical from equivalents
Max. and min. transmission	1.00000 and 0.62792
Refinement method	Full-matrix least-squares on F ²
Data / restraints / parameters	2986 / 6 / 237
Goodness-of-fit on F ²	1.089
Final R indices [I>2sigma(I)]	$R_1 = 0.0371$, $wR_2 = 0.0951$
R indices (all data)	$R_1 = 0.0418$, $wR_2 = 0.0979$
Largest diff. peak and hole	0.434 and -0.426 e.Å ⁻³

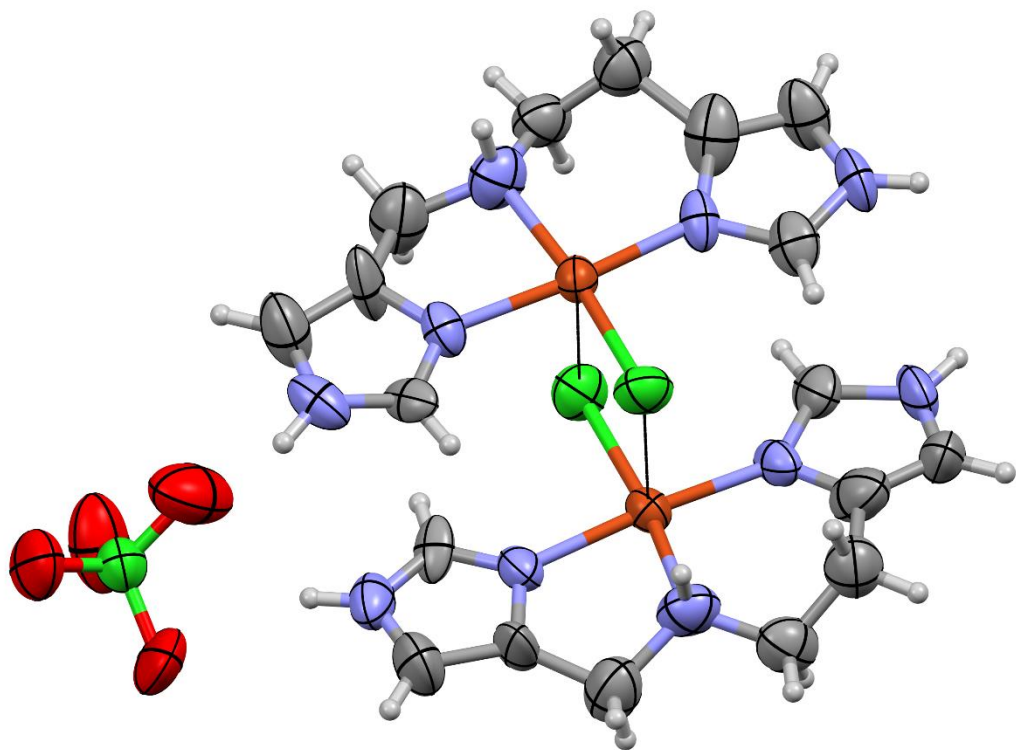


Figure S3: Ortep representation of **3** with displacement ellipsoids drawn at the 50% probability level. The dashed lines between the Cu and Cl atoms are added to show the proximity of both complexes, such that both shown complexes could be considered a dimer.

Table S3: Crystal data and structure refinement for **3**

Identification code	Complex 3
CCDC Deposition Number	2369753
Empirical formula	C9 H12 Cl2 Cu N5 O4
Formula weight	388.68
Temperature	297(2) K
Wavelength	0.71073 Å
Crystal system	Orthorhombic
Space group	Pna2 ₁
Unit cell dimensions	$a = 6.3467(8)$ Å $b = 17.642(2)$ Å $c = 13.4662(12)$ Å $\alpha = 90^\circ$. $\beta = 90^\circ$. $\gamma = 90^\circ$.
Volume	1507.8(3) Å ³
Z	4
Density (calculated)	1.717 Mg/m ³
Absorption coefficient	1.824 mm ⁻¹
F(000)	788
Crystal size	0.24 x 0.12 x 0.07 mm ³
Theta range for data collection	3.411 to 26.391°.
Reflections collected	7905
Independent reflections	2959 [$R_{(int)} = 0.0616$]
Completeness to theta = 25.242°	99.6 %
Absorption correction	Semi-empirical from equivalents
Max. and min. transmission	1.00000 and 0.85609
Refinement method	Full-matrix least-squares on F ²
Data / restraints / parameters	2959 / 118 / 191
Goodness-of-fit on F ²	1.057
Final R indices [I>2sigma(I)]	$R_1 = 0.0595$, $wR_2 = 0.1541$
R indices (all data)	$R_1 = 0.0769$, $wR_2 = 0.1660$
Largest diff. peak and hole	0.559 and -0.382 e.Å ⁻³

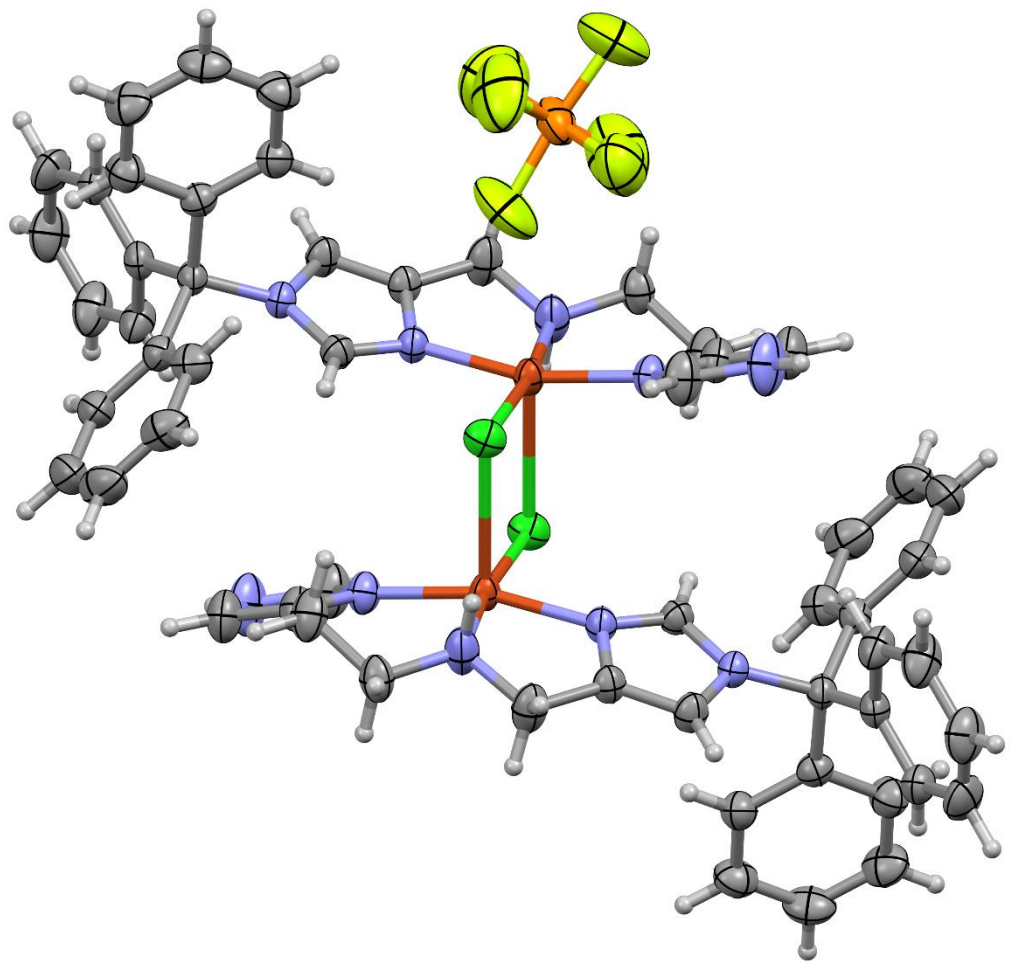


Figure S4: Ortep representation of 3^{Tr} with displacement ellipsoids drawn at the 50% probability level.

Table S4: Crystal data and structure refinement for **3^{Tr}**

Identification code	Complex 3 ^{Tr}
CCDC Deposition Number	2369758
Empirical formula	C56 H54 Cl2 Cu2 F12 N10 P2
Formula weight	1355.01
Temperature	297(2) K
Wavelength	0.71073 Å
Crystal system	Monoclinic
Space group	C2/c
Unit cell dimensions	$a = 33.2550(11)$ Å $a = 90^\circ$. $b = 7.3015(3)$ Å $b = 99.704(3)^\circ$. $c = 23.7923(8)$ Å $\gamma = 90^\circ$.
Volume	5694.4(3) Å ³
Z	4
Density (calculated)	1.581 Mg/m ³
Absorption coefficient	0.985 mm ⁻¹
F(000)	2760
Crystal size	0.50 x 0.12 x 0.02 mm ³
Theta range for data collection	3.018 to 26.332°.
Independent reflections	5755 [$R_{\text{int}} = 0.0411$]
Completeness to theta = 25.242°	99.8 %
Absorption correction	Semi-empirical from equivalents
Max. and min. transmission	1.00000 and 0.90673
Refinement method	Full-matrix least-squares on F ²
Data / restraints / parameters	5755 / 18 / 404
Goodness-of-fit on F ²	1.039
Final R indices [I>2sigma(I)]	$R_1 = 0.0421$, $wR_2 = 0.1061$
R indices (all data)	$R_1 = 0.0558$, $wR_2 = 0.1129$
Largest diff. peak and hole	0.497 and -0.410 e.Å ⁻³

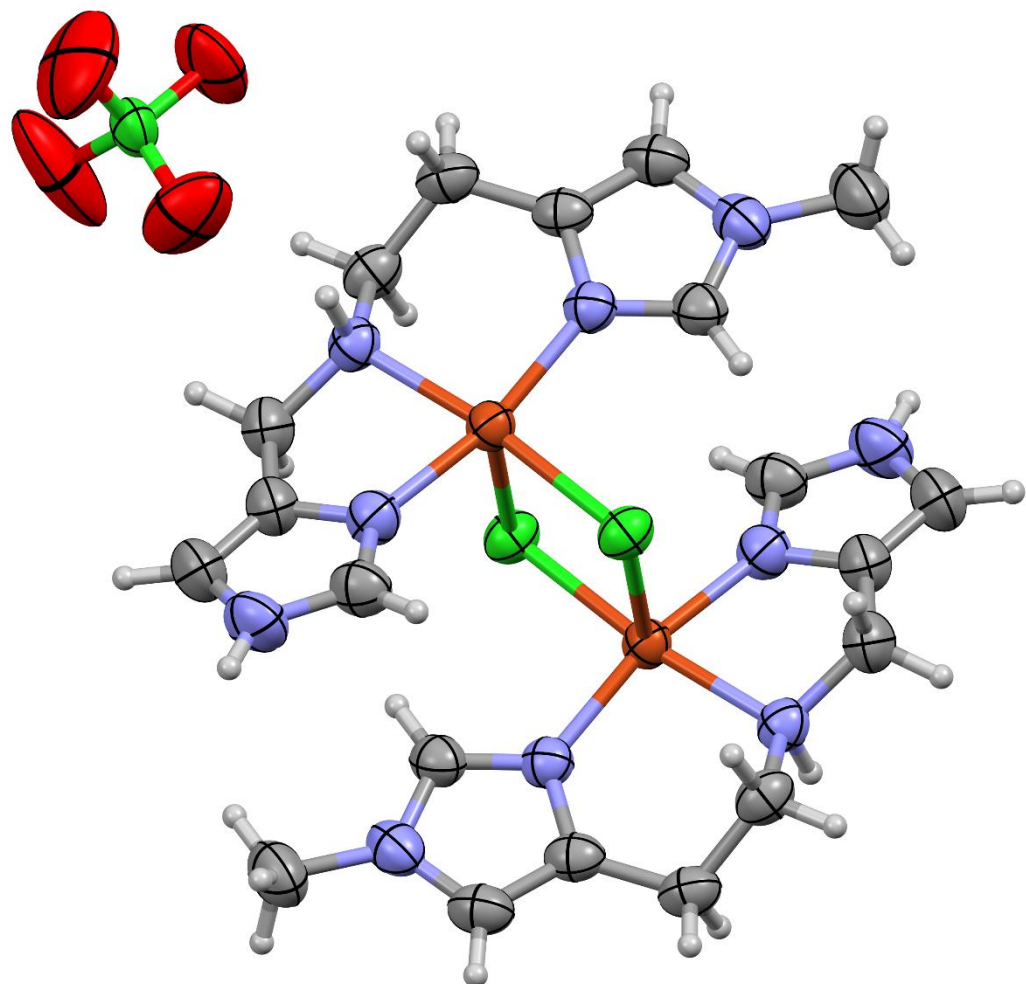


Figure S5: Ortep representation of **4** with displacement ellipsoids drawn at the 50% probability level. The minor part of the disordered perchlorate anion was omitted for clarity.

Table S5: Crystal data and structure refinement for **4**

Identification code	Complex 4
CCDC Deposition Number	2369754
Empirical formula	C ₂₀ H ₃₀ Cl ₄ Cu ₂ N ₁₀ O ₈
Formula weight	807.42
Temperature	297(2) K
Wavelength	0.71073 Å
Crystal system	Triclinic
Space group	P-1
Unit cell dimensions	$a = 7.5005(15)$ Å $b = 8.931(2)$ Å $c = 12.916(2)$ Å $\alpha = 80.624(17)^\circ$. $\beta = 73.129(16)^\circ$. $\gamma = 69.64(2)^\circ$.
Volume	774.4(3) Å ³
Z	1
Density (calculated)	1.731 Mg/m ³
Absorption coefficient	1.779 mm ⁻¹
F(000)	410
Crystal size	0.13 x 0.12 x 0.04 mm ³
Theta range for data collection	2.849 to 26.203°.
Reflections collected	10998
Independent reflections	3043 [$R_{(int)} = 0.0329$]
Completeness to theta = 25.242°	98.5 %
Absorption correction	Semi-empirical from equivalents
Max. and min. transmission	1.00000 and 0.85032
Refinement method	Full-matrix least-squares on F ²
Data / restraints / parameters	3043 / 56 / 246
Goodness-of-fit on F ²	1.051
Final R indices [I>2sigma(I)]	$R_1 = 0.0422$, $wR_2 = 0.1098$
R indices (all data)	$R_1 = 0.0479$, $wR_2 = 0.1130$
Largest diff. peak and hole	0.504 and -0.549 e.Å ⁻³

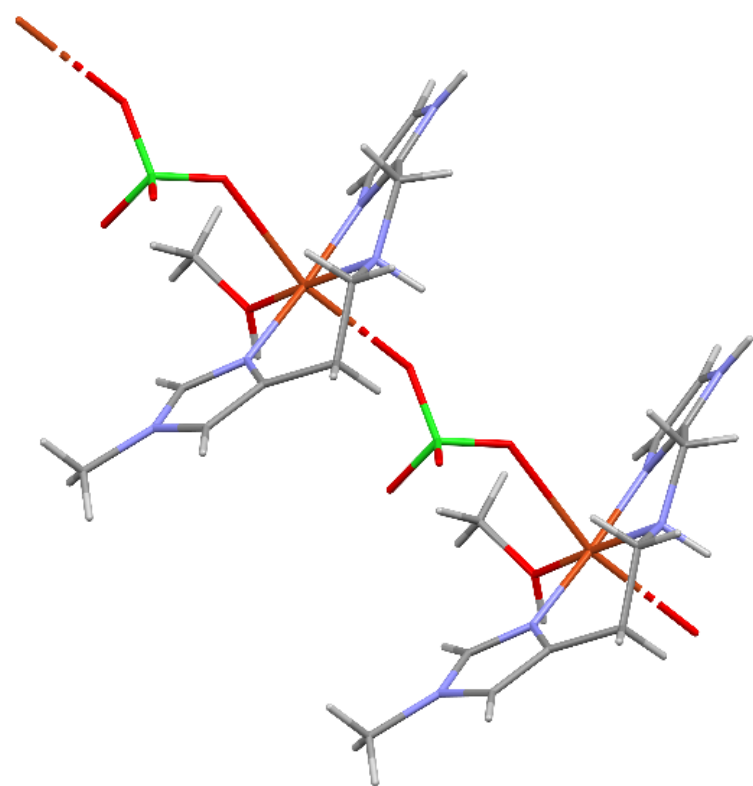
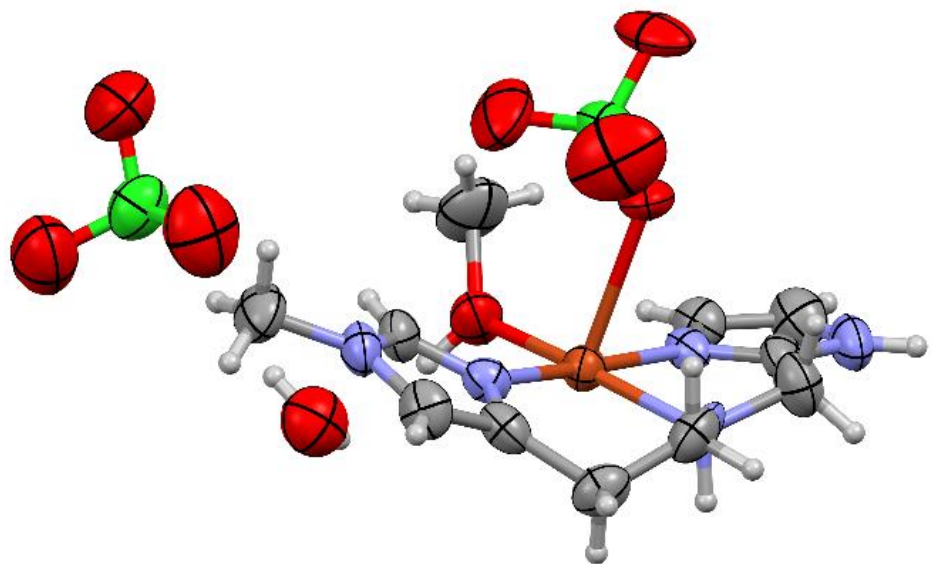


Figure S6: (top) Ortep representation of **5** with displacement ellipsoids drawn at the 50% probability level. (Bottom) 1D coordination chain where the complexes are linked by coordinating perchlorate anions. The minor parts of the disordered perchlorate anions were omitted for clarity.

Table S6: Crystal data and structure refinement for **5**

Identification code	Complex 5
CCDC Deposition Number	2369755
Empirical formula	C11 H21 Cl2 Cu N5 O10
Formula weight	517.77
Temperature	297(2) K
Wavelength	0.71073 Å
Crystal system	Orthorhombic
Space group	P2 ₁ 2 ₁ 2 ₁
Unit cell dimensions	 a = 7.2615(9) Å b = 16.4041(17) Å c = 16.7373(16) Å α= 90°. β= 90°. γ = 90°.
Volume	1993.7(4) Å ³
Z	4
Density (calculated)	1.725 Mg/m ³
Absorption coefficient	1.424 mm ⁻¹
F(000)	1060
Crystal size	0.15 x 0.06 x 0.05 mm ³
Theta range for data collection	3.301 to 25.349°.
Reflections collected	8064
Independent reflections	3518 [R _(int) = 0.0834]
Completeness to theta = 25.242°	99.1 %
Absorption correction	Semi-empirical from equivalents
Max. and min. transmission	1.00000 and 0.69867
Refinement method	Full-matrix least-squares on F ²
Data / restraints / parameters	3518 / 259 / 326
Goodness-of-fit on F ²	1.092
Final R indices [I>2sigma(I)]	R ₁ = 0.0802, wR ₂ = 0.1801
R indices (all data)	R ₁ = 0.1136, wR ₂ = 0.1975
Largest diff. peak and hole	0.946 d -0.398 e.Å ⁻³

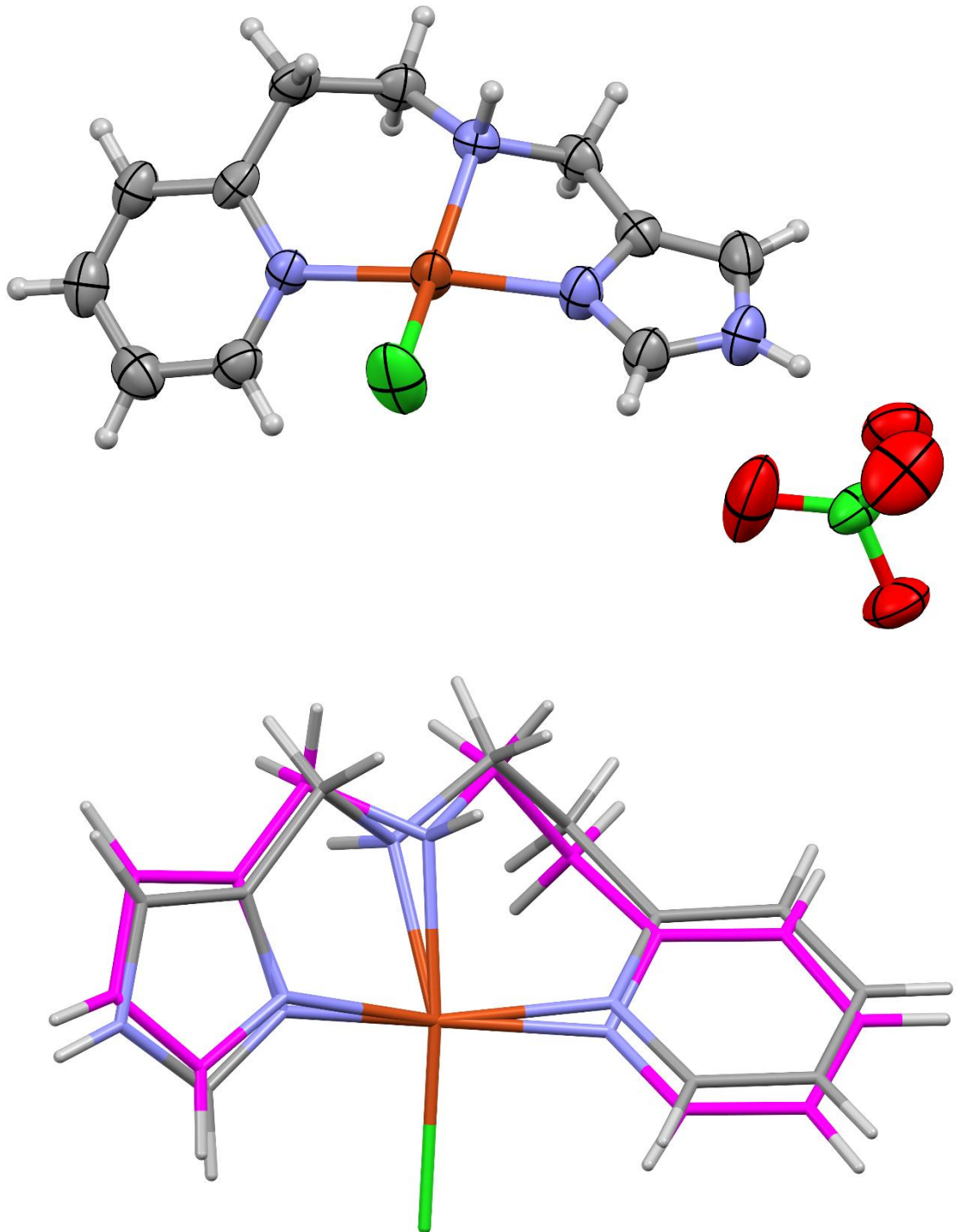


Figure S7: (top) Ortep representation of **6** with displacement ellipsoids drawn at the 50% probability level. The minor part of the disordered perchlorate anion was omitted for clarity. (Bottom) The observed disorder of the ligand, minor part shown with carbon atom.

Table S7: Crystal data and structure refinement for **6**

Identification code	Complex 6
CCDC Deposition Number	2369756
Empirical formula	C11 H14 Cl2 Cu N4 O4
Formula weight	400.70
Temperature	297(2) K
Wavelength	0.71073 Å
Crystal system	Monoclinic
Space group	P21/n
Unit cell dimensions	$a = 12.8007(9)$ Å $a = 90^\circ$. $b = 8.0922(4)$ Å $b = 108.525(7)^\circ$. $c = 15.2526(10)$ Å $\gamma = 90^\circ$.
Volume	1498.09(18) Å ³
Z	4
Density (calculated)	1.777 Mg/m ³
Absorption coefficient	1.837 mm ⁻¹
F(000)	812
Crystal size	0.40 x 0.15 x 0.04 mm ³
Theta range for data collection	3.104 to 26.323°.
Reflections collected	12848
Independent reflections	3021 [R(int) = 0.0271]
Completeness to theta = 25.242°	99.5 %
Absorption correction	Semi-empirical from equivalents
Max. and min. transmission	1.00000 and 0.45546
Refinement method	Full-matrix least-squares on F2
Data / restraints / parameters	3021 / 74 / 236
Goodness-of-fit on F2	0.872
Final R indices [I>2sigma(I)]	R1 = 0.0333, wR2 = 0.0827
R indices (all data)	R1 = 0.0372, wR2 = 0.0855
Largest diff. peak and hole	0.706 and -0.323 e.Å ⁻³

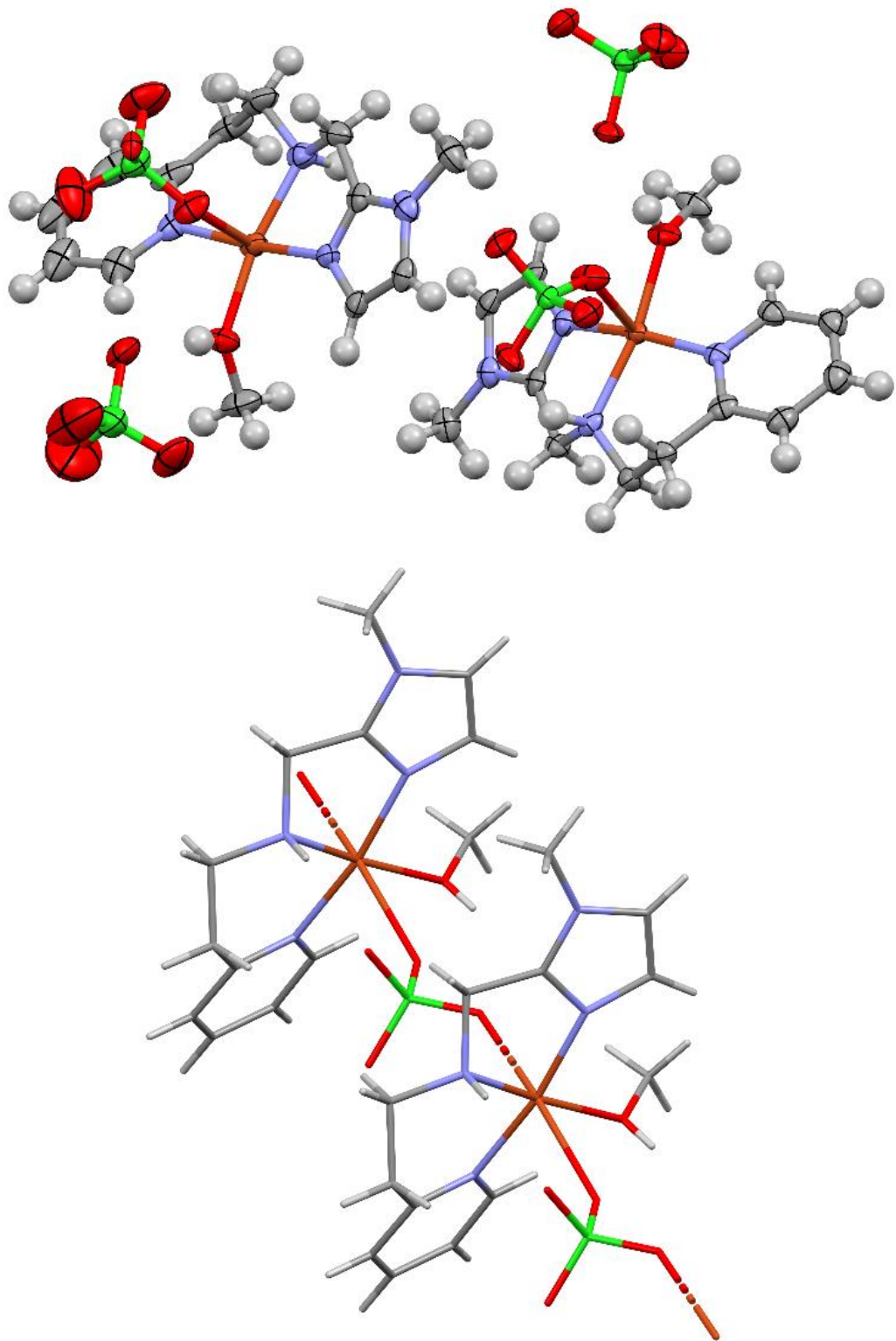


Figure S8: (top) Ortep representation of **7** with displacement ellipsoids drawn at the 50% probability level. (bottom) 1D coordination chain where the complexes are linked by coordinating perchlorate anions. The minor parts of the disordered perchlorate anions were omitted for clarity.

Complex **7** is reported previously by the Simaan group⁷ but with a coordinated acetonitrile (CCDC 1476063) instead of a coordinated methanol.

Table S8: Crystal data and structure refinement for 7

Identification code	Complex 7
CCDC Deposition Number	2369757
Empirical formula	C13 H20 Cl2 Cu N4 O9
Formula weight	510.77
Temperature	150(2) K
Wavelength	0.71073 Å
Crystal system	Monoclinic
Space group	P2 ₁ /c
Unit cell dimensions	 a = 29.258(2) Å b = 7.1874(3) Å c = 19.1948(19) Å α = 90°. β = 99.360(10)°. γ = 90°.
Volume	3982.7(5) Å ³
Z	8
Density (calculated)	1.704 Mg/m ³
Absorption coefficient	1.420 mm ⁻¹
F(000)	2088
Crystal size	0.50 x 0.14 x 0.03 mm ³
Theta range for data collection	2.921 to 26.002°.
Reflections collected	21207
Independent reflections	7701 [R _(int) = 0.0455]
Completeness to theta = 25.242°	99.5 %
Absorption correction	Semi-empirical from equivalents
Max. and min. transmission	1.00000 and 0.67010
Refinement method	Full-matrix least-squares on F ²
Data / restraints / parameters	7701 / 330 / 641
Goodness-of-fit on F ²	1.112
Final R indices [I>2sigma(I)]	R ₁ = 0.0705, wR ₂ = 0.1593
R indices (all data)	R ₁ = 0.0790, wR ₂ = 0.1638
Largest diff. peak and hole	1.510 and -1.098 e.Å ⁻³

4) EPR spectroscopy

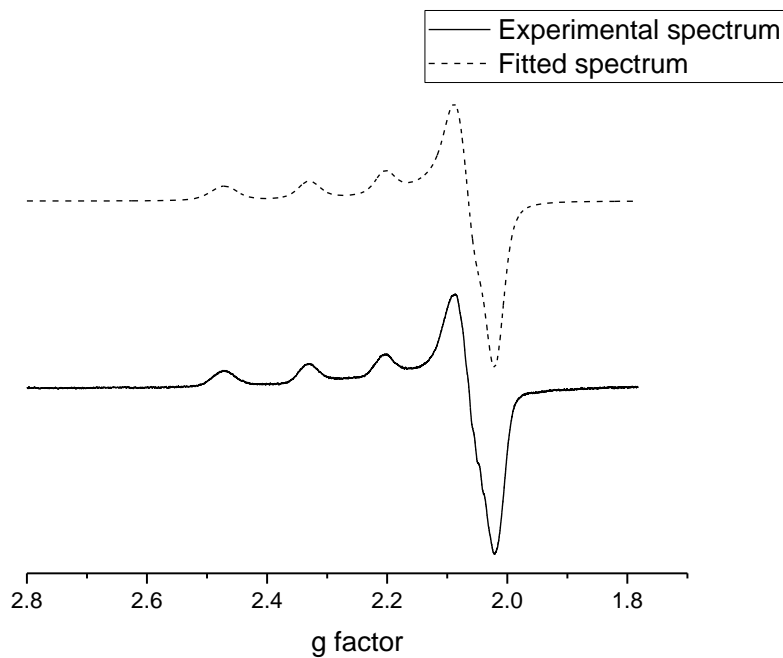


Figure S9: X-band (~9.5 GHz) EPR spectrum of **1** recorded at 100 K in methanol.

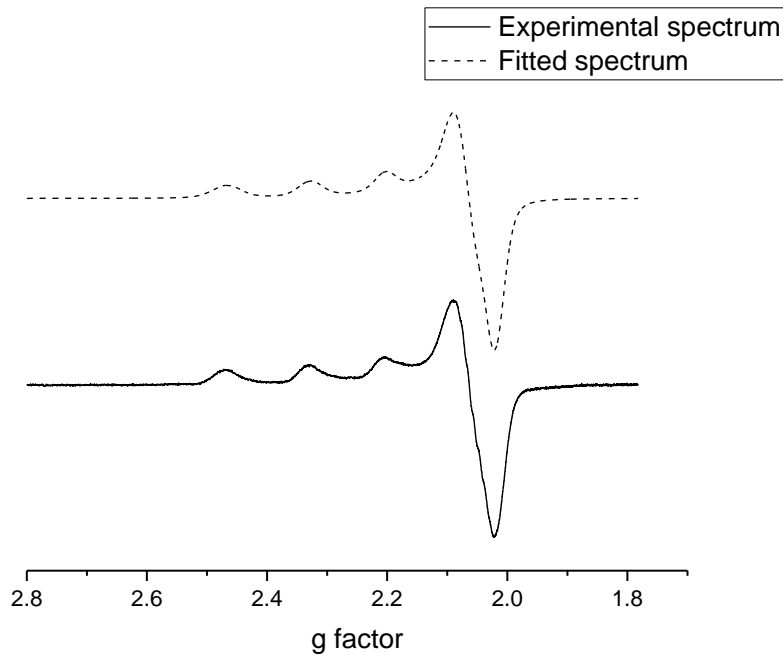


Figure S10: X-band (~9.5 GHz) EPR spectrum of **2** recorded at 100 K in methanol.

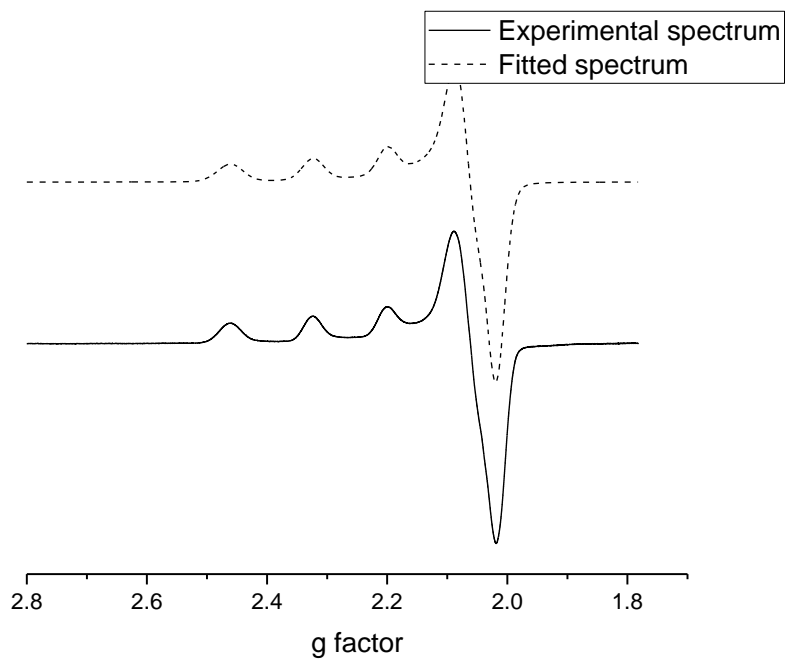


Figure S11: X-band (~9.5 GHz) EPR spectrum of **3** recorded at 100 K in methanol.

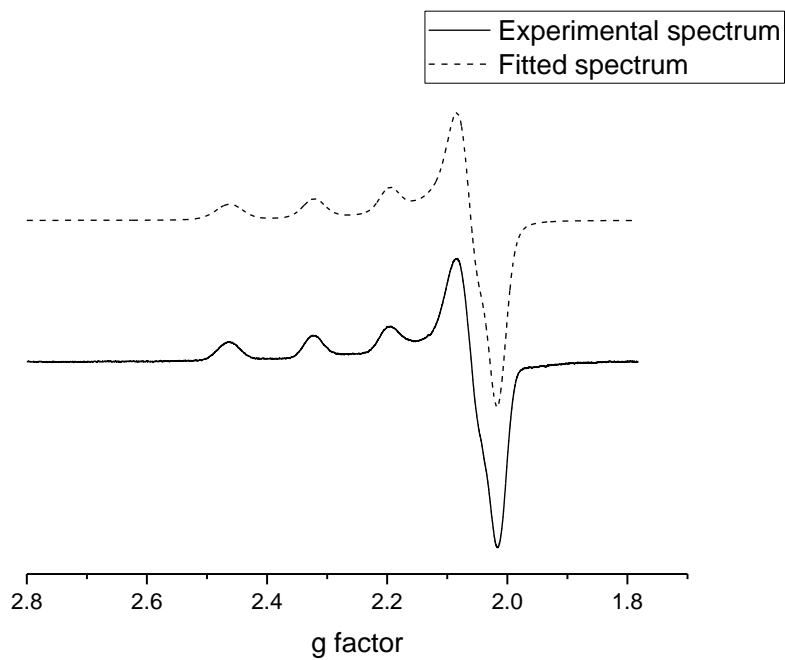


Figure S12: X-band (~9.5 GHz) EPR spectrum of **4** recorded at 100 K in methanol.

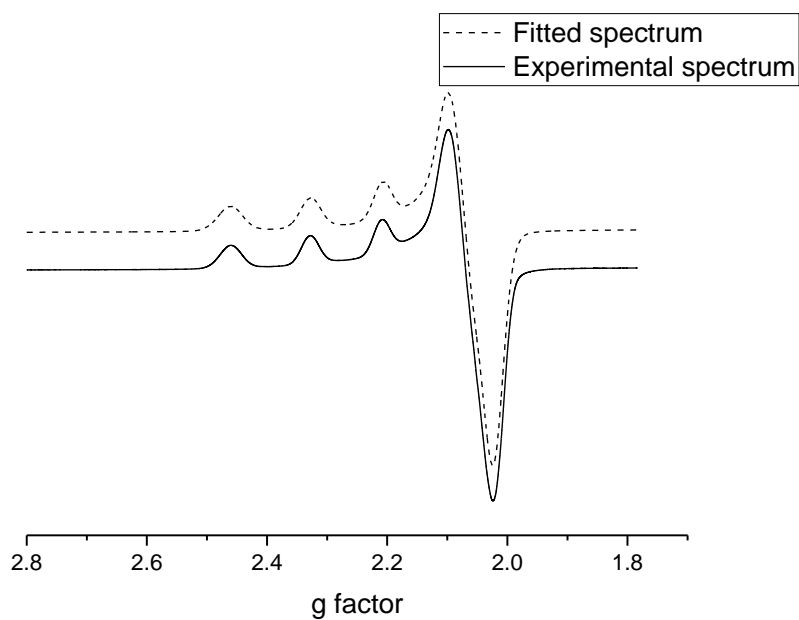


Figure S13: X-band (~9.5 GHz) EPR spectrum of **5** recorded at 100 K in methanol.

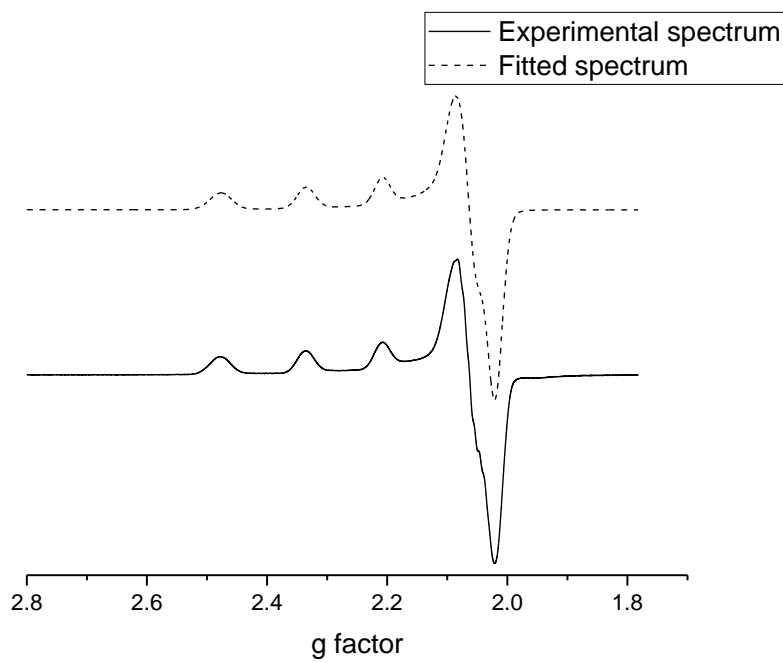


Figure S14: X-band (~9.5 GHz) EPR spectrum of **6** recorded at 100 K in methanol.

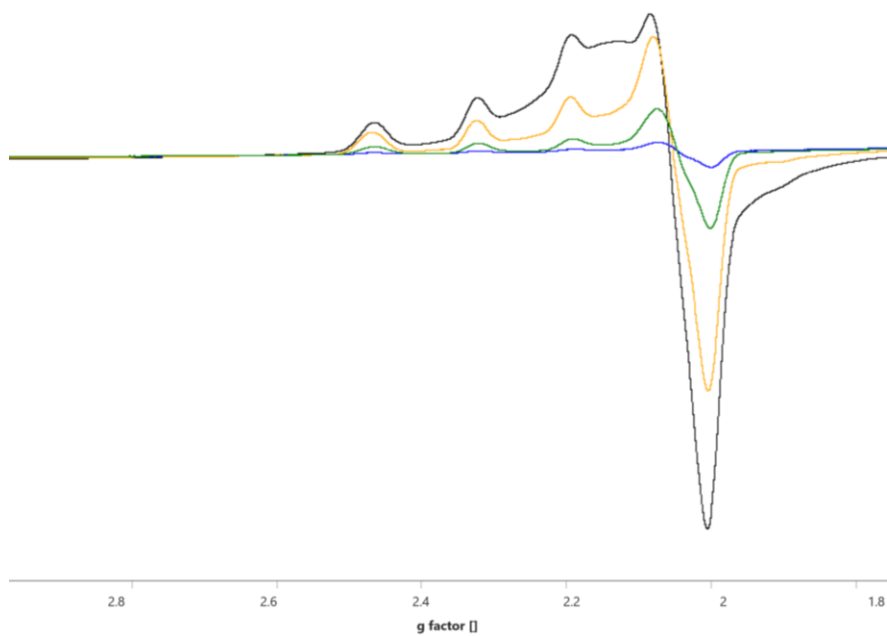


Figure S15: X-band (~ 9.5 GHz) EPR spectrum of **3** recorded at 100 K in methanol at different concentrations: (black) $C \approx 5.10^{-2}$ M ; (yellow) $C \approx 1.10^{-2}$ M ; (green) $C \approx 5.10^{-3}$ M ; (blue) $C \approx 1.10^{-3}$ M.

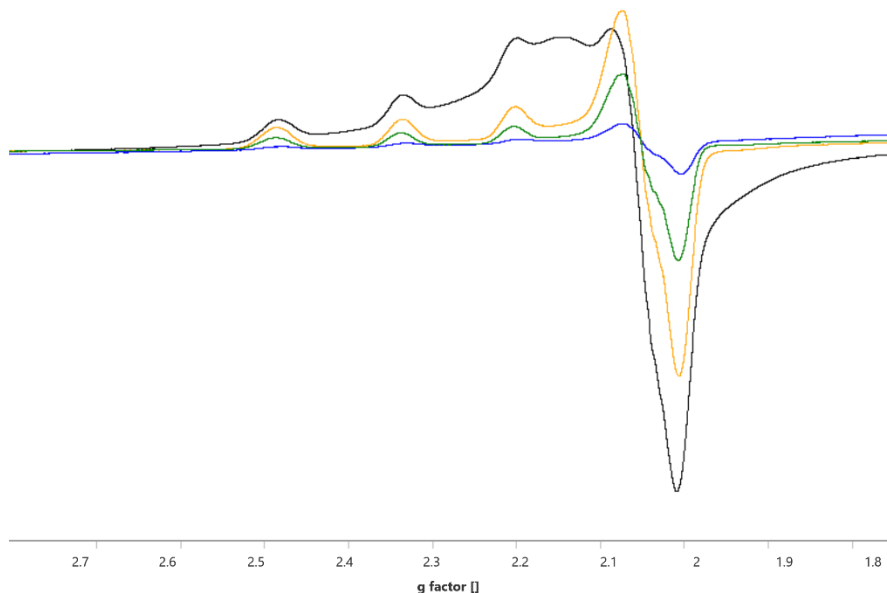


Figure S16: X-band (~ 9.5 GHz) EPR spectrum of **6** recorded at 100 K in methanol at different concentrations: (black) $C \approx 5.10^{-2}$ M ; (yellow) $C \approx 1.10^{-2}$ M ; (green) $C \approx 5.10^{-3}$ M ; (blue) $C \approx 1.10^{-3}$ M.

Table S9: Quantification of the spin concentration by EPR spectroscopy in frozen methanolic solutions and comparison with the molar concentration. Error estimated at $\pm 15\%$.

Compound (in MeOH)	Spin C (M)	Molar C (M)	C ratio (Spin C/Molar C)
1	0.00175	0.00201	0.87
2	0.00196	0.00200	0.98
3	0.02315	0.01989	1.16
4	0.00213	0.00202	1.05
5	0.00237	0.00199	1.19
6	0.00533	0.00499	1.07

5) UV-visible spectra

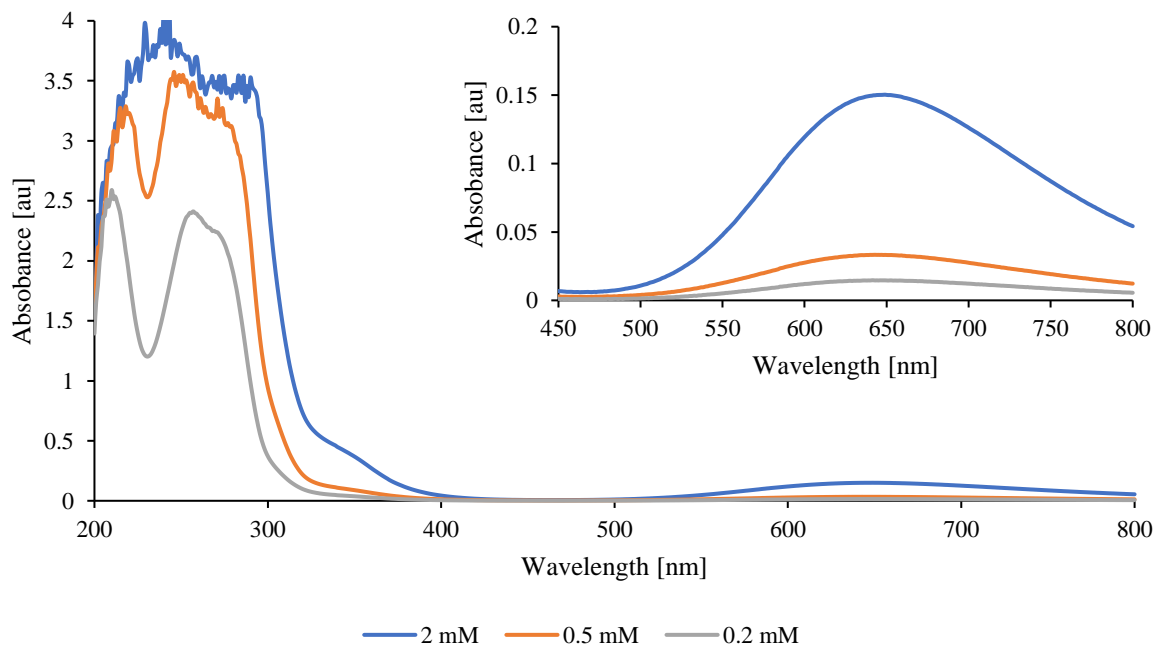


Figure S17: UV spectra of **1** at various concentrations in water.

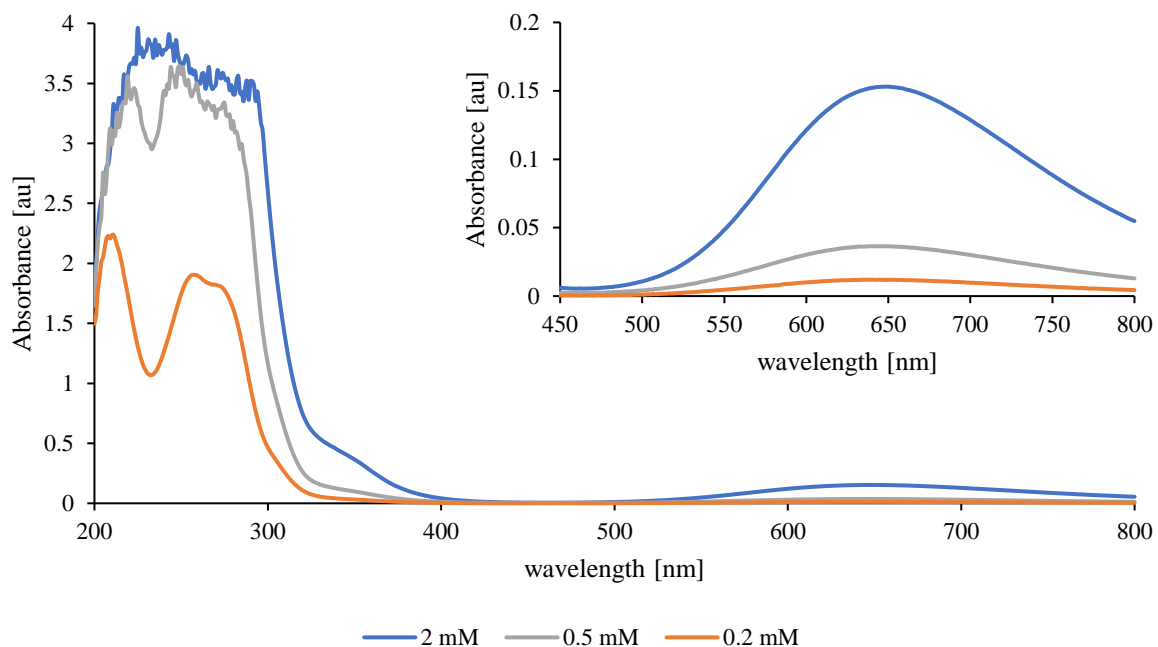


Figure S18: UV spectra of **2** at various concentrations in water.

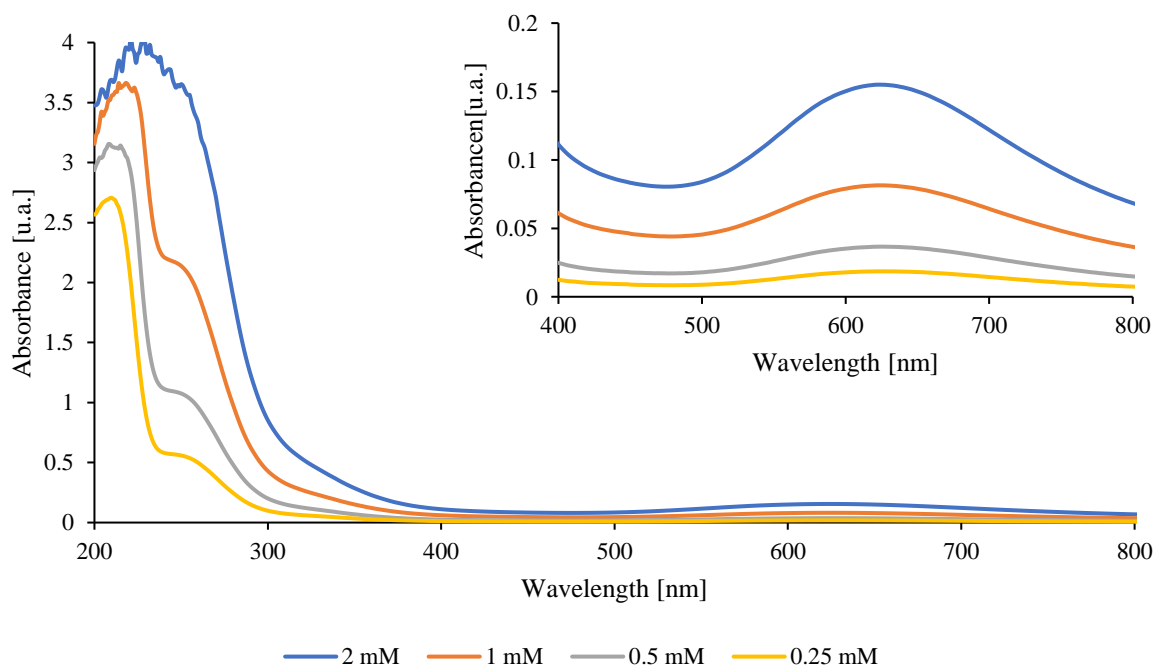


Figure S19: UV spectra of **3** at various concentrations in water.

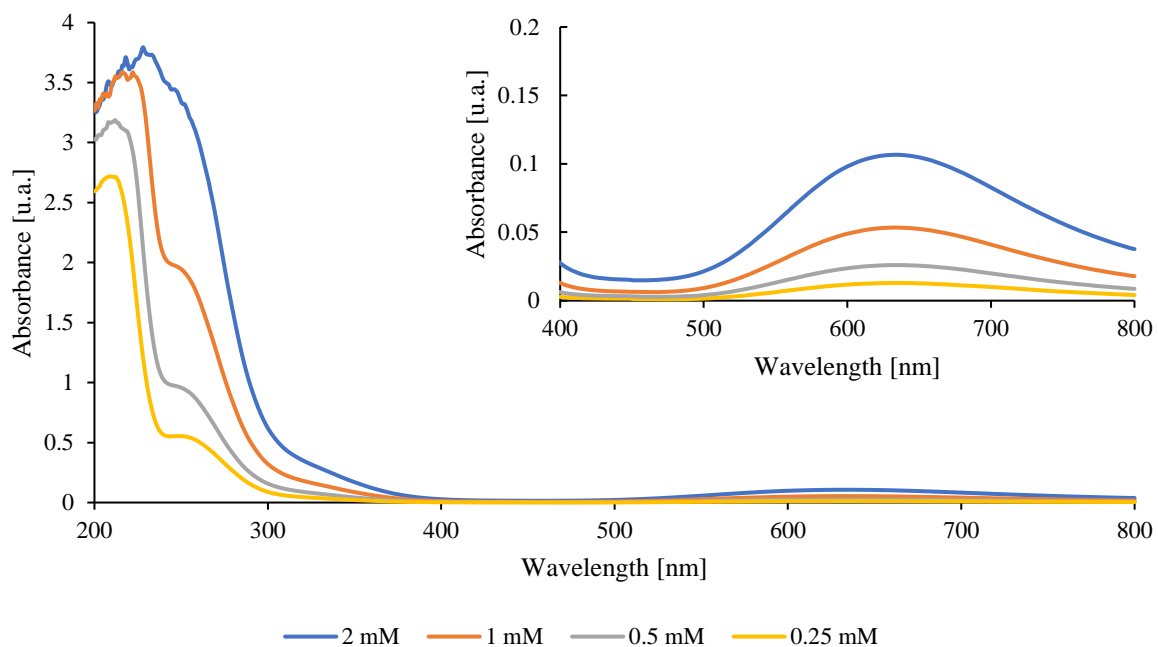


Figure S20: UV spectra of **4** at various concentrations in water.

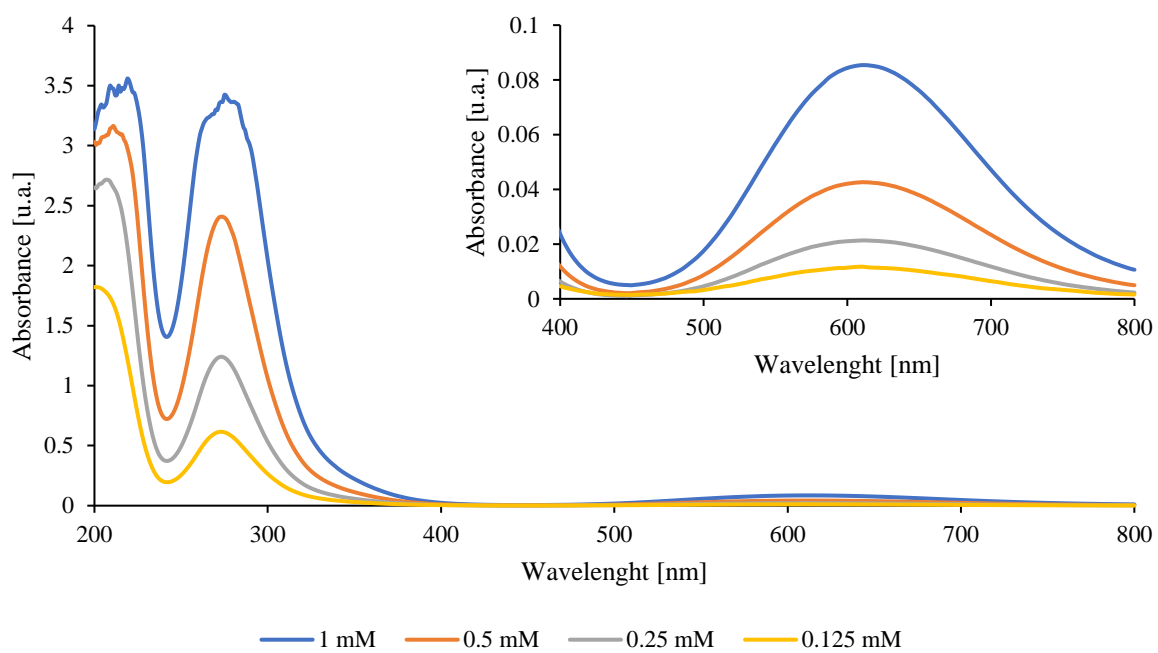


Figure S21: UV spectra of **4** at various concentrations in acetonitrile.

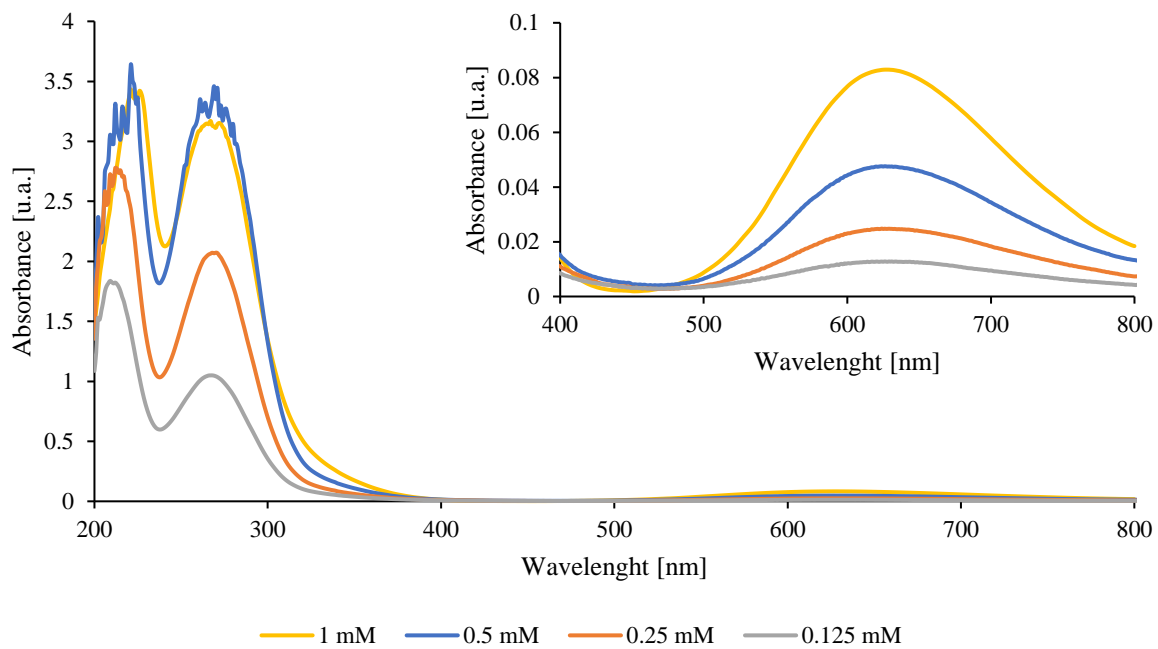


Figure S22: UV spectra of **4** at various concentrations in methanol.

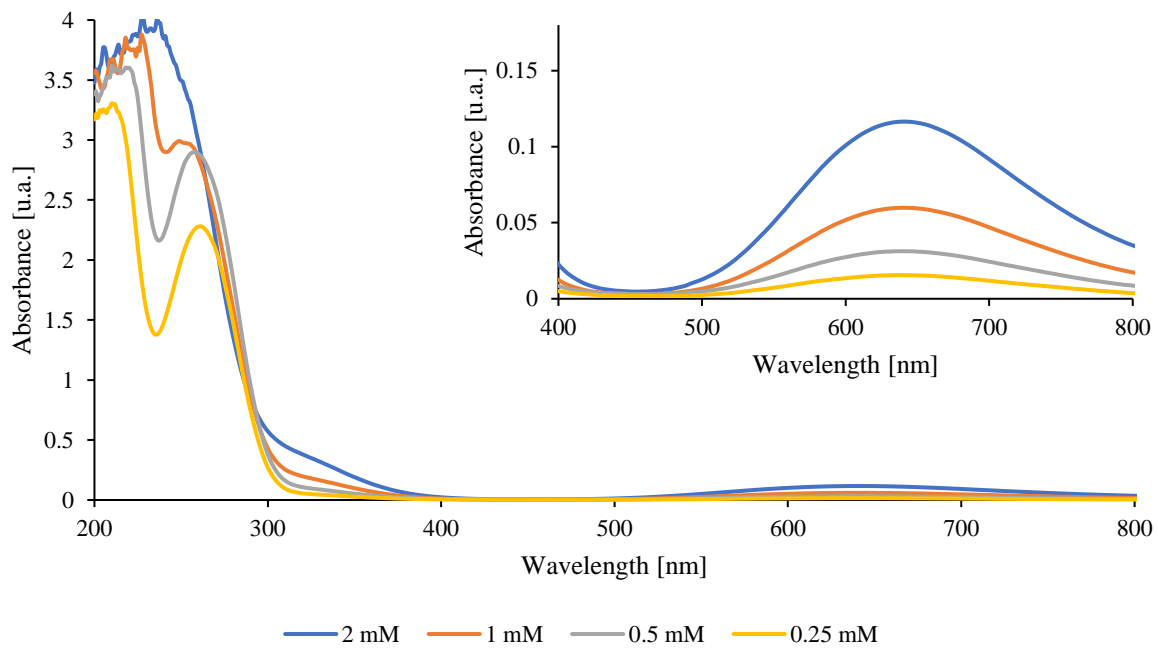


Figure S23: UV spectra of **5** at various concentrations in water.

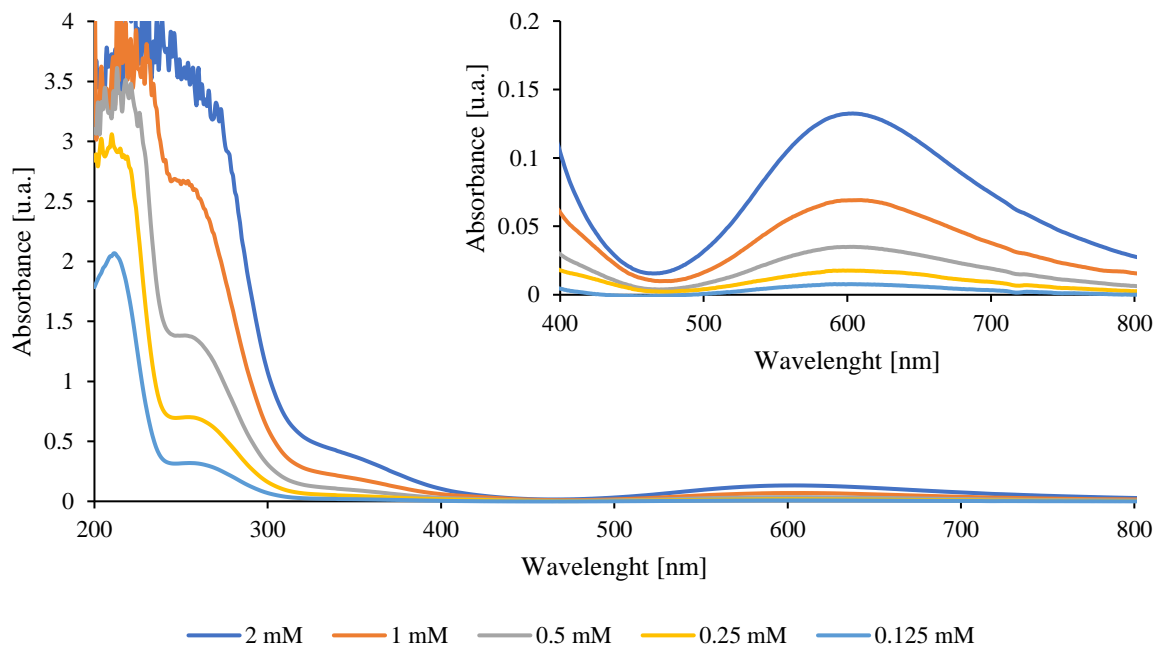


Figure S24: UV spectra of **5** at various concentrations in acetonitrile.

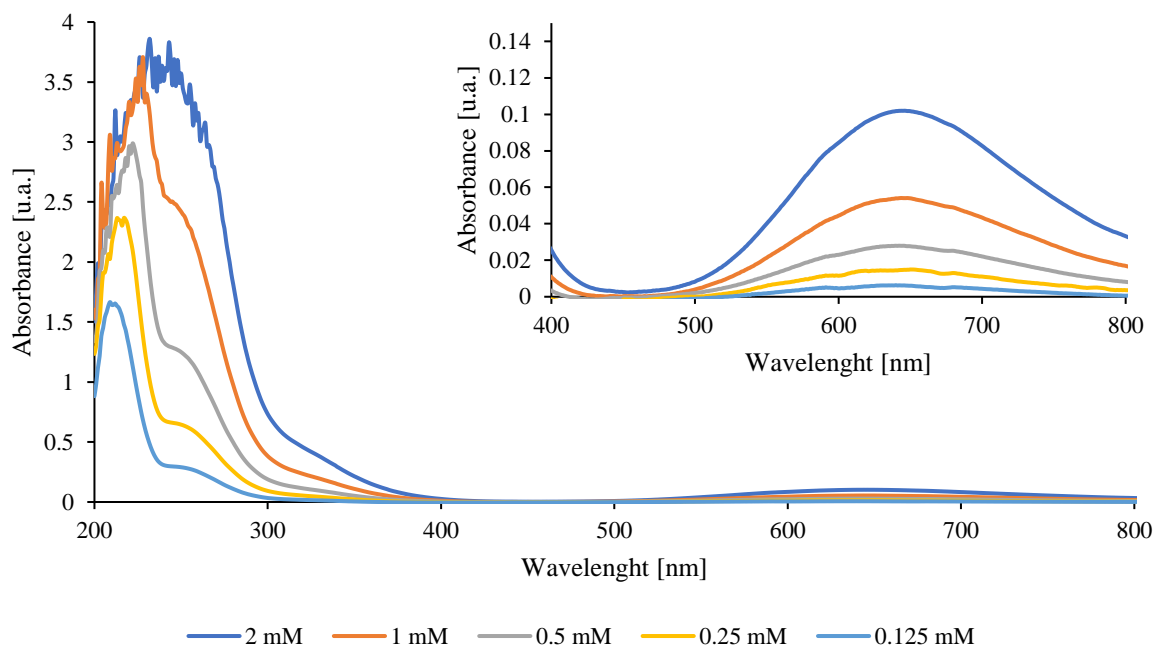


Figure S25: UV spectra of **5** at various concentrations in methanol.

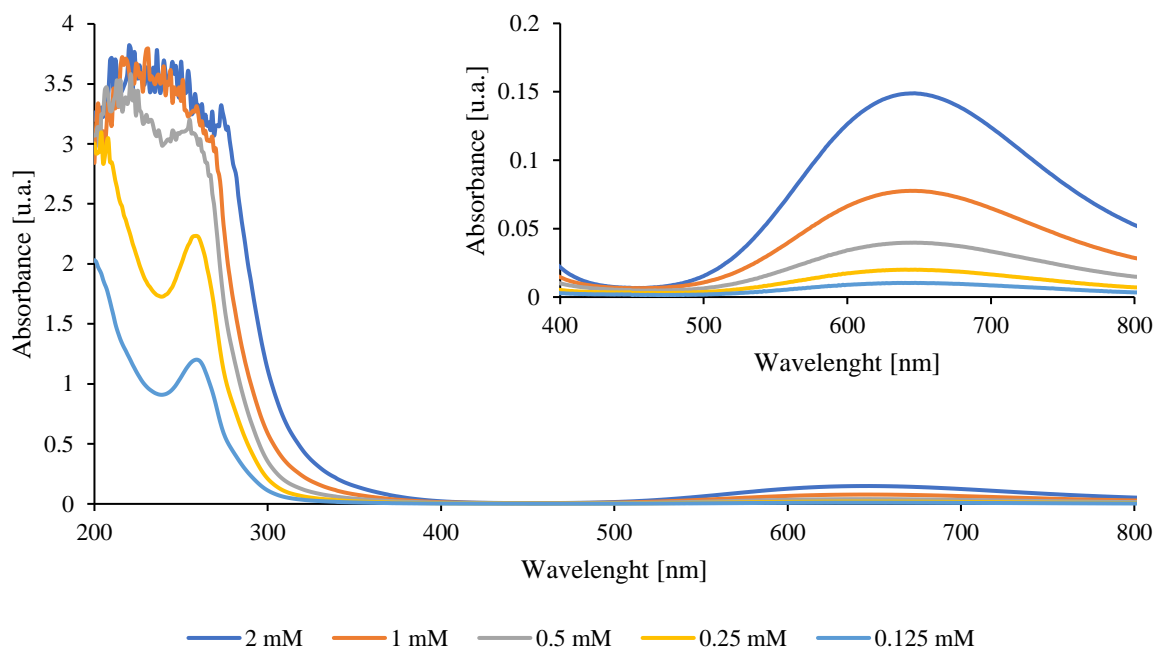


Figure S26: UV spectra of **6** at various concentrations in water.

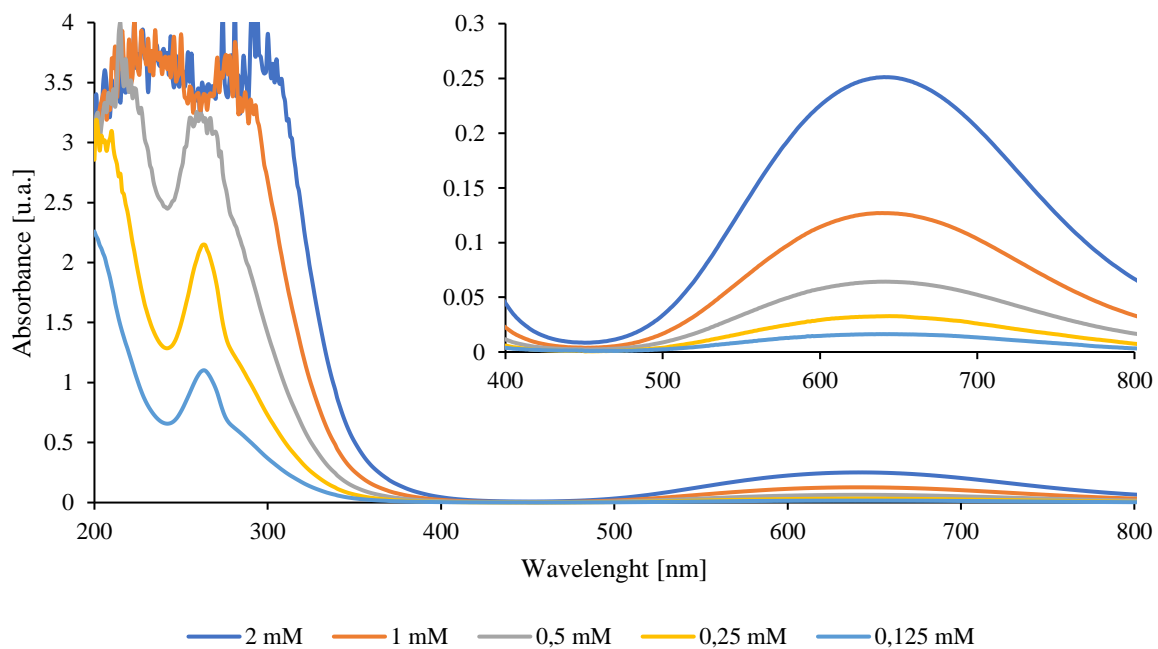


Figure S27: UV spectra of **6** at various concentrations in acetonitrile.

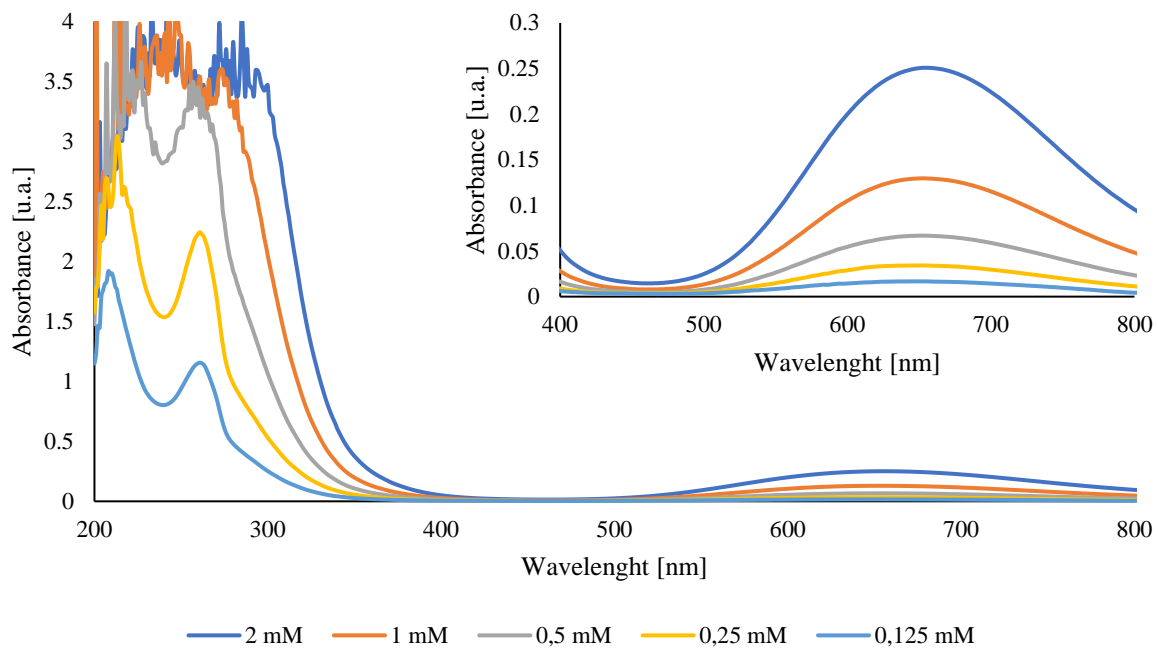


Figure S28: UV spectra of **6** at various concentrations in methanol.

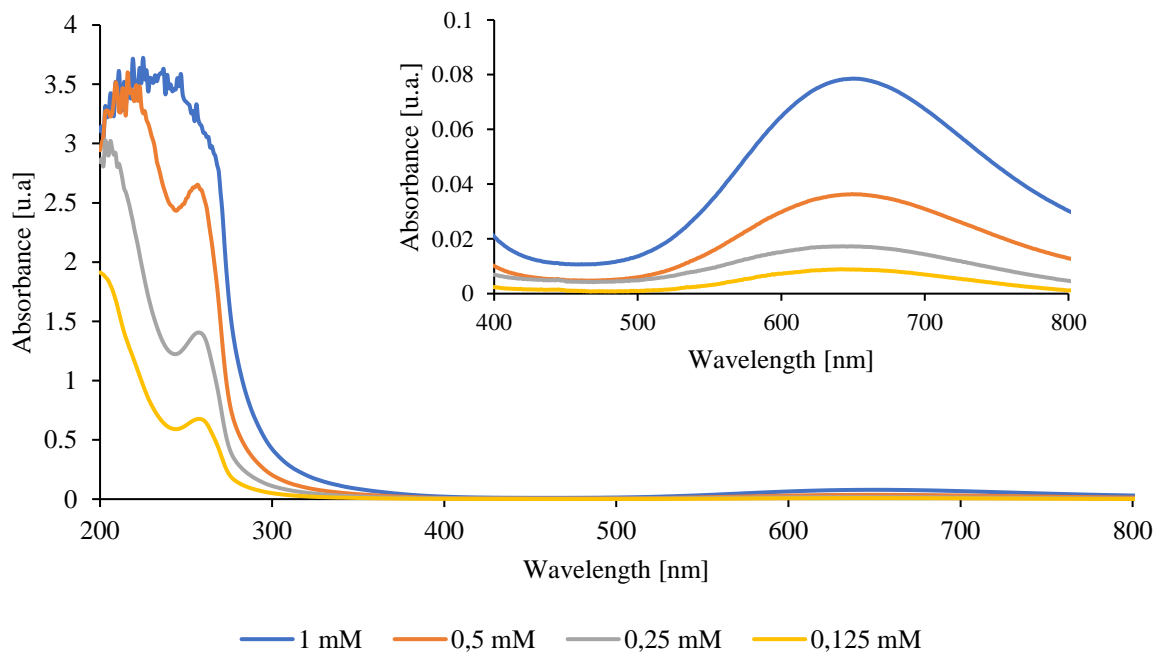


Figure S29: UV spectra of **7** at various concentrations in water.

6) Cyclic voltammetry

The experiments were carried out in a 10 mL three electrode glass cell with a glassy carbon working electrode ($d = 3$ mm), a platinum wire counter electrode, and a Ag^+/Ag pseudo reference electrode. Unless otherwise stated, voltammograms were recorded in methanol with 0.1 M tetrabutylammonium perchlorate under an argon atmosphere, at room temperature and at a scan rate of 100 mV/s. Ferrocene was used as an internal standard.

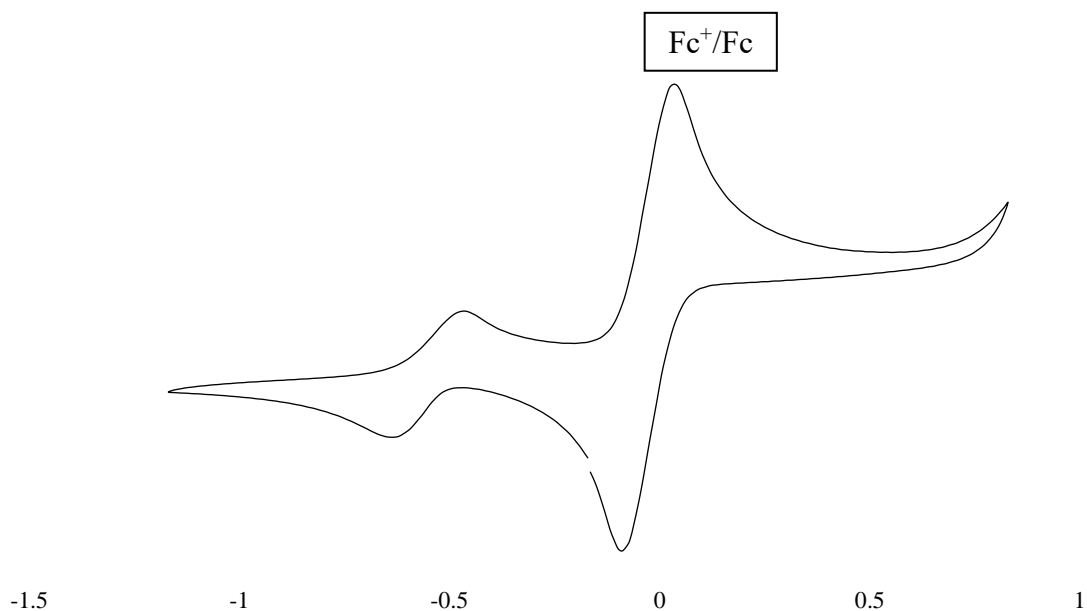


Figure S30: Cyclic voltammogram of **1** (1 mM in 100 mM TBAP/methanol, scan rate: 100mV/s).

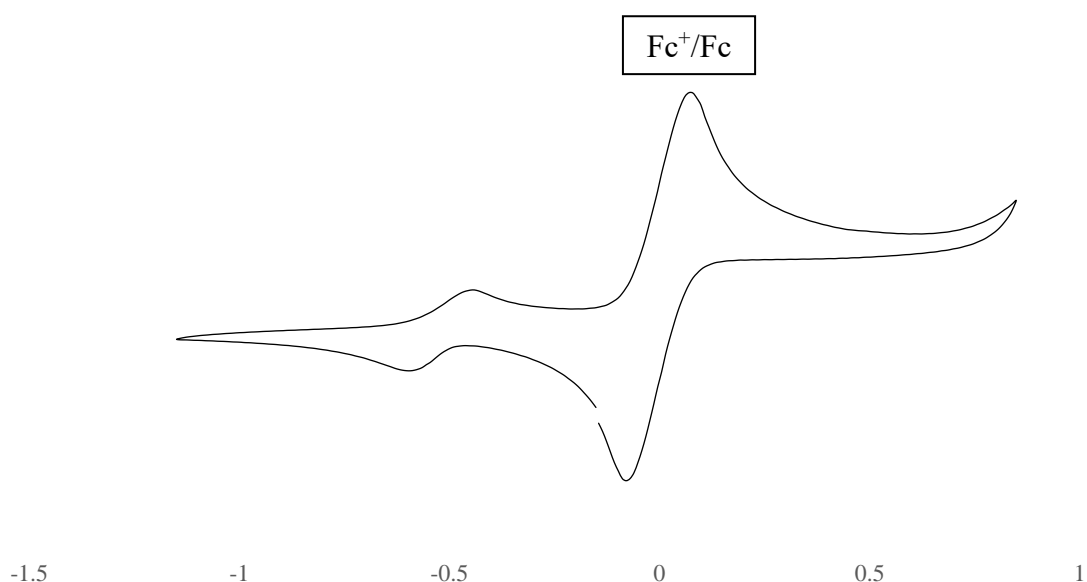


Figure S31: Cyclic voltammogram of **2** (1 mM in 100 mM TBAP/methanol, scan rate: 100mV/s).

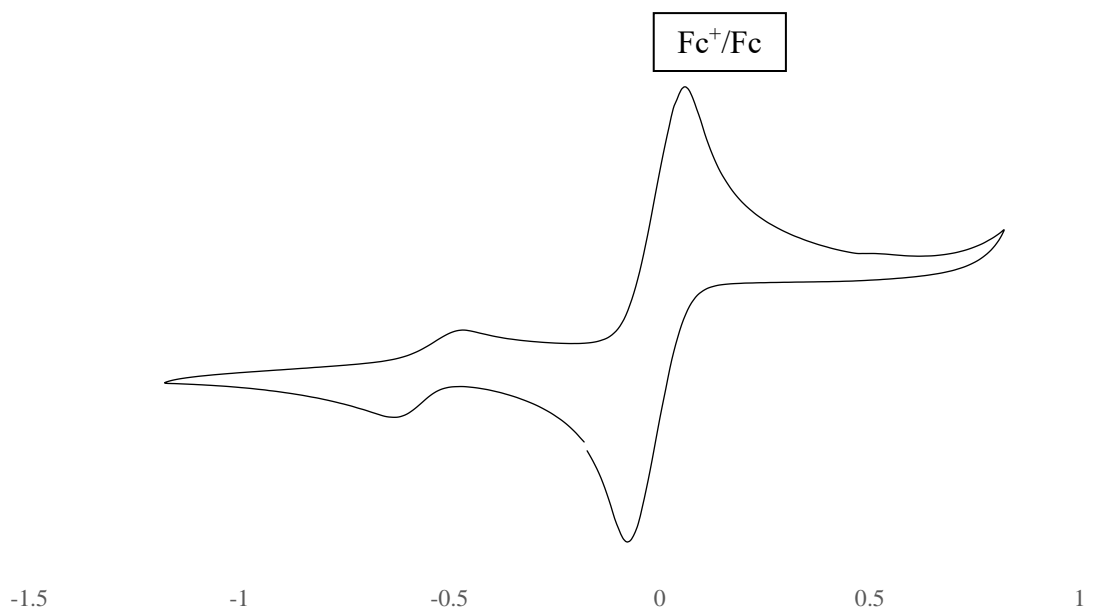


Figure S32: Cyclic voltammogram of **3** (1 mM in 100 mM TBAP/methanol, scan rate: 100mV/s).

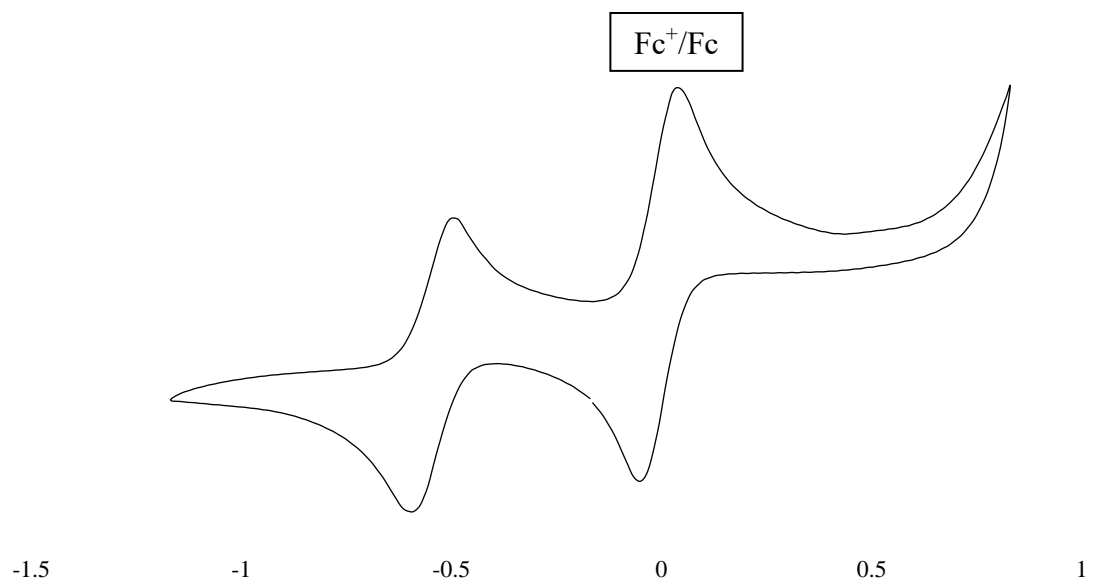


Figure S33: Cyclic voltammogram of **4** (1 mM in 100 mM TBAP/methanol, scan rate: 100mV/s).

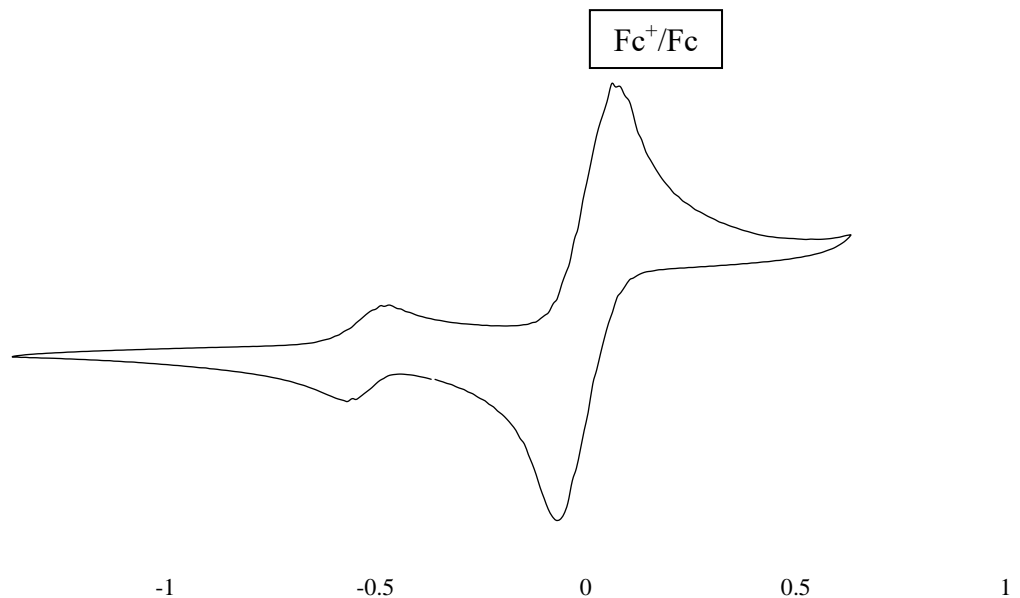


Figure S34: Cyclic voltammogram of **5** (1 mM in 100 mM TBAP/methanol, scan rate: 100mV/s).

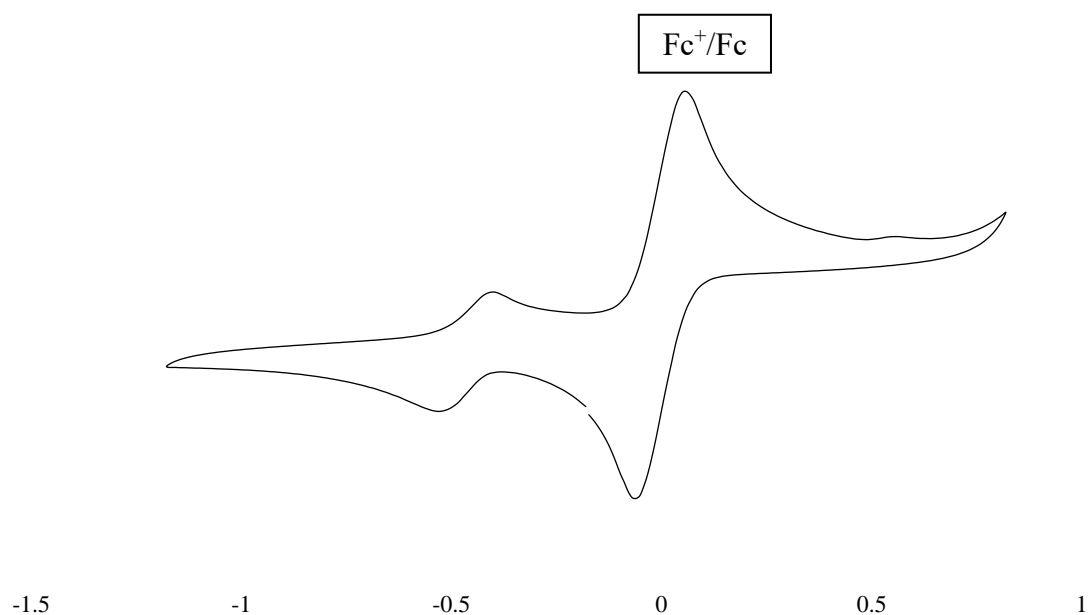


Figure S35: Cyclic voltammogram of **6** (1 mM in 100 mM TBAP/methanol, scan rate: 100mV/s).

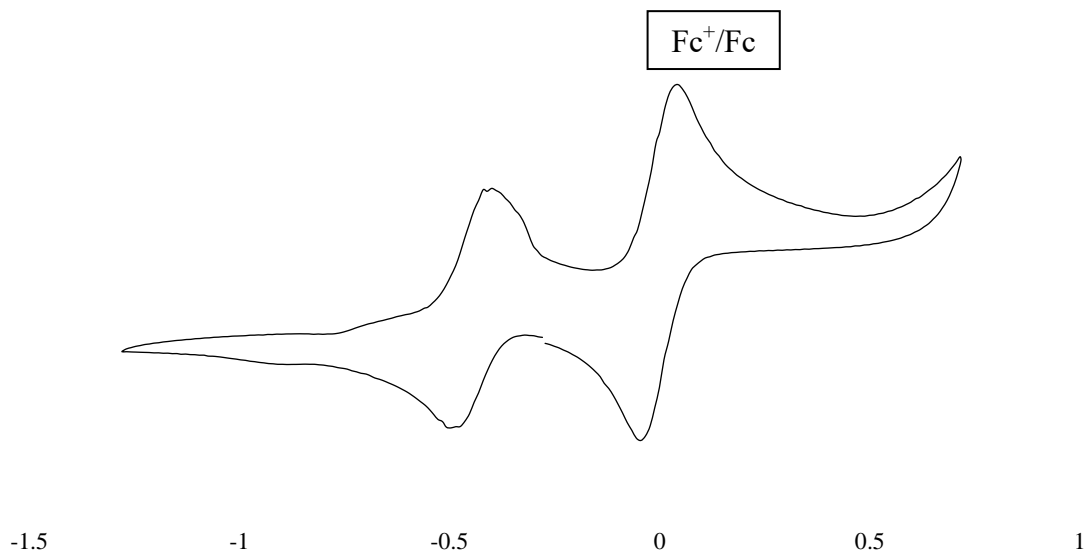


Figure S36: Cyclic voltammogram of **7** (1 mM in 100 mM TBAP/methanol, scan rate: 100mV/s).

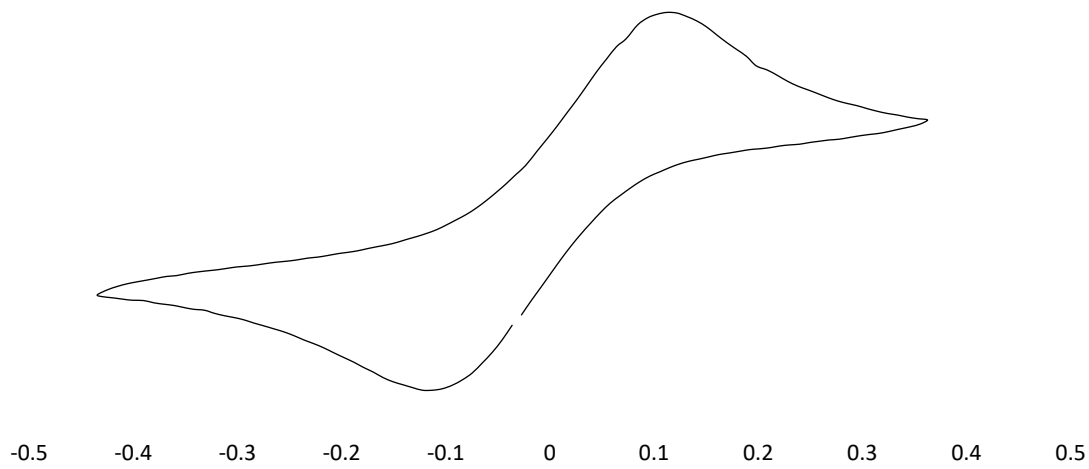


Figure S37: Cyclic voltammogram of **CuCl₂** (1 mM in 100 mM TBAP/methanol, scan rate: 100mV/s). The Cu^{II}/Cu^I reduction overlaps with the Fc⁺/Fc reduction.

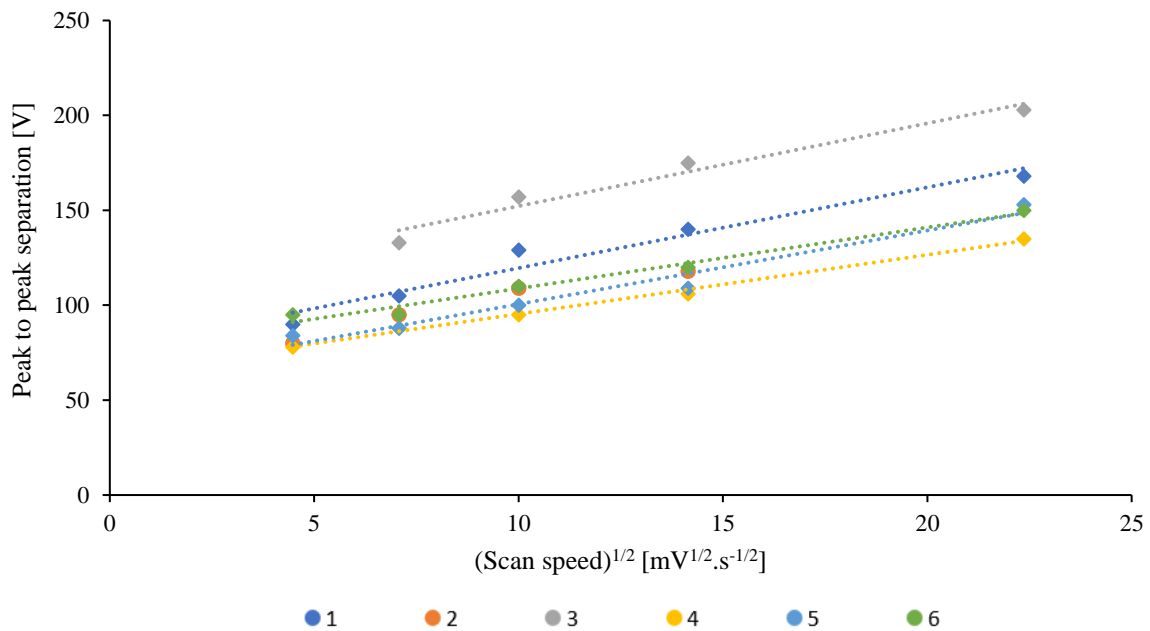


Figure S38: Dependence of the peak to peak separation with the square root of the scan rate (1 mM in 100 mM TBAP/methanol).

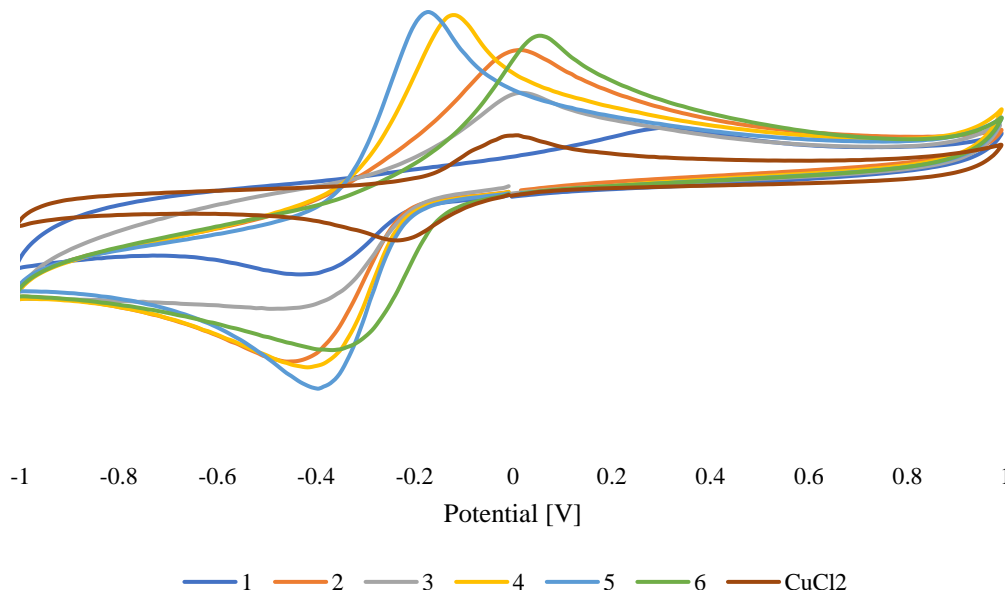


Figure S39: Cyclic voltammogram of **1-7** (1 mM in 10 mM pH 7.5 aqueous phosphate buffer, scan rate: 100 mV/s, reference electrode: AgCl/Ag in 3 M KCl).

Table S10: Summary of the electrochemical parameters in pH 7.5 aqueous phosphate buffer.

Compound	$E_{\text{red}} [\text{V}]$	$E_{\text{ox}} [\text{V}]$	$E_{1/2} [\text{V}]$	$\Delta E [\text{V}]$
1	-0.431	0.325	-0.053	0.756
2	-0.441	0.016	-0.2125	0.457
3	-0.445	0.032	-0.2065	0.477
4	-0.413	-0.116	-0.2645	0.297
5	-0.394	-0.163	-0.2785	0.231
6	-0.366	0.053	-0.1565	0.419

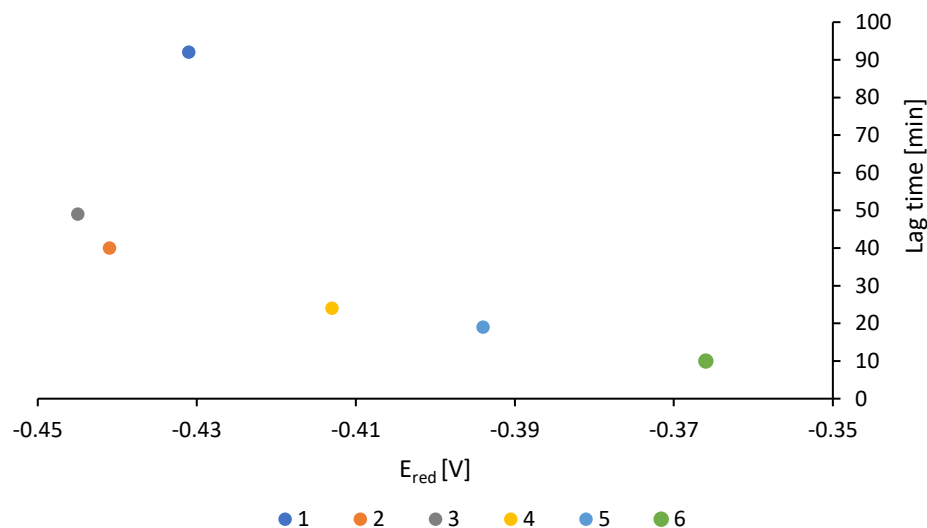


Figure S40: Correlation between the reduction potential (E_{red}) of compound **1** - **6** measured in phosphate buffer (pH 7.5) and the lag time obtained from the catalytic assays.

7) Catalytic evaluation

7.1) Reactivity test of catalytic oxidation cleavage of PNPG

The following solutions were prepared:

- Phosphate buffer (80 mM, pH = 7.5): $\text{K}_2\text{HPO}_4 \cdot 3\text{H}_2\text{O}$ (15.340 g, 0.0672 mol) and NaH_2PO_4 (1.534 g, 0.0128 mol) were dissolved in distilled water to reach 1 L. before each use a volume of this stock solution as diluted 8 times to reach a concentration of 10 mM.
- Catalyst solution (0.1 mM): Each copper compound (2.5 μmol) was dissolved in the buffer solution to reach 25 mL.

- H_2O_2 solution (400 mM): The commercial 35% (wt%) hydrogen peroxide aqueous solution was regularly titrated using a known concentration of potassium permanganate in acid conditions. The corresponding volume of peroxide was each time diluted in the buffer solution to reach 2 mL.
- Substrate solution, PNPG (100 mM): PNPG (0.0602 g, 0.2 mmol) was dissolved in the buffer solution to reach 2 mL.

The reactivity tests were performed as follow: a 1 mL UV quartz cuvette was charged, thanks to micropipettes, with 500 μL of the catalyst solution, 100 μL of the PNPG solution, the total volume was brought to 0.9 mL with buffer. The assay was started with the addition of 100 μL of the H_2O_2 solution. Reference tests were performed without catalyst in all cases the total volume was brought to 1 mL with buffer. The reaction mixtures were manually stirred prior to each measurement to prevent the formation of gas bubbles in the cuvette. Quantification of the product (4-nitrophenolate) was performed by measuring the absorbance at 400 nm ($\varepsilon = 1.85 \times 10^4 \text{ M}^{-1}\text{cm}^{-1}$) every minute for the first 20 minutes or 2 hours and after 24 h. Note that for the measurement after 24 h, the catalytic solution was diluted 10 times. The assays were performed at room temperature ($18^\circ\text{C} - 25^\circ\text{C}$) protected from light.

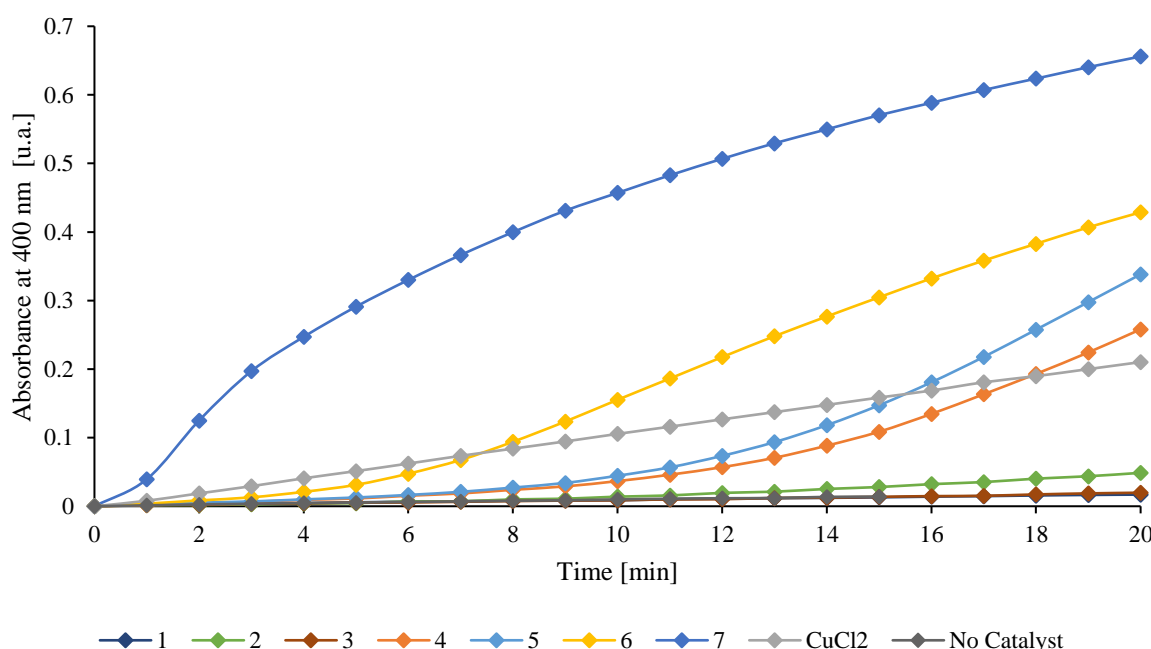


Figure S41: Evolution of the absorbance of paranitrophenolate at 400 nm as a function of time over 20 minutes. Conditions: 10 mM phosphate buffer pH 7.5; [catalyst] = 50 μM ; [PNPG] = 10 mM and $[\text{H}_2\text{O}_2]$ = 40 mM, temperature = r.t.

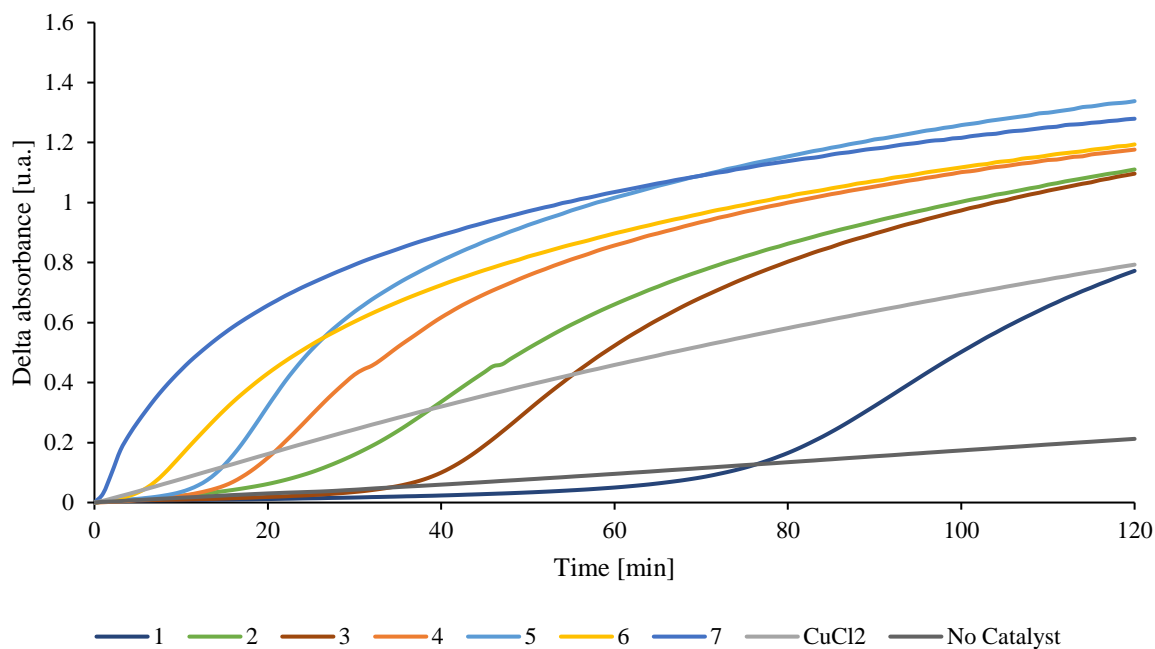


Figure S42: Evolution of the absorbance of paranitrophenolate at 400 nm as a function of time over 2 hours. Conditions: 10 mM phosphate buffer pH 7.5; [catalyst]= 50 μ M; [PNPG]= 10 mM and $[\text{H}_2\text{O}_2]$ = 40 mM, temperature = r.t.

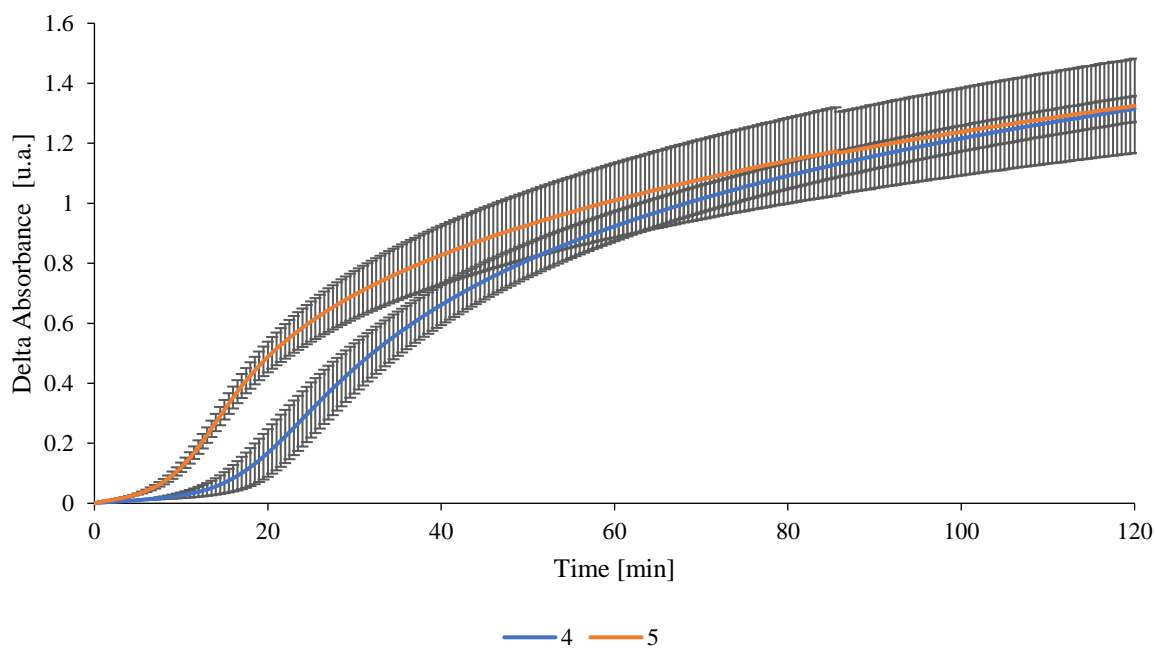


Figure S43: Mean of the evolution of the absorbance of paranitrophenolate at 400 nm as a function of time over 2 hours for compound 4 (blue) and 5 (orange) over three separate runs with standard deviations (grey). Conditions: 10 mM phosphate buffer pH 7.5; [catalyst]= 50 μ M; [PNPG]= 10 mM and $[\text{H}_2\text{O}_2]$ = 40 mM, temperature = r.t.

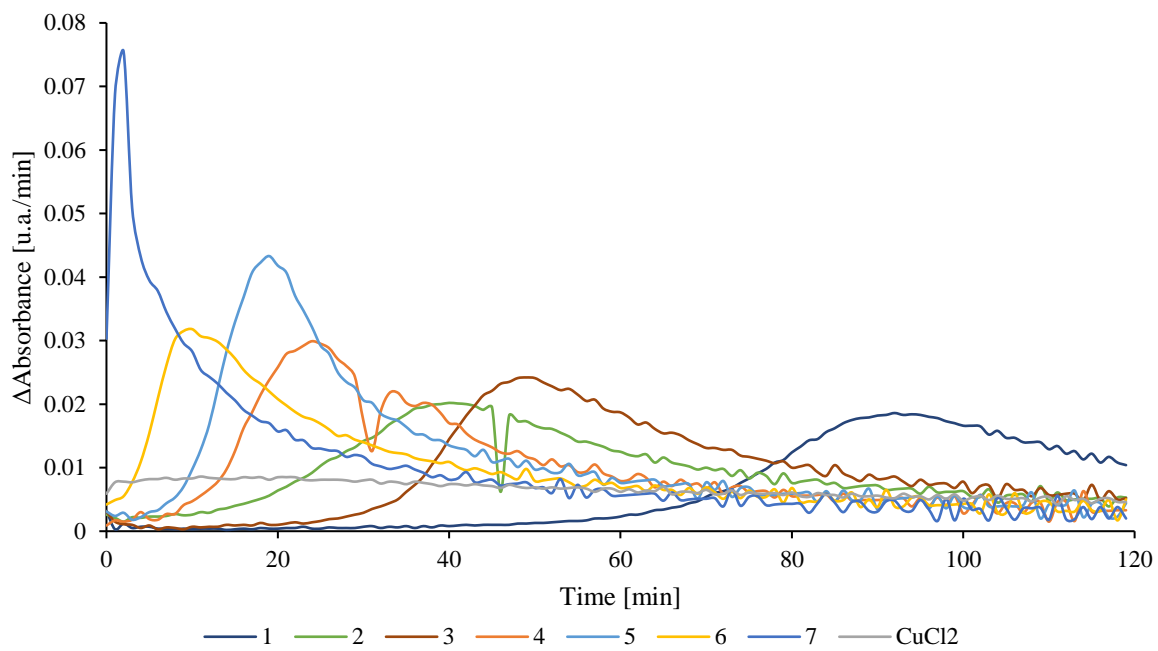


Figure S44: First derivative of the absorbance of paranitrophenolate at 400 nm as a function of time over 2 hours. Conditions: 10 mM phosphate buffer pH 7.5; [catalyst] = 50 μ M; [PNPG] = 10 mM and $[H_2O_2]$ = 40 mM, temperature = r.t.

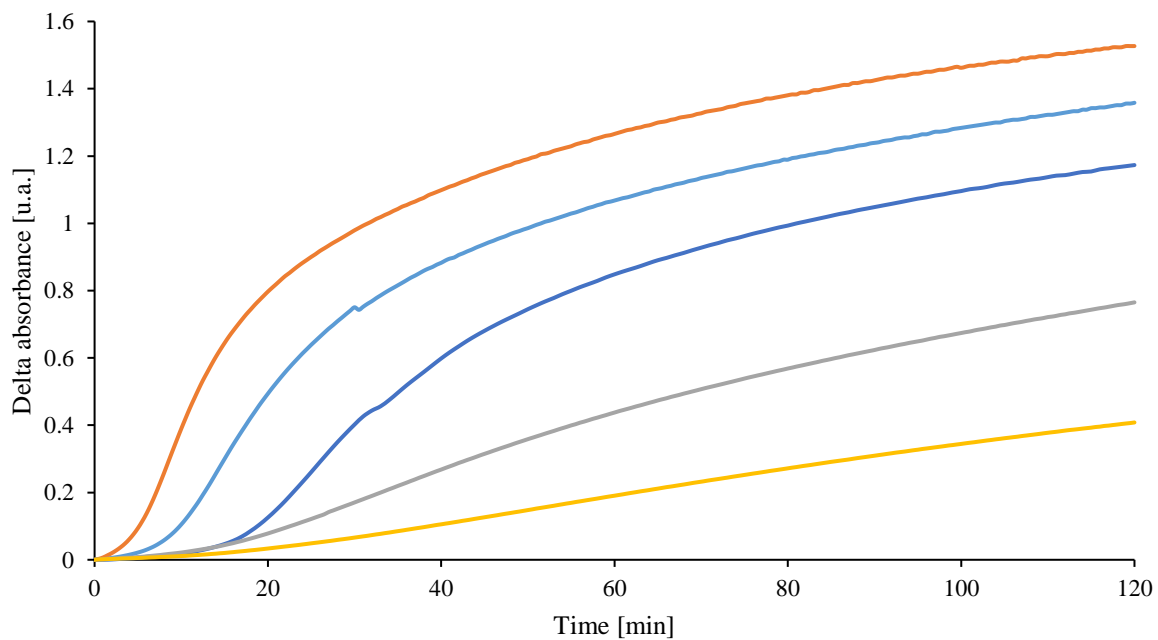


Figure S45 : Evolution of the absorbance of paranitrophenolate at 400 nm as a function of time over 2 hours with various concentration of compound 4 or H_2O_2 . Initial conditions: 10

mM phosphate buffer pH 7.5; [catalyst]= 50 μ M; [PNPG]= 10 mM and $[\text{H}_2\text{O}_2]$ = 40 mM, temperature = r.t. Light blue: [4]= 100 μ M, orange: $[\text{H}_2\text{O}_2]$ = 80 mM, grey: $[\text{H}_2\text{O}_2]$ = 40 mM, yellow: $[\text{H}_2\text{O}_2]$ = 20 mM.

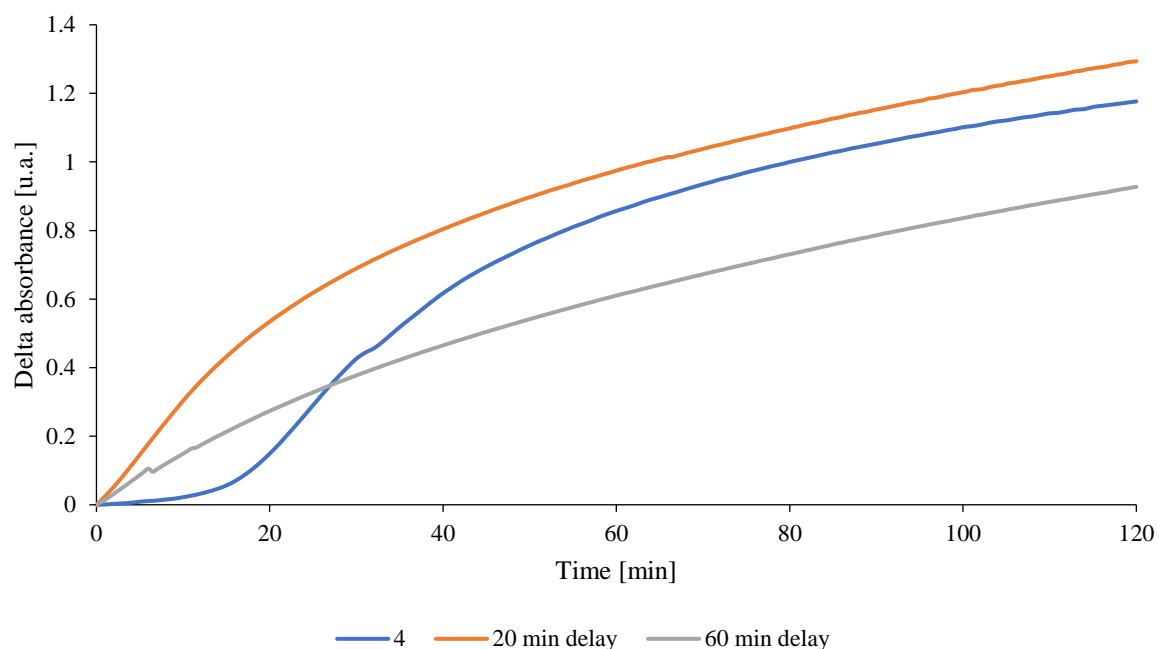


Figure S46: Evolution of the absorbance of paranitrophenolate at 400 nm as a function of time over 2 hours. The substrate was added as described in section 7.1 [blue], after a 20-minute [Orange] or a 60-minute [grey] incubation of compound 4 with H_2O_2 .

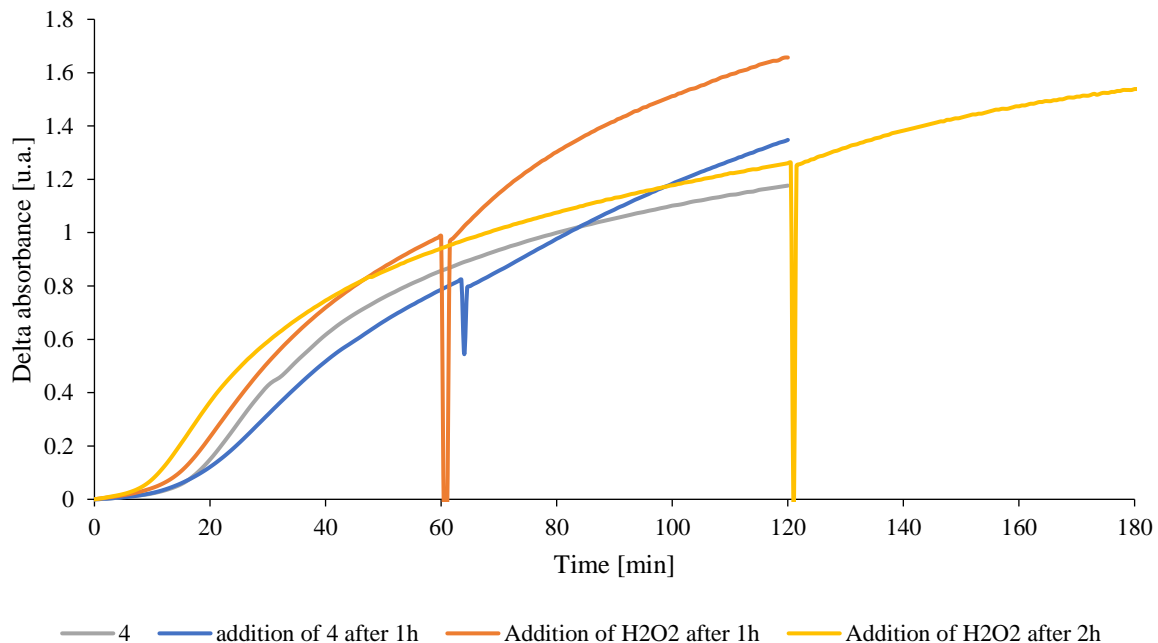


Figure S47: Evolution of the absorbance of paranitrophenolate at 400 nm as a function of time over 2 hours. Addition of another equivalent of compound 4 after 1 hour, (Blue) or H₂O₂ after 1 hour (Orange) or 2 hours (Yellow). Initial conditions (Grey): 10 mM phosphate buffer pH 7.5; [catalyst]= 50 μ M; [PNPG]= 10 mM and [H₂O₂]= 40 mM, temperature = r.t. Note: the variations in the first hour between the assays are explained by the accumulation of experimental errors and temperature variations.

7.2) Reactivity test of catalytic oxidation cleavage of 4-nitrophenol (PNP)

The following solutions were prepared:

- Phosphate buffer (80 mM, pH = 7.5): K₂HPO₄.3H₂O (15.340 g, 0.0672 mol) and NaH₂PO₄ (1.534 g, 0.0128 mol) were dissolved in distilled water to reach 1 L. before each use a volume of this stock solution as diluted 8 times to reach a concentration of 10 mM.
- Catalyst solution (0.1 mM): Each copper compound (2.5 μ mol) was dissolved in the buffer solution to reach 25 mL.
- H₂O₂ solution (400 mM): The commercial 35% (wt%) hydrogen peroxide aqueous solution was regularly titrated using a known concentration of potassium permanganate in acid conditions. The corresponding volume of peroxide was each time diluted in the buffer solution to reach 2 mL.
- Substrate solution, PNP (100 mM): PNP (0.010 g) was dissolved in the buffer solution to reach 1 mL.

The reactivity tests were performed as follow: a 1 mL UV quartz cuvette was charged, thanks to micropipettes, with 500 μ L of the catalyst solution, 100 μ L of the PNP solution, the total volume was brought to 0.9 mL with buffer. The assay was started with the addition of 100 μ L of the H₂O₂ solution. Reference tests were performed without catalyst or H₂O₂ in all cases the total volume was brought to 1 mL with buffer. The reaction mixtures were manually stirred prior to each measurement to prevent the formation of gas bubbles in the cuvette. Quantification of the substrate (4-nitorophenolate) was performed by measuring the absorbance at 400 nm ($\varepsilon = 1.85 \times 10^4 \text{ M}^{-1} \cdot \text{cm}^{-1}$) over 2 hours. The assays were performed at room temperature (18 °C – 25 °C) protected from light, and using fresh PNP solution for each measurement.

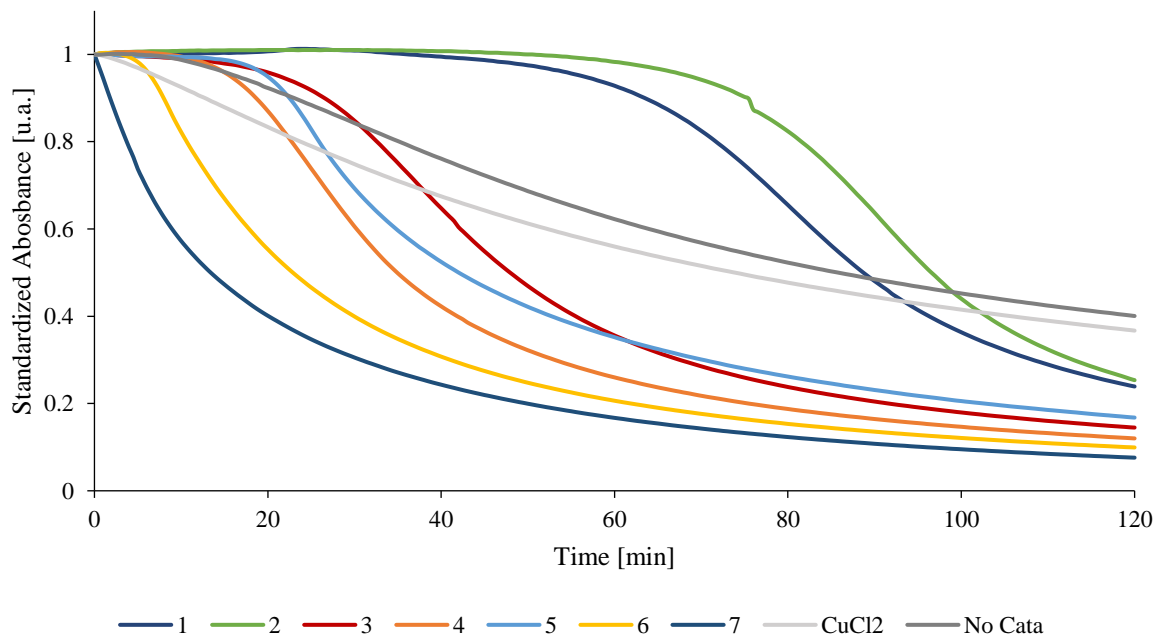


Figure S48: Evolution of the absorbance of paranitrophenolate at 400 nm as a function of time over 2 hours. Conditions: 10 mM phosphate buffer pH 7.5; [catalyst] = 50 μ M; [PNP] = 72 μ M and [H₂O₂] = 40 mM, temperature = r.t.

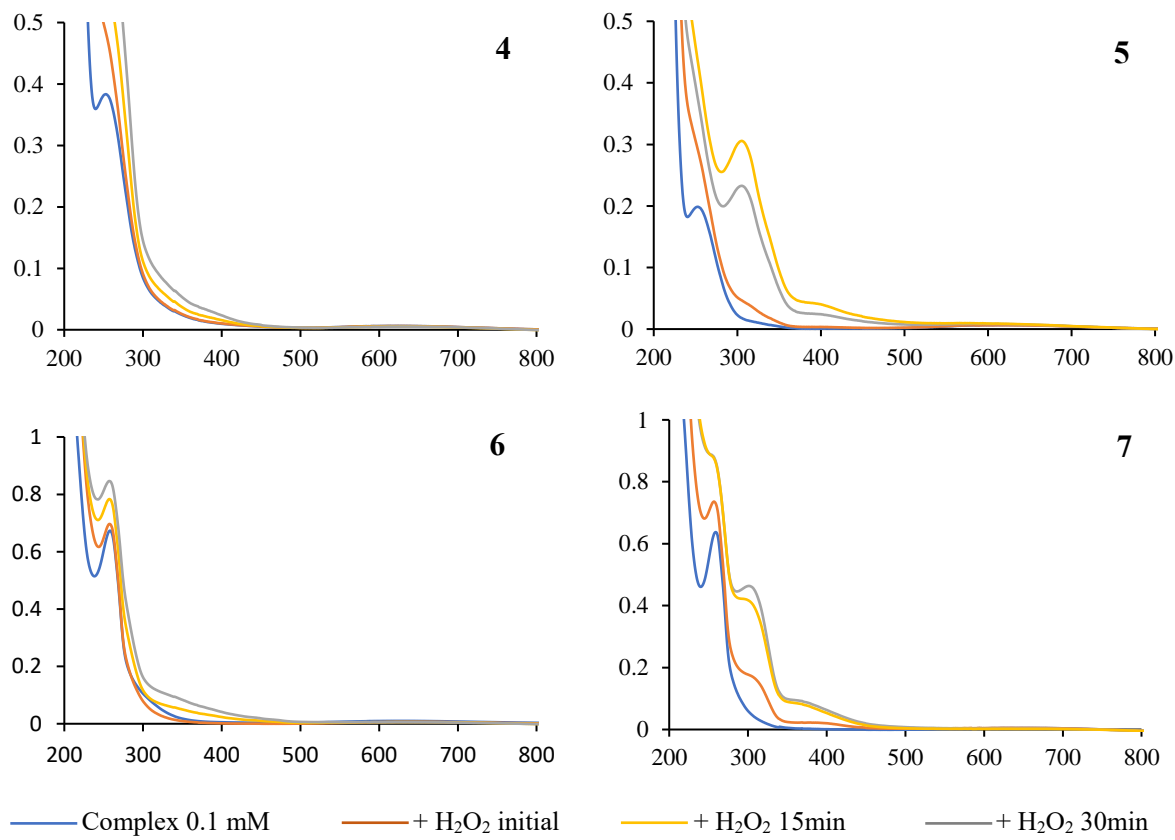


Figure S49: Evolution of the absorption spectra of compounds **4** – **7** after addition of 10 equivalents of H_2O_2 . Conditions: 10 mM phosphate buffer pH 7.5; [Complex] = 0.1 mM; and $[\text{H}_2\text{O}_2] = 1 \text{ mM}$, temperature = r.t.

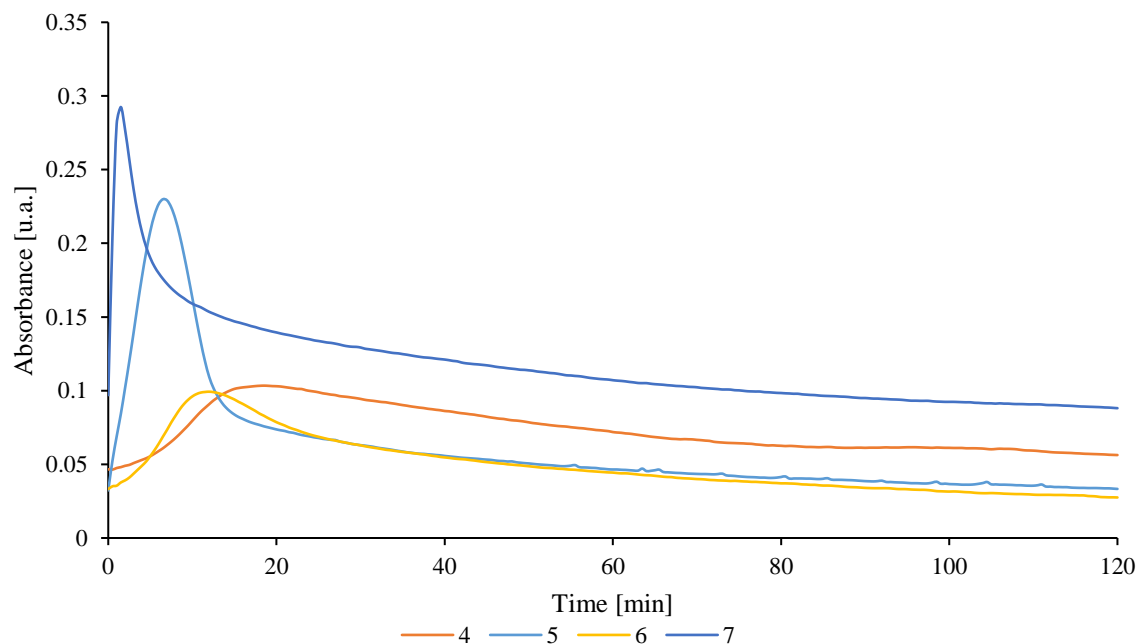


Figure S50: Evolution of the absorbance at 305 nm as a function of time over 2 hours of complexes **4** – **7** after addition of 800 equivalents H_2O_2 .

7.3) Radical trap experiments

The following solutions were prepared:

- Phosphate buffer (80 mM, pH = 7.5): $K_2HPO_4 \cdot 3H_2O$ (15.340 g, 0.0672 mol) and NaH_2PO_4 (1.534 g, 0.0128 mol) were dissolved in distilled water to reach 0.1 L. before each use a volume of this stock solution as diluted 8 times to reach a concentration of 10 mM.
- Catalyst solution (0.1 mM): Each copper compound (2.5 μ mol) was dissolved in the buffer solution to reach 25 mL.
- H_2O_2 solution (400 mM): The commercial 35% (wt%) hydrogen peroxide aqueous solution was regularly titrated using a known concentration of potassium permanganate in acid conditions. The corresponding volume of peroxide was each time diluted in the buffer solution to reach 2 mL.
- Coumarin-3-carboxylic acid (CCA) solution, (5 mM): CCA (0.0119 g, 0.125 mmol) was dissolved in the buffer solution to reach 25 mL.

The hydroxy radical trap experiments were performed as follow: a 4 mL fluorimetry quartz cuvette was charged, thanks to micropipettes, with 2 mL of the catalyst solution, 800 μ L of buffer, 800 μ L of the CCA solution. The experiment was started with the addition of 400 μ L of the H_2O_2 solution. Reference tests were performed without catalyst in all cases the total volume was brought to 4 mL with buffer. For each assay the following fluorimetry parameters were used; Excitation wavelength: 495 nm, Emission wavelength measured: 410-550 nm, Emission slit: 2.5 nm, Absorption slit: 5 nm. The assays were performed at room temperature (20 °C – 25 °C) protected from light.

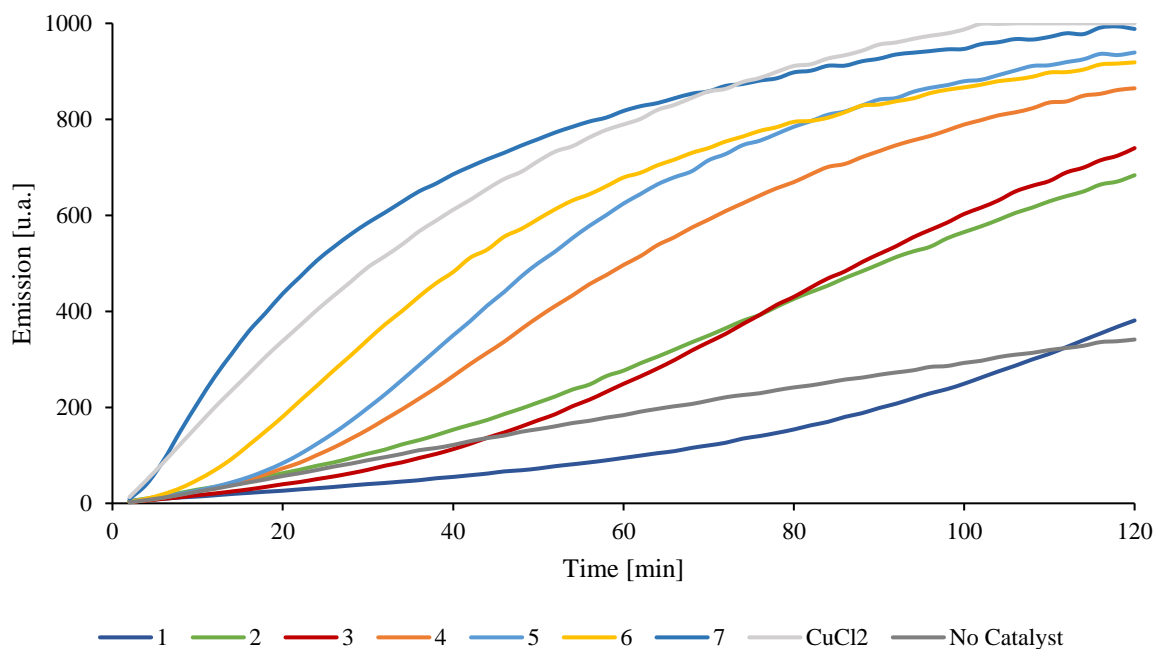


Figure S51: Evolution of the emission of 7-hydroxyCoumarin-3carboxylic acid at 447 nm as a function of time over 2 hours. Conditions: 10 mM phosphate buffer pH 7.5; [catalyst]= 50 μ M; [CCA]= 0.5 mM and $[\text{H}_2\text{O}_2]$ = 40 mM, temperature = r.t.

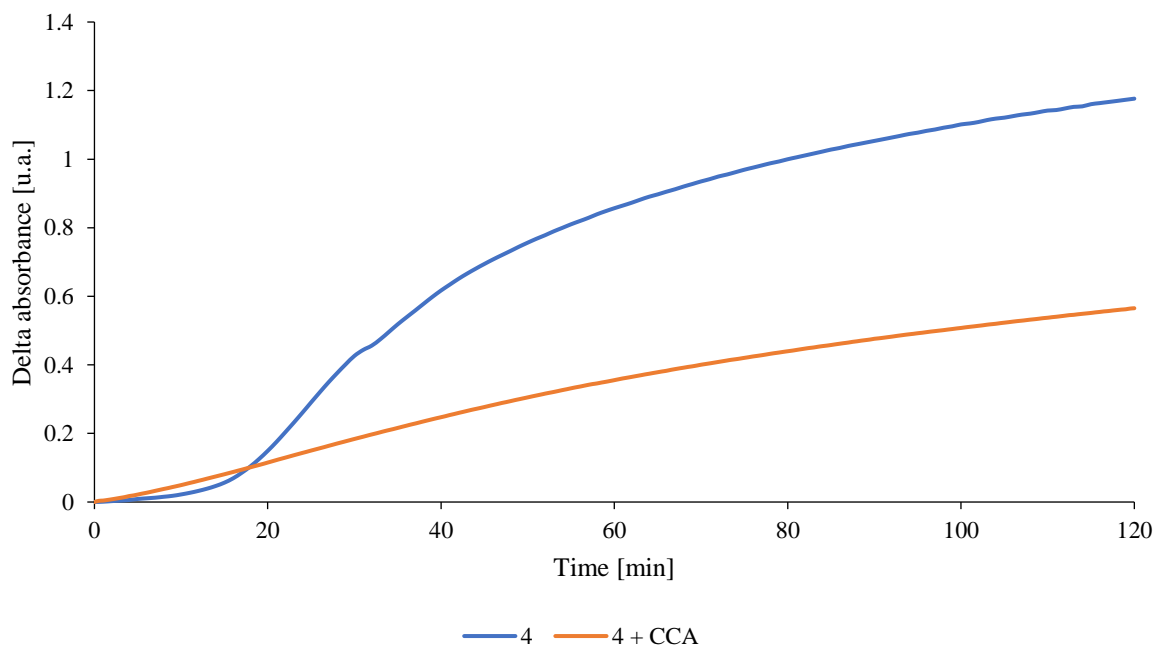


Figure S52: Evolution of the absorbance of paranitrophenolate at 400 nm as a function of time over 2 hours for compound 4 without (blue) and with CCA (orange) as radical trap. Conditions: 10 mM phosphate buffer pH 7.5; [catalyst]= 50 μ M; [PNPG]= 10 mM; [CCA]= 2.5 mM and $[\text{H}_2\text{O}_2]$ = 40 mM, temperature = r.t.

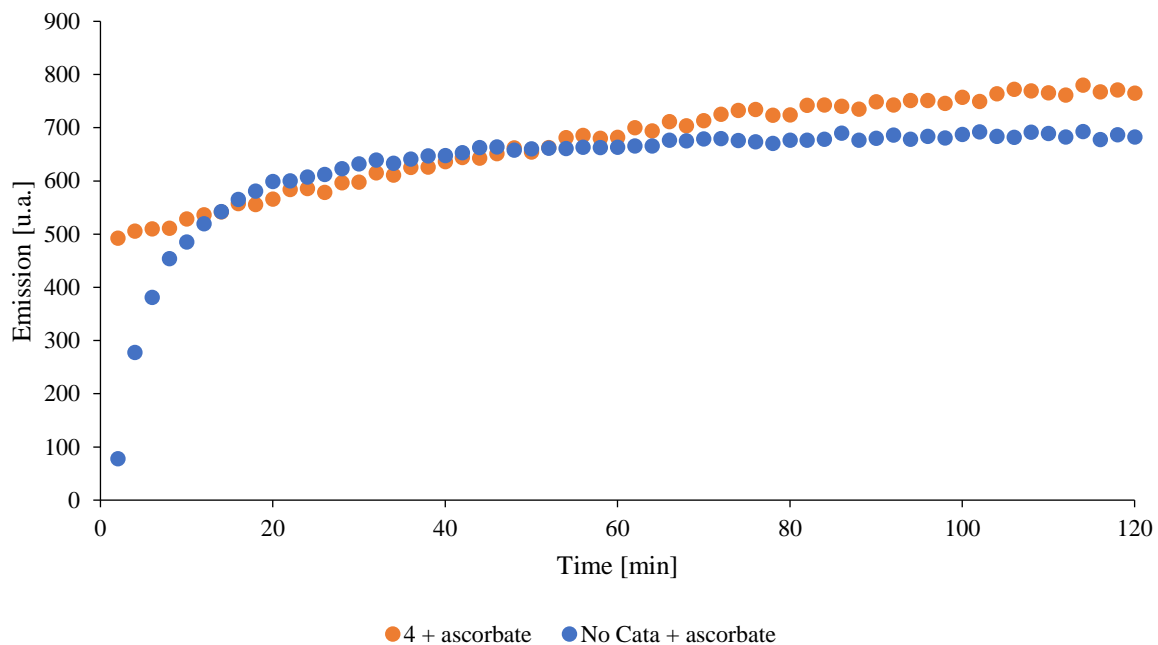


Figure S53 : Evolution of the emission of 7-hydroxyCoumarin-3carboxylic acid at 447 nm as a function of time over 1 hour without catalyst and with sodium ascorbate. Conditions: 10 mM phosphate buffer pH 7.5; [CCA]= 0.5 mM, [Ascorbate]= 1 mM, [catalyst]= 50 μ M and [H₂O₂]= 40 mM, temperature = r.t.

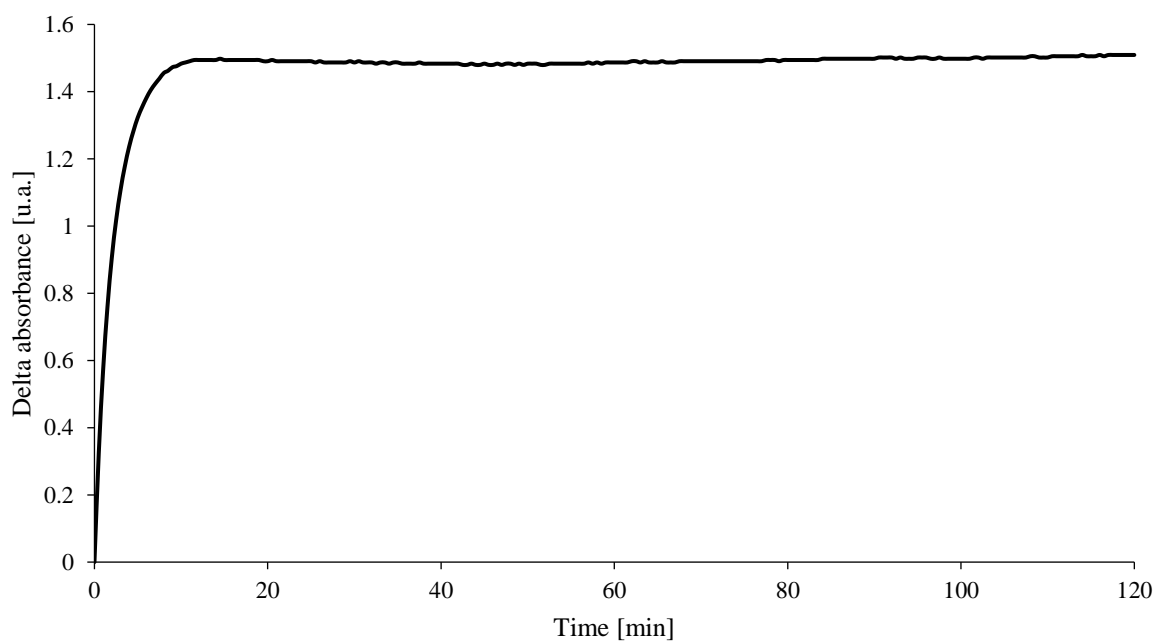


Figure S54 : Evolution of the absorbance of paranitrophenolate at 400 nm as a function of time over 2 hours without catalyst and with sodium ascorbate. Conditions: 10 mM phosphate buffer pH 7.5; [CCA]= 0.5 mM, [Ascorbate]= 1 mM and [H₂O₂]= 40 mM, temperature = r.t.

8) Computational Studies

Computations have been carried out using the Jaguar 8.5 pseudospectral program package 8 (Jaguar 8.5, Schrodinger, Inc., New York, NY, 2014). All species have been fully geometry optimized, and the Cartesian coordinates are given in the annex. Density Functional Theory (DFT) was applied by the means of the B3LYP functional^{8,9} corrected for dispersion as proposed by Grimme (D3 correction)¹⁰. The LACV3P basis set as implemented in Jaguar was used for the copper atom and the standard split valence polarized 6-31+G(d) basis set¹¹ was used for all other atoms. Electronic energies were obtained after corresponding fully analytical single point calculations, at the BP86/6-31+G(d) level of theory. Thermal and entropic contributions to free energy (at 298.15 K) and zero-point energy have been obtained by performing frequency calculations at the B3LYP-D3/6-31+G(d) level of theory.

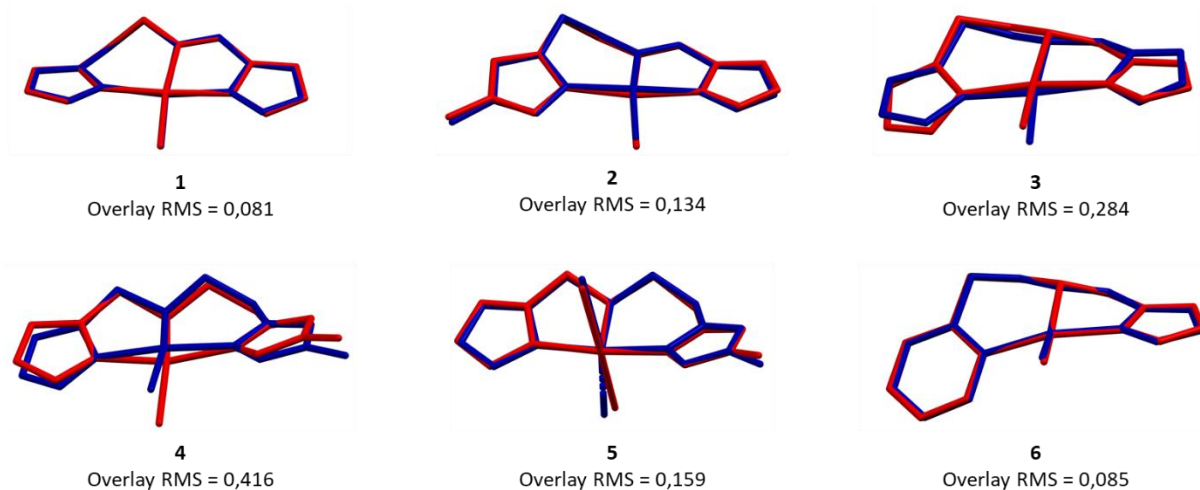


Figure S55: Overlay of the X-ray diffraction crystallography structure (Blue) and the DFT geometry optimization (red) for compounds **1-6**.

Complex 1

$E(\text{B3LYP-d3/6-31+G}^*) = -1279.7284 \text{ Ha}$

Solvent = methanol

Cu1 -0.9696006373 2.6163715215 5.7766344641
 Cl2 0.0615620860 0.5581207053 6.0728913009
 N3 -1.1668936951 2.9033624477 7.7799827262
 C4 -0.8740813599 2.3288055983 8.9359078154
 H5 -0.3852630330 1.3723170512 9.0697074741
 N6 -1.2894210899 3.1198591673 9.9620167540

H7 -1.1865028217 2.8999148815 10.9544974017
 C8 -1.8712237982 4.2528281955 9.4429863257
 H9 -2.2812582348 5.0377788819 10.0669498284
 C10 -1.7907439756 4.1096959009 8.071679831
 C11 -2.1910907619 4.9150775859 6.9372530786
 H12 -2.6921654736 5.8774018272 7.0824785013
 N13 -1.9341184987 4.4412187994 5.7646276588
 C14 -2.3269948751 5.1523344609 4.5449659673
 H15 -2.5721958652 6.1965510995 4.7784147589
 H16 -3.2298956579 4.6657217148 4.1538800112
 C17 -1.2075155617 5.0948277507 3.4902321927
 H18 -1.4777498784 5.7603567842 2.6623412328
 H19 -0.2853397588 5.4962065698 3.9343622920

C20 -0.9626971690 3.7166494724 2.9454621234
 N21 -0.8052614029 2.6014211442 3.7675871013
 C22 -0.5815064254 1.5532055182 2.9683256803
 H23 -0.4156506638 0.5363518242 3.2924355423
 N24 -0.5849845189 1.9464756835 1.6802633514
 H25 -0.4353204625 1.3362626188 0.8761935265
 C26 -0.8259220882 3.3086750535 1.6398563187
 H27 -0.8703071419 3.8612322819 0.7100054504

Complex 2

E(B3LYP-d3/6-31+G*) = -1319.0402 Ha

Solvent = methanol

Cu1 4.0657823861 2.4674112151 6.2550382707
 Cl2 5.0027608761 0.3545075142 6.5105011373
 N3 3.9995960102 2.2882327323 4.2387896938
 C4 4.3649469089 1.4660515836 3.2684561256
 H5 4.8741615529 0.5185820487 3.3909123647
 N6 4.0064786753 1.9877805751 2.0643690428
 H7 4.1742211315 1.5472140754 1.1578032792
 C8 3.3842466370 3.1970842592 2.2708167941
 H9 3.0048619823 3.8051806897 1.4585611715
 C10 3.3837337952 3.3796563142 3.6393864741
 C11 2.8926896306 4.4084255918 4.5325606676
 H12 2.3873417172 5.2976689640 4.1421982413
 N13 3.0738320201 4.2174230979 5.7956562427
 C14 2.5963775221 5.1743588612 6.7967728623
 H15 1.7071098768 4.7404493119 7.2727011888
 H16 2.3062261408 6.1168117958 6.3146937347
 C17 3.6761277125 5.4368148990 7.8600728195
 H18 4.5898199606 5.7862114080 7.3581913679
 C19 3.9790136899 4.2413333638 8.7152057062
 N20 4.1855645686 2.9662313811 8.1944357542
 C21 4.4499804886 2.1627188670 9.2308398193
 H22 4.6584349513 1.1040541701 9.1703331766
 N23 4.4242685938 2.8569272913 10.3841376736
 C24 4.1252686505 4.1742152093 10.0795451786
 H25 4.0502405859 4.9363615413 10.8459915956
 C26 4.6855679816 2.3246354751 11.7253340065
 H27 4.8518467053 1.2465814253 11.6528469810
 H28 3.8232649145 2.5183172506 12.3713890468
 H29 3.3350758005 6.2542735757 8.5061018241
 H30 5.5765333493 2.8042257803 12.1436916225

Complex 3

E(B3LYP-d3/6-31+G*) = -1280.9463 Ha

Solvent = methanol

Cu1 2.3096684824 12.3761581681 8.5633282475
 Cl2 1.9333329246 14.6814486626 8.6795669179
 N3 2.4946695804 12.1380063023 10.5453877118
 C4 2.8902936443 13.0617017024 11.4272616347

H5 3.1093779715 14.0958164061 11.2028098205
 N6 2.9820849842 12.5163687099 12.6554679421
 H7 3.2614177564 13.0127488829 13.5025968807
 C8 2.6338564402 11.1795357223 12.5670423710
 C9 2.3268218791 10.9463868989 11.2476441050
 C10 1.8740761204 9.6772479921 10.5866352790
 H11 2.0316981337 8.8419914566 11.2796032163
 H12 0.7923797620 9.7122756411 10.3834350484
 C13 2.6199982711 9.3676677828 9.2829844977
 H14 2.4130528253 8.3340162696 8.9732888830
 H15 3.7009784078 9.4693236597 9.4286167924
 N16 2.2265084898 10.2926190899 8.1856718243
 H17 1.2275327587 10.1466846542 7.9855531444
 C18 2.9924762439 10.0202082269 6.9312535398
 H19 4.0508910369 9.9423280638 7.2115683109
 H20 2.6906962510 9.0631766367 6.4862524900
 C21 2.7922242373 11.1742618436 5.9965802877
 N22 2.5201626025 12.4055516769 6.5693137218
 C23 2.4391715997 13.2958292758 5.5798741035
 H24 2.2259120996 14.3505185559 5.6888550881
 N25 2.6609610416 12.6785774063 4.3998532144
 H26 2.6606956327 13.1346514470 3.4863477402
 C27 2.8817974584 11.3302862721 4.6356348938
 H28 3.0959603781 10.6304241154 3.8374201956
 H29 2.6292524381 10.5251181491 13.4292935091

Complex 4

E(B3LYP-d3/6-31+G*) = -1320.2580 Ha

Solvent = methanol

Cu1 5.3181741291 4.4522203440 5.2121528427
 Cl2 5.1853076532 6.5512288282 6.2414155758
 N3 6.2803271441 5.1760306365 3.6195385129
 C4 6.7053205526 6.3575371691 3.1717060488
 H5 6.5904522775 7.3068403762 3.6761878750
 N6 7.3097366478 6.1936832623 1.9758937117
 H7 7.7234053962 6.9410262842 1.4175334995
 C8 7.2648717181 4.8510497327 1.6327604438
 H9 7.6919326308 4.4736317820 0.7125402521
 C10 6.6206968101 4.2258355420 2.6712497029
 C11 6.2993453030 2.7972800125 2.9923114996
 H12 6.0841428493 2.2041524341 2.0946656593
 H13 7.1473876328 2.3308748386 3.5096923940
 N14 5.1434981373 2.7714716520 3.9400706449
 H15 4.2889427475 2.9806354074 3.4066129720
 C16 4.9791774307 1.4319870906 4.5694663585
 H17 5.9323890058 1.1698671775 5.0405789459
 H18 4.7687025781 0.6903888203 3.7874737739
 C19 3.8553053344 1.4234980286 5.6136156380
 H20 2.9414321060 1.8448621993 5.1687059781
 H21 3.6273228201 0.3821626579 5.8692423461
 C22 4.2199643913 2.1630263758 6.8656424979
 N23 4.7803901609 3.4354297390 6.8393800417
 C24 4.9841936105 3.7985972739 8.1103013670
 H25 5.4123908752 4.7353489315 8.4383301919

N26 4.5860406048 2.8214574537 8.9467328733
 C27 4.0998267507 1.7763132092 8.1780719149
 H28 3.7176771735 0.8671690176 8.6255979796
 C29 4.6535918321 2.8518552833 10.4112751077
 H30 5.0687396134 3.8125537914 10.7261905936
 H31 5.2973136298 2.0414545499 10.7679776532
 H32 3.6475822020 2.7362422274 10.8269407242

Complex 5 (Cl as counter ion)

E(B3LYP-d3/6-31+G*) = -1320.2573 Ha

Solvent = methanol

Cu1 6.1326616525 6.0719871282 13.0485871996
 N2 5.9621543613 7.9706780869 12.4692825342
 C3 5.9795883822 8.6924110386 11.2866421698
 H4 6.1809717591 8.2155533217 10.3375210462
 C5 5.7135820122 10.0061563551 11.5779547610
 H6 5.6380089505 10.8828742088 10.9481331516
 N7 5.5384219433 10.0713593636 12.9542525546
 H8 5.3235610182 10.9131222982 13.4899846538
 C9 5.6936884847 8.8275851956 13.4532149643
 C10 5.5331037111 8.3513378521 14.8598756393
 H11 4.4638746781 8.2464014646 15.0860367341
 H12 5.9688953786 9.0479378384 15.5874181013
 N13 6.1620839194 7.0016515189 14.9550218811
 H14 7.1704847379 7.1337255967 15.1096411555
 C15 5.6101527717 6.2254803625 16.0997700681
 H16 4.5306756051 6.1308771104 15.9394131111
 C17 6.2564441541 4.8410098847 16.2119238107
 C18 5.8216431607 3.8930718350 15.1359652538
 N19 5.8069499837 4.2449356376 13.7904500158
 C20 5.3901831010 3.1695024605 13.1118832594
 H21 5.2704464033 3.1064408193 12.0393438732
 N22 5.1408549911 2.1495512877 13.9554942356
 C23 5.4026804667 2.5896274920 15.2423184138
 H24 5.2793369284 1.9445450750 16.1035938712
 C25 4.6454121045 0.8182606055 13.5903218647
 H26 3.6203317084 0.6915976640 13.9548424360
 H27 5.2919972664 0.0547250301 14.0347495626
 H28 4.6621794665 0.7193717920 12.5019131664
 Cl29 6.6453238450 5.3090010953 10.8993075185
 H30 5.7719930380 6.7894235673 17.0277966877
 H31 7.3518483060 4.9513667590 16.2081471407
 H32 5.9916812845 4.4156713487 17.1870897981

Complex 5 (ClO₄ as counter ion)

E(B3LYP-d3/6-31+G*) = -2497.4063 Ha

Solvent = methanol

Cu1 6.0418555846 6.0332471037 12.9048289409

N2 6.1566118194 7.9449098451 12.2584704249
 C3 6.4353274864 8.6734160051 11.1214967322
 H4 6.7335688789 8.1976195755 10.2019705395
 C5 6.3620511349 10.0051316113 11.4221408179
 H6 6.5317847752 10.8901369313 10.8289592139
 N7 6.0455014929 10.0715607245 12.7711943040
 H8 5.9327069669 10.9165287243 13.3140923047
 C9 5.9315746936 8.8071762506 13.2373414981
 C10 5.6214982712 8.3449711297 14.6248314520
 H11 4.5421892774 8.1925030438 14.7313677218
 H12 5.9577636840 9.0684461209 15.3819981228
 N13 6.2701553454 7.0280158448 14.7812741152
 H14 7.2878930459 7.1431472152 14.7659520337
 C15 5.8616784425 6.3045268085 16.0027807474
 H16 4.7769095288 6.1702195562 15.9590432792
 C17 6.5586126357 4.9370790611 16.0758229866
 C18 6.0076024480 3.9581731166 15.0876601177
 N19 5.8885623840 4.2572460097 13.7423884247
 C20 5.3357639022 3.2080746088 13.1509327350
 H21 5.0791494233 3.1508836071 12.1068514036
 N22 5.0928306622 2.2352713721 14.0506291366
 C23 5.5110158097 2.6973985831 15.2875514380
 H24 5.4071269692 2.1027062104 16.1826693733
 C25 4.3691450662 0.9974801637 13.7955719720
 H26 3.3690711614 1.0548248800 14.2358197916
 H27 4.9159038354 0.1505773145 14.2194683827
 H28 4.2742444726 0.8592669627 12.7168631705
 O29 6.1734908662 5.2047227394 11.0220975121
 H30 7.0573707237 5.5285797767 10.7134721501
 C31 5.1299770913 5.5099465200 10.0734064161
 H32 5.0322536928 6.5902792658 9.9315447601
 H33 4.2026445707 5.1255887142 10.4988357128
 H34 5.3510835955 5.0187707675 9.1201856548
 Cl35 2.7099612730 5.4911138055 13.3400434329
 O36 1.3961910575 6.1774420338 13.3290512666
 O37 3.0246125556 4.9389407715 14.6976455649
 O38 2.7565901156 4.3940600411 12.3164043484
 O39 3.7978276258 6.5158576643 12.9802870991
 O40 8.3769881391 5.8524966457 13.0560934700
 O41 9.2237871834 8.0727891397 12.4356540645
 O42 8.5984351294 6.4525264483 10.6879981442
 Cl43 9.2400520185 6.6290311306 12.0602953233
 O44 10.6116838697 6.0797630023 12.0542480371
 H45 6.1140038306 6.9004989127 16.8931202546
 H46 6.4310128931 4.5325235471 17.0855015331
 H47 7.6390204704 5.0686021197 15.9182748399

Complex 6

E(B3LYP-d3/6-31+G*) = -1303.0014 Ha

Solvent = methanol

Cu1 3.7546713132 5.5834947965 3.6832390367
 Cl2 1.7580437629 4.4263715658 3.9089309119
 N3 3.9824970725 5.8914362152 5.6426235902
 C4 3.4040566567 5.5170200377 6.7833102740

H5 2.5416506816 4.8711864624 6.8775596968
N6 4.0509439250 6.0890984057 7.8209434539
H7 3.8073056561 5.9705031992 8.8045714399
C8 5.0855401700 6.8701735457 7.3287663582
H9 5.7485662693 7.4283267924 7.9768222997
C10 5.0328468047 6.7359147838 5.9639647417
C11 5.8652016840 7.2432767887 4.8232880052
H12 6.6933284986 6.5527613873 4.6196537316
N13 5.0000783380 7.2633103870 3.6062331912
H14 4.3299107298 8.0382267755 3.7038565833
C15 5.7565546546 7.4707320716 2.3466424338
H16 6.5854396717 6.7554339164 2.3279957620
C17 4.8493857217 7.2711648701 1.1232210811
H18 3.8908177692 7.7848061917 1.2888845202

H19 5.3180490391 7.7534105783 0.2590037145
C20 4.6011668109 5.8167308867 0.7934440108
N21 4.1407288615 4.9924832051 1.7694015088
C22 3.9477414666 3.6810111562 1.4935159838
H23 3.5795111167 3.0688824258 2.3087990221
C24 4.1846003437 3.1338240179 0.2363840440
C25 4.8596532507 5.3232919375 -0.4922261135
C26 4.6418647635 3.9753919468 -0.7819515667
H27 4.0047420904 2.0753800092 0.0659321505
H28 5.2220672910 6.0029905022 -1.2595558276
H29 4.8336124829 3.5894425070 -1.7815031377
H30 6.1815935444 8.4827097141 2.3362674222
H31 6.2902413973 8.2352696494 5.0202780266

9) NMR spectra

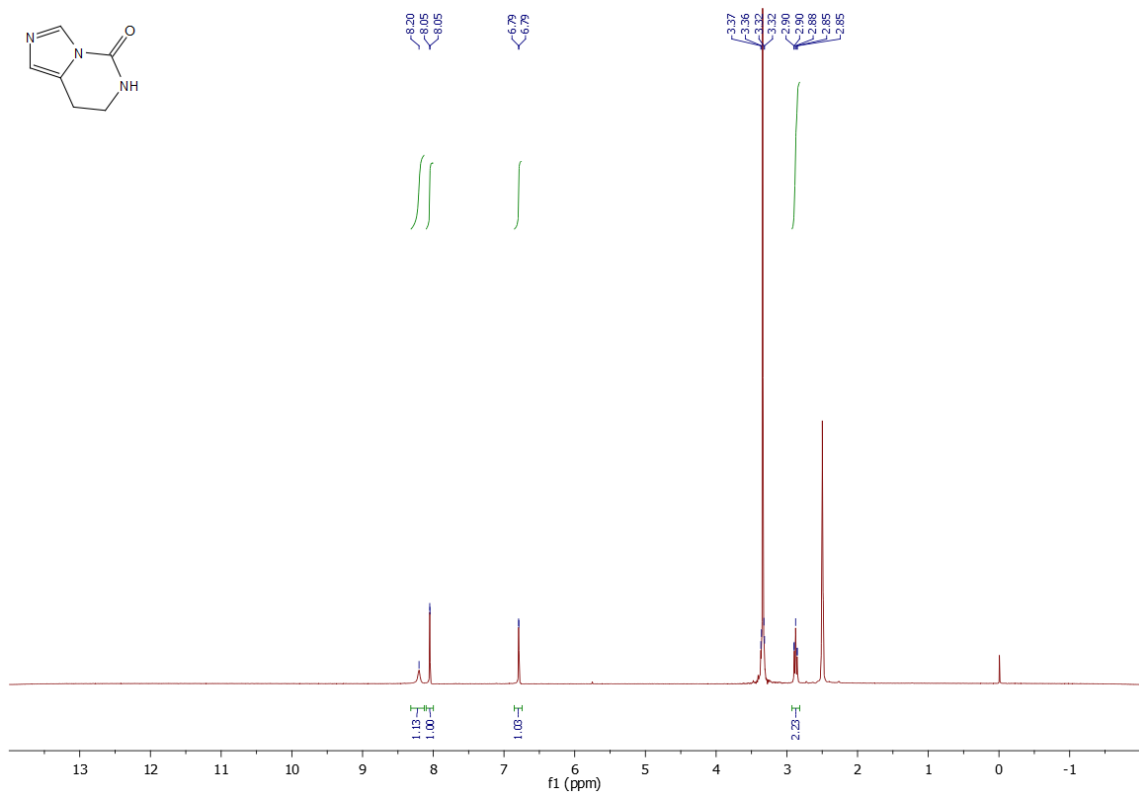


Figure S56: ^1H NMR spectrum of **a1** in $d_6\text{-DMSO}$ at 25°C.

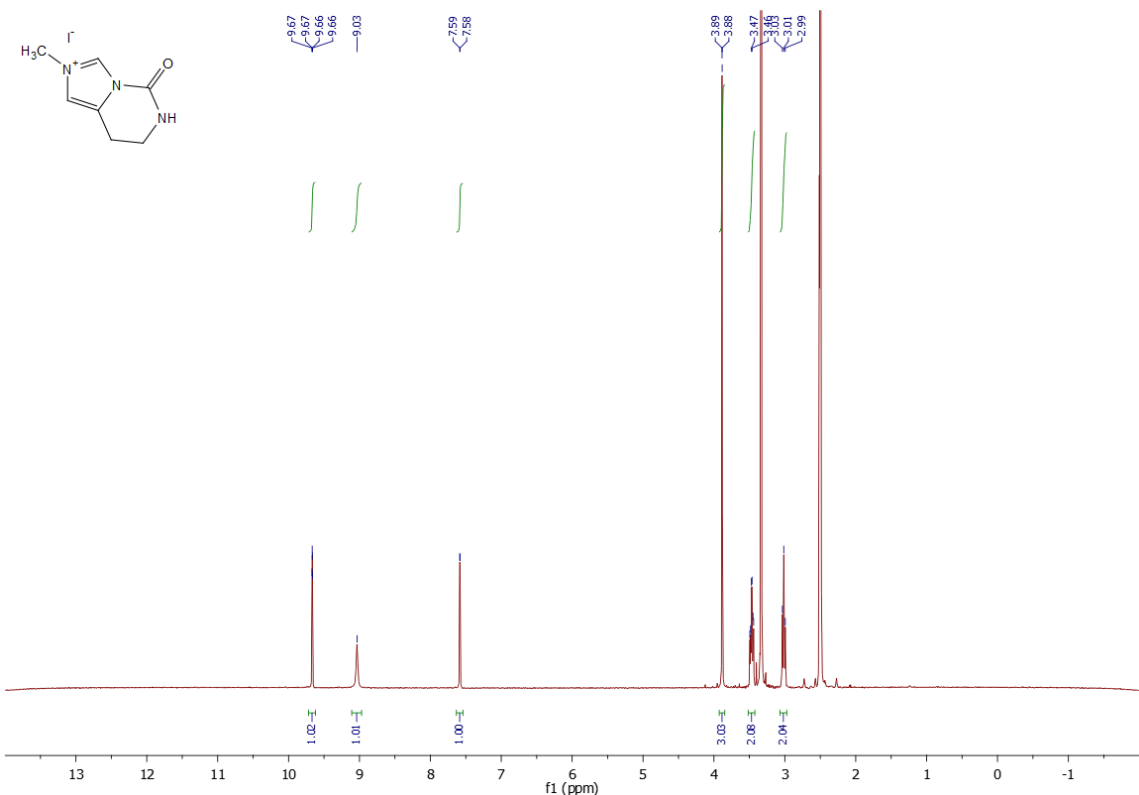


Figure S57: ^1H NMR spectrum of **a2** in $d_6\text{-DMSO}$ at 25°C.

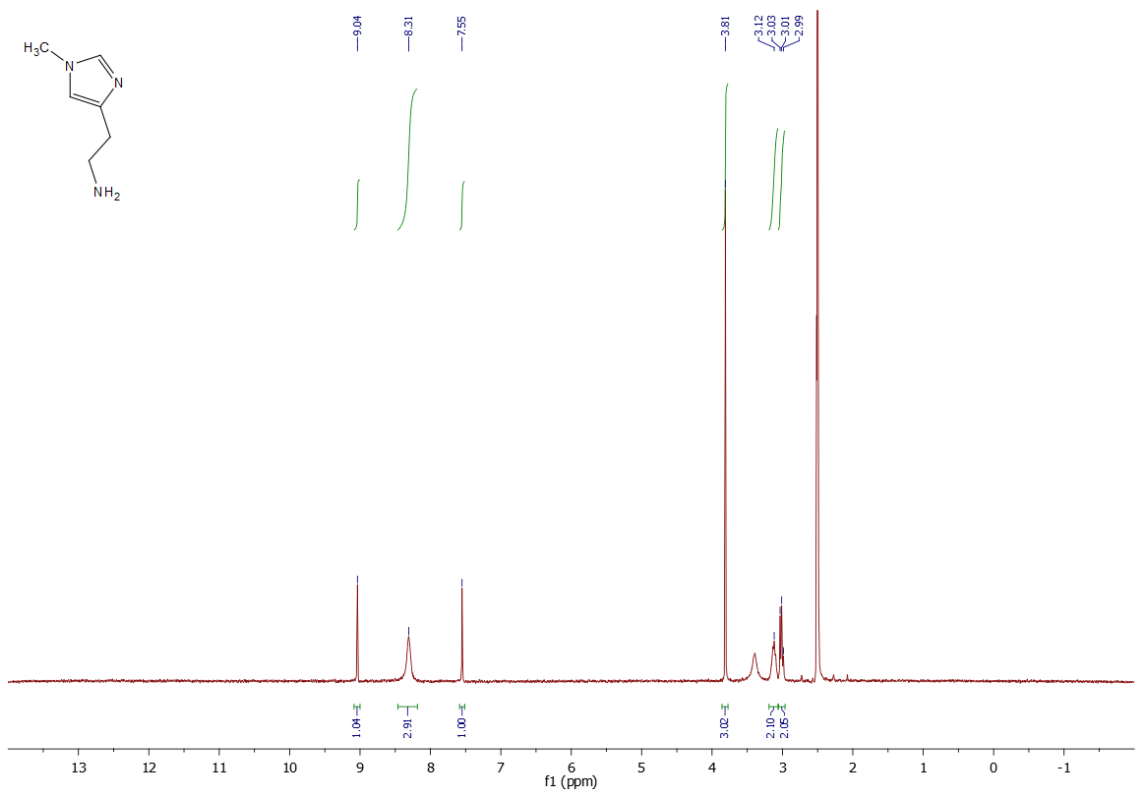


Figure 58: ^1H NMR spectrum of **a3** in d_6 -DMSO at 25°C.

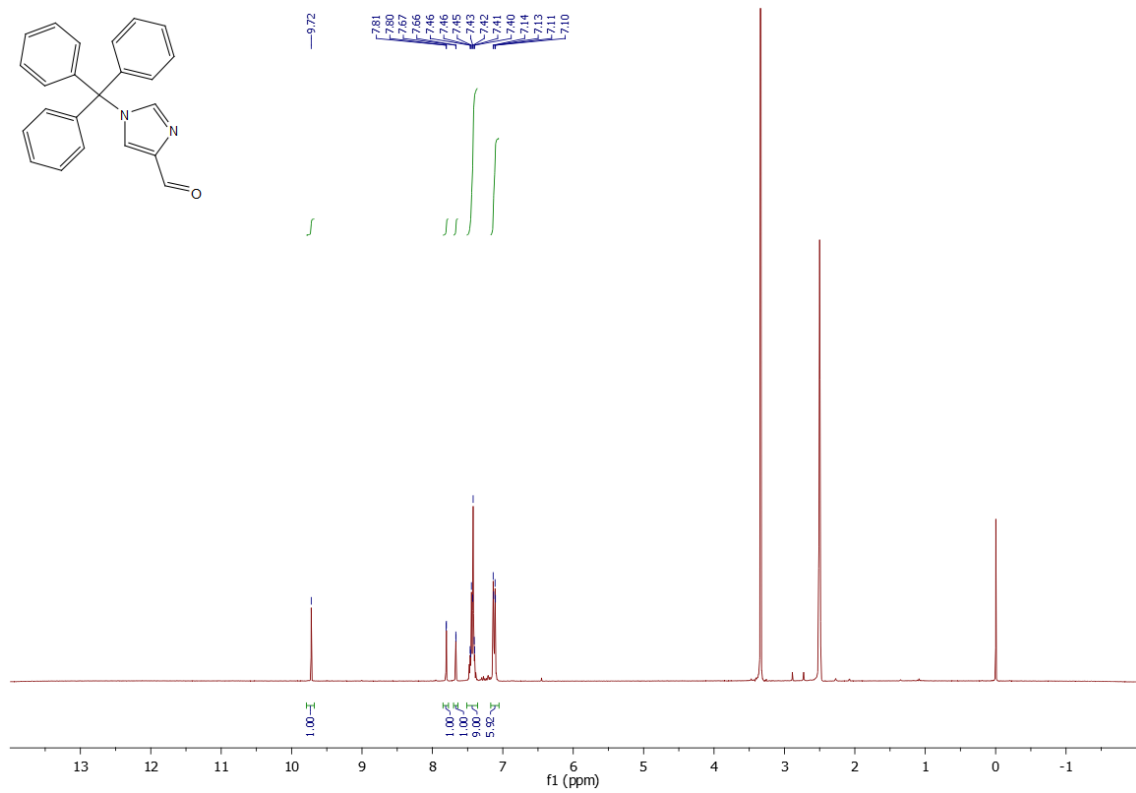


Figure S59: ^1H NMR spectrum of **a4** in d_6 -DMSO at 25°C.

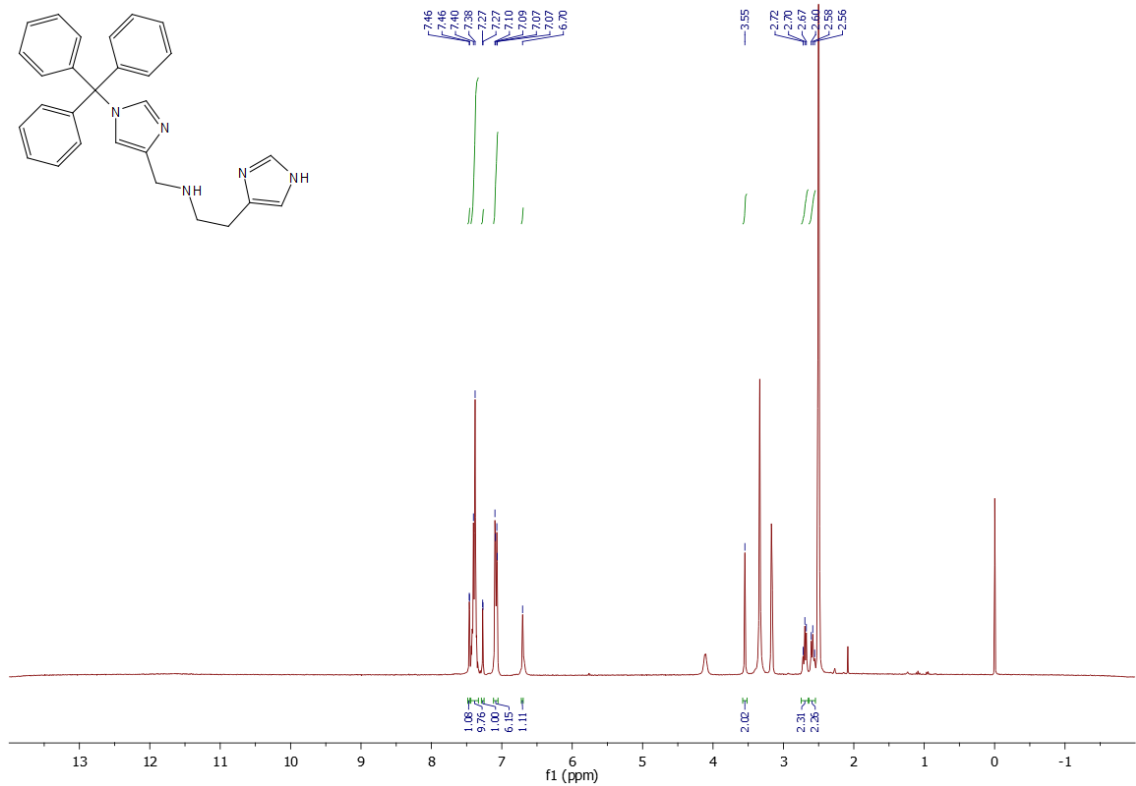


Figure S60: ^1H NMR spectrum of $\mathbf{L3}^{\text{Tr}}$ in $d_6\text{-DMSO}$ at 25°C .

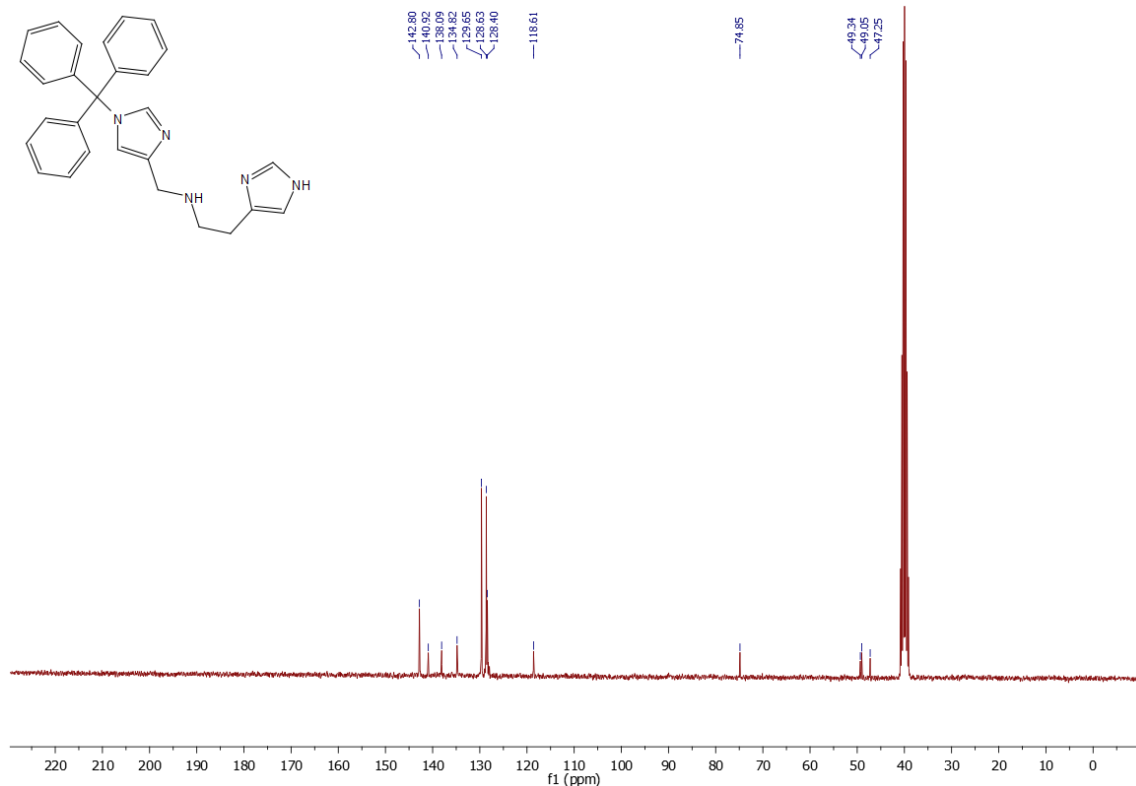


Figure S61: ^{13}C NMR spectrum of $\mathbf{L3}^{\text{Tr}}$ in $d_6\text{-DMSO}$ at 25°C .

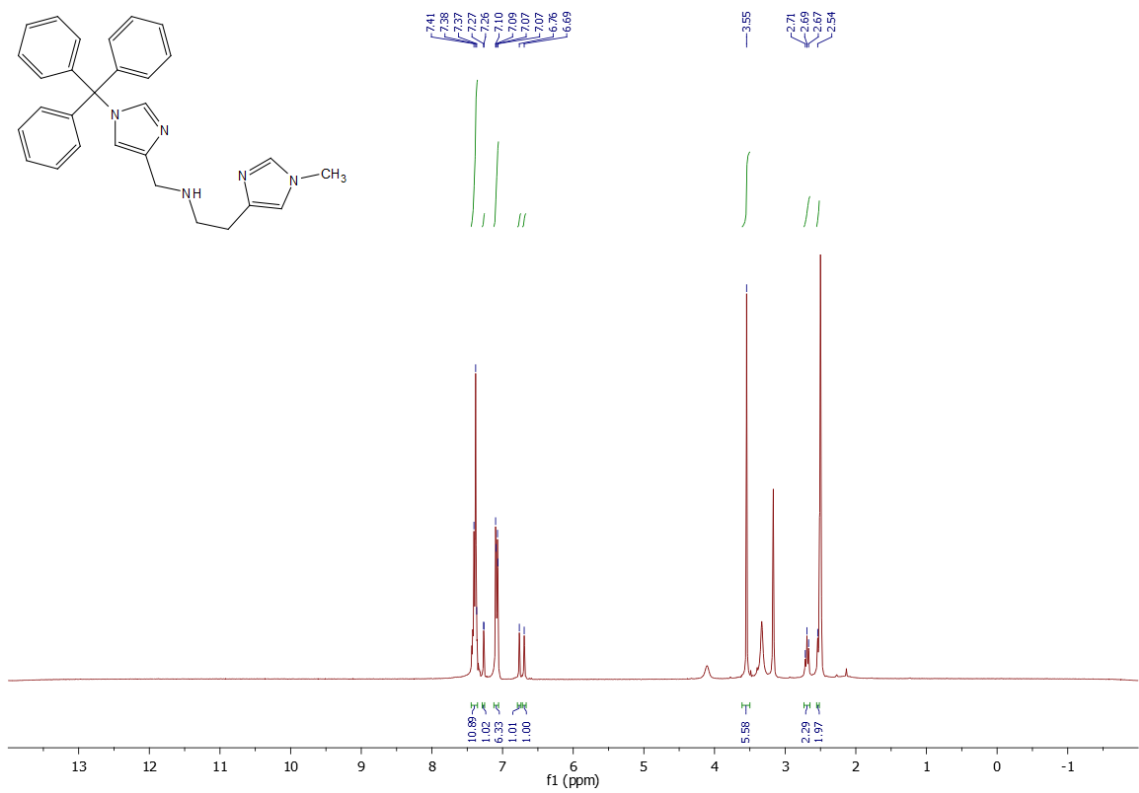


Figure S62: ^1H NMR spectrum of **L4^{Tr}** in d_6 -DMSO at 25°C.

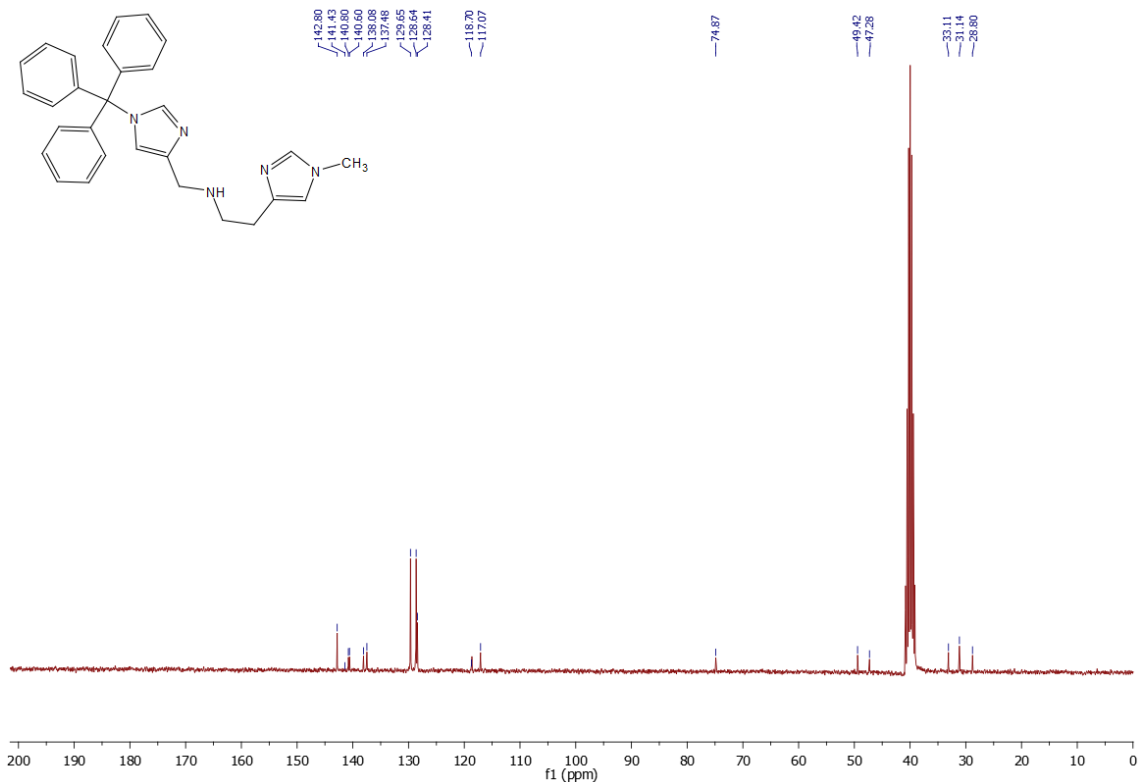


Figure S63: ^{13}C NMR spectrum of **L4^{Tr}** in d_6 -DMSO at 25°C.

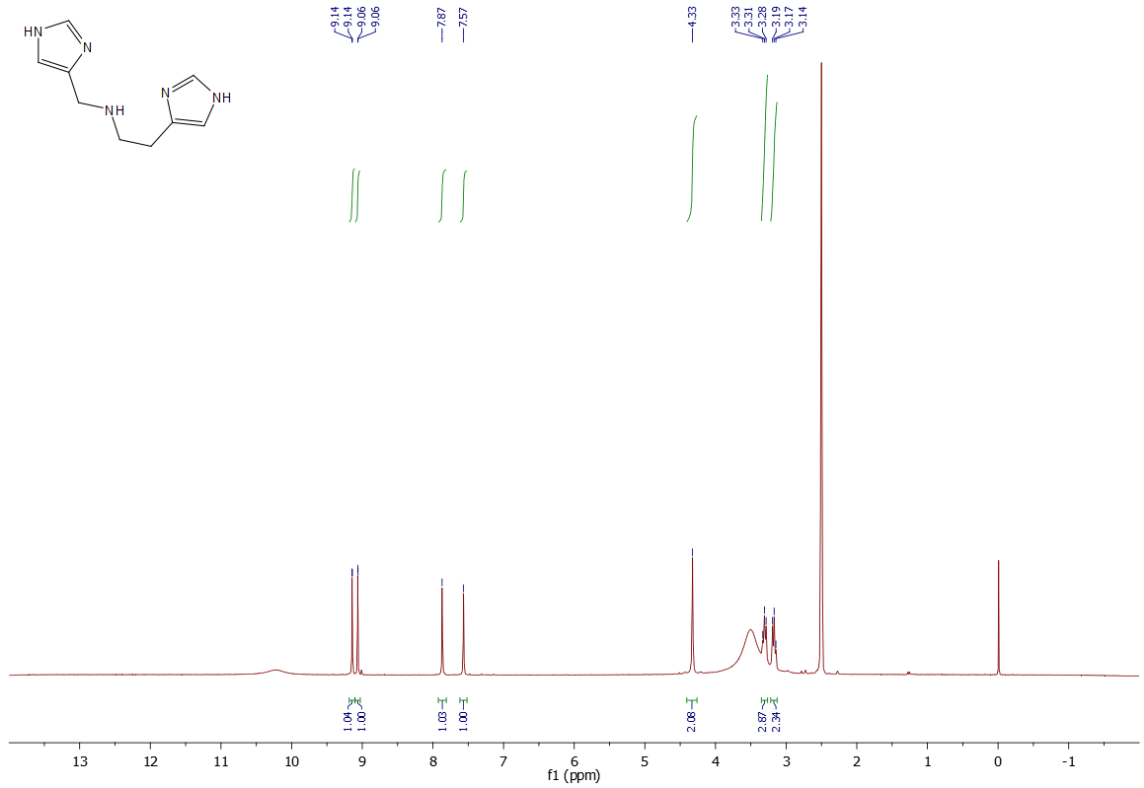


Figure S64: ^1H NMR spectrum of **L3** in d_6 -DMSO at 25°C.

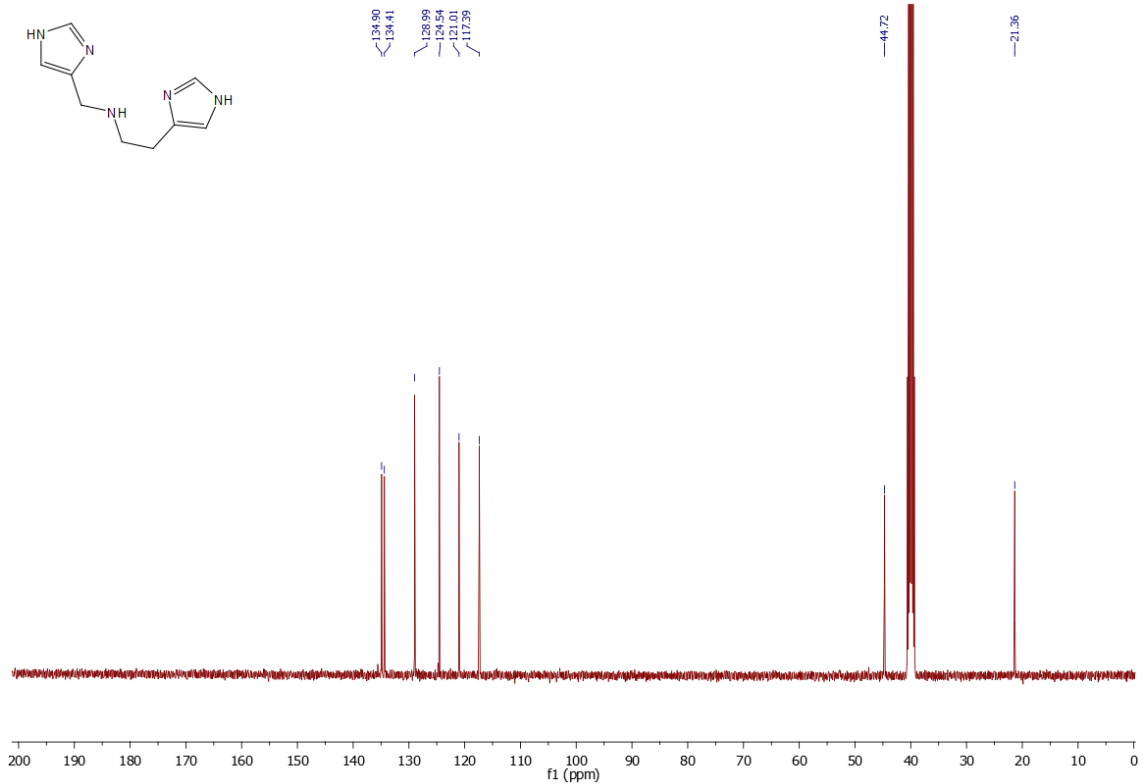


Figure S65: ^{13}C NMR spectrum of **L3** in d_6 -DMSO at 25°C.

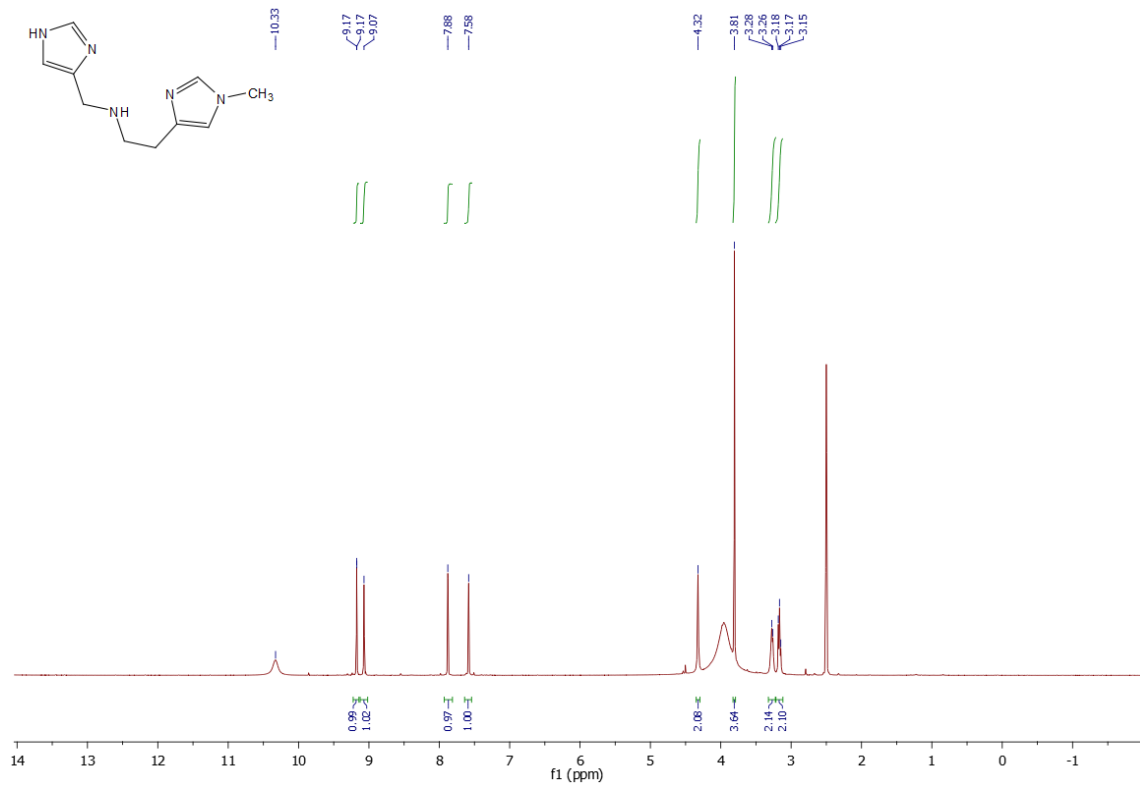


Figure S66: ^1H NMR spectrum of L4 in d_6 -DMSO at 25°C.

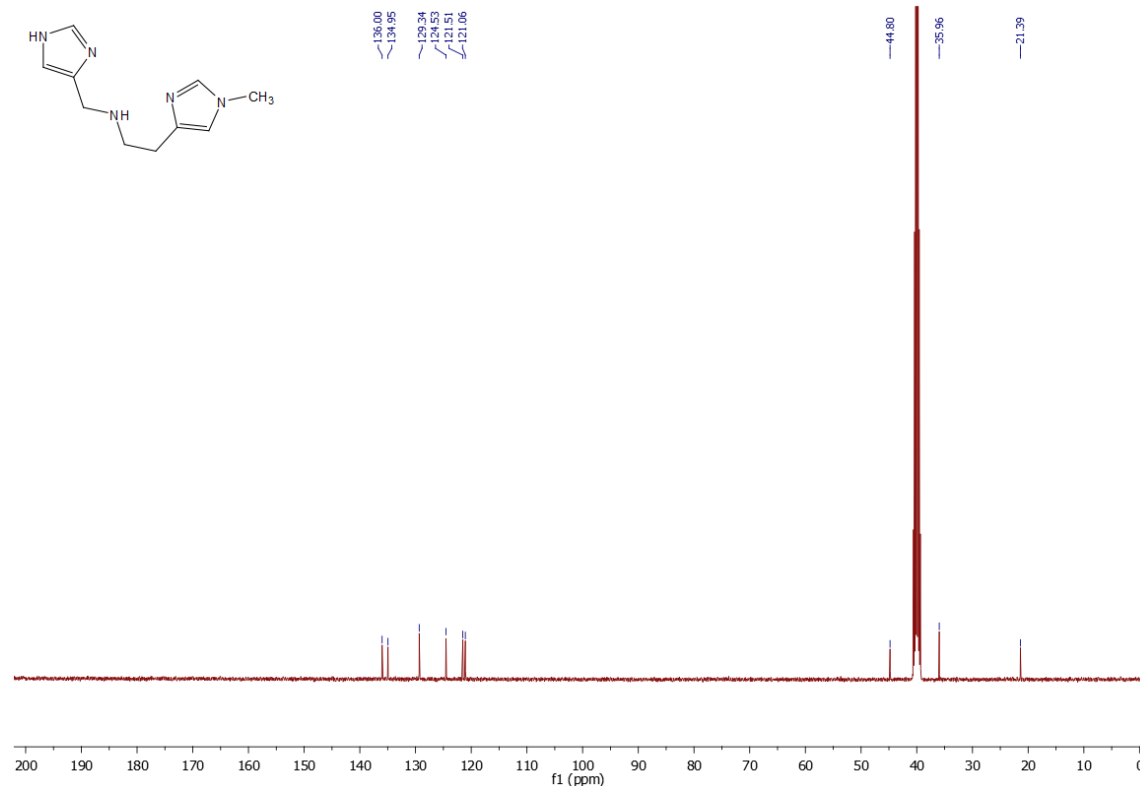


Figure S67: ^{13}C NMR spectrum of L4 in d_6 -DMSO at 25°C.

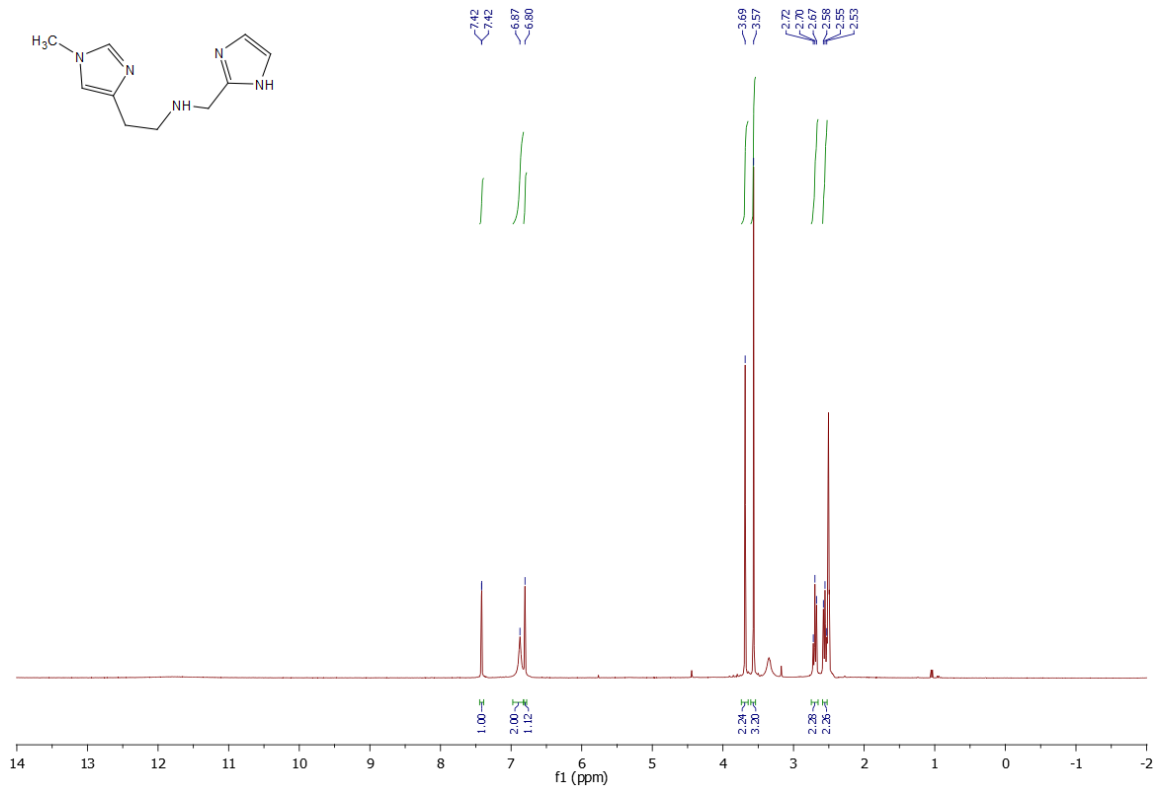


Figure S68: ^1H NMR spectrum of **L5** in d_6 -DMSO at 25°C.

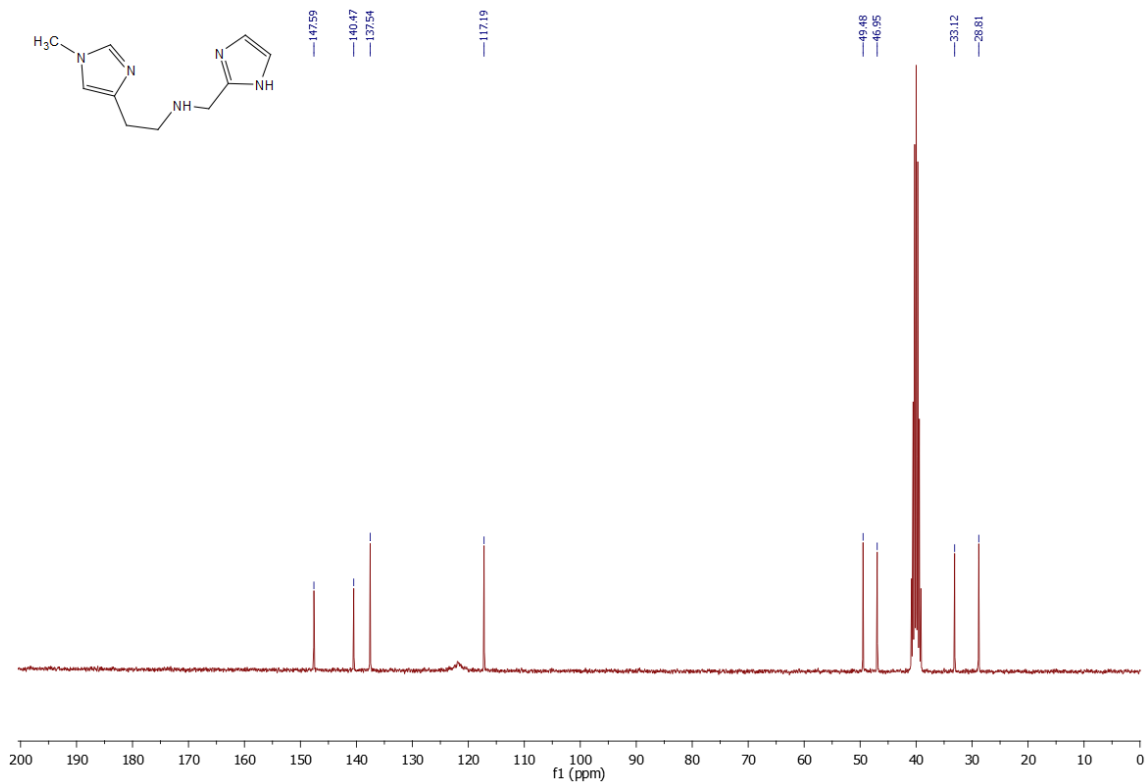


Figure S69: ^{13}C NMR spectrum of **L5** in d_6 -DMSO at 25°C.

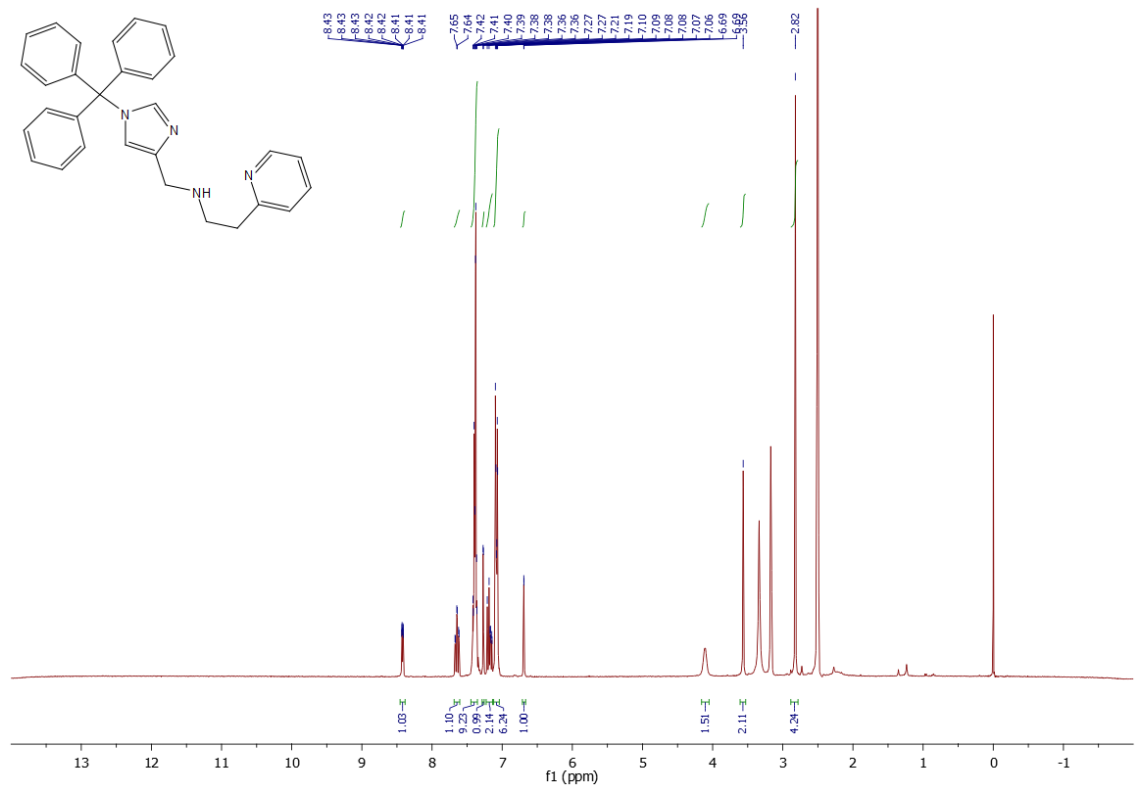


Figure S70: ^1H NMR spectrum of **L6^{Tr}** in *d*6-DMSO at 25°C.

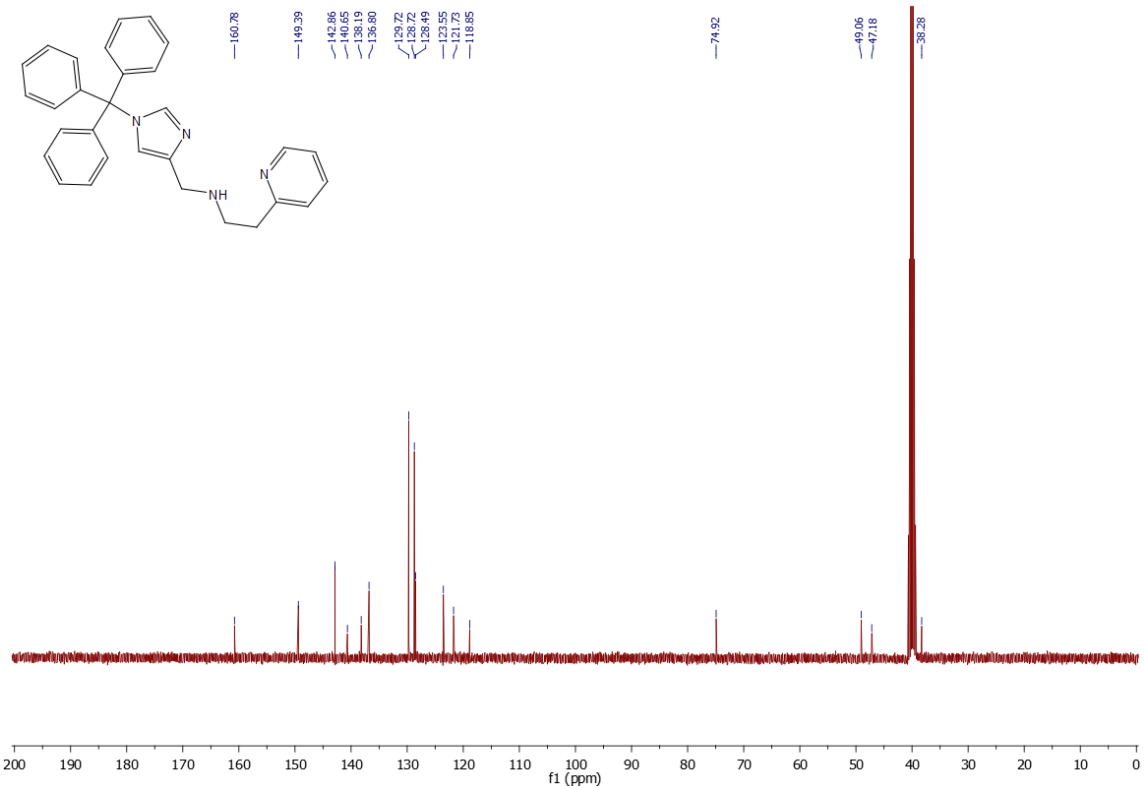


Figure S71: ^{13}C NMR spectrum of **L6^{Tr}** in *d*6-DMSO at 25°C.

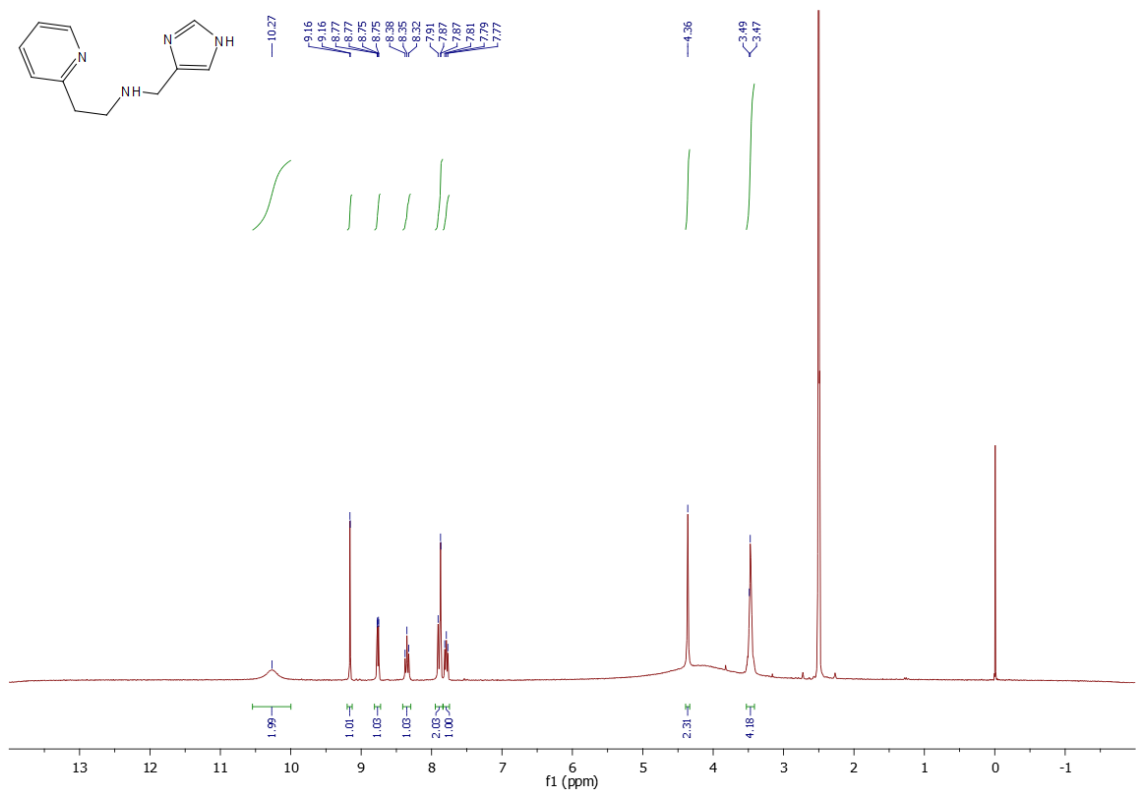


Figure S72: ^1H NMR spectrum of **L6** in d_6 -DMSO at 25°C.

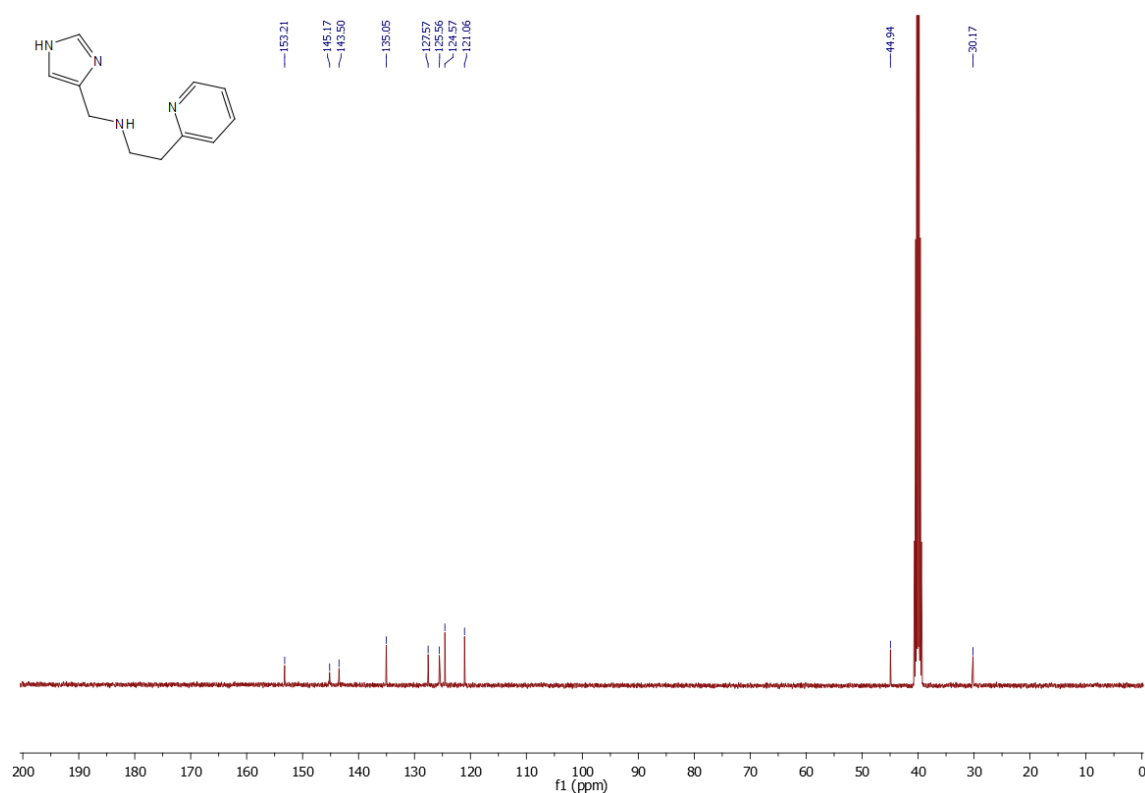


Figure S73: ^{13}C NMR spectrum of **L6** in d_6 -DMSO at 25°C.

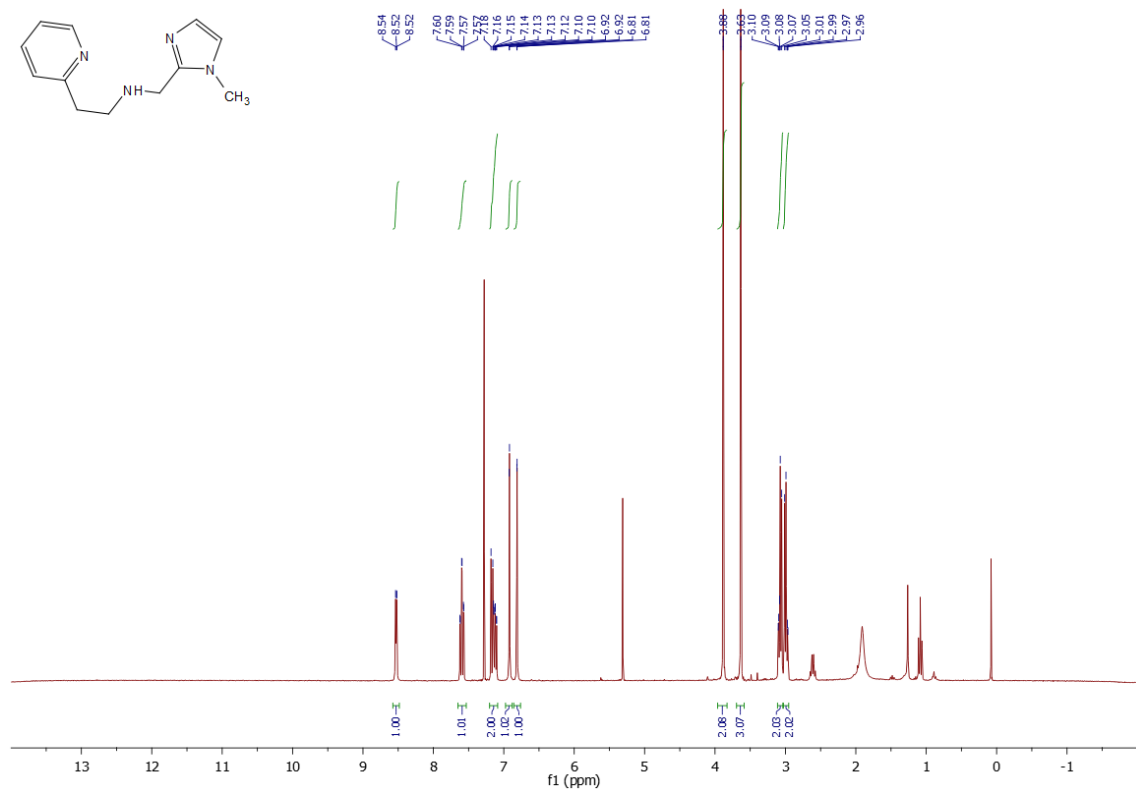


Figure S74: ^1H NMR spectrum of **L7** in d_6 -DMSO at 25°C .

10) References

- (1) Stoll, S.; Schweiger, A. EasySpin, a Comprehensive Software Package for Spectral Simulation and Analysis in EPR. *Journal of Magnetic Resonance* **2006**, *178* (1), 42–55. <https://doi.org/10.1016/j.jmr.2005.08.013>.
- (2) Durmus, S.; Garrison, J. C.; Panzner, M. J.; Tessier, C. A.; Youngs, W. J. Synthesis of an Imidazolium-Linked Cyclophane from Histamine. *Tetrahedron* **2005**, *61* (1), 97–101. <https://doi.org/10.1016/j.tet.2004.10.056>.
- (3) Saulnier, M. G.; Frennesson, D. B.; Wittman, M. D.; Zimmermann, K.; Velaparthi, U.; Langley, D. R.; Struzynski, C.; Sang, X.; Carboni, J.; Li, A.; Greer, A.; Yang, Z.; Balimane, P.; Gottardis, M.; Attar, R.; Vyas, D. 2-(1H-Imidazol-4-Yl)Ethanamine and 2-(1H-Pyrazol-1-Yl)Ethanamine Side Chain Variants of the IGF-1R Inhibitor BMS-536924. *Bioorg Med Chem Lett* **2008**, *18* (5), 1702–1707. <https://doi.org/10.1016/j.bmcl.2008.01.049>.
- (4) Ohkanda, J.; Lockman, J. W.; Kothare, M. A.; Qian, Y.; Blaskovich, M. A.; Sebti, S. M.; Hamilton, A. D. Design and Synthesis of Potent Nonpeptidic Farnesyltransferase

Inhibitors Based on a Terphenyl Scaffold. *J Med Chem* **2002**, *45* (1), 177–188. <https://doi.org/10.1021/jm0103099>.

(5) Casella, L.; Gullotti, M.; Pallanza, G.; Buga, M. *Spectroscopic and Binding Studies of Azide-Copper (II) Model Complexes+*; 1991; Vol. 30.

(6) Galli, U.; Hysenlika, R.; Meneghetti, F.; Grossi, E. Del; Pelliccia, S.; Novellino, E.; Giustiniano, M.; Tron, G. C. Exploiting the Nucleophilicity of the Nitrogen Atom of Imidazoles: One-Pot Three-Component Synthesis of Imidazo-Pyrazines. *Molecules* **2019**, *24* (10). <https://doi.org/10.3390/molecules24101959>.

(7) Concia, A. L.; Beccia, M. R.; Orio, M.; Ferre, F. T.; Scarpellini, M.; Biaso, F.; Guigliarelli, B.; Réglier, M.; Simaan, A. J. Copper Complexes as Bioinspired Models for Lytic Polysaccharide Monooxygenases. *Inorg Chem* **2017**, *56* (3), 1023–1026. <https://doi.org/10.1021/acs.inorgchem.6b02165>.

(8) Becke, A. D. Density-Functional Thermochemistry. III. The Role of Exact Exchange. *J Chem Phys* **1993**, *98* (7), 5648–5652. <https://doi.org/10.1063/1.464913>.

(9) Stephens, P. J.; Devlin, F. J.; Chabalowski, C. F.; Frisch, M. J. *Ab Initio Calculation of Vibrational Absorption and Circular Dichroism Spectra Using Density Functional Force Fields*; 1994; Vol. 0.

(10) Grimme, S.; Antony, J.; Ehrlich, S.; Krieg, H. A Consistent and Accurate Ab Initio Parametrization of Density Functional Dispersion Correction (DFT-D) for the 94 Elements H–Pu. *Journal of Chemical Physics* **2010**, *132* (15). <https://doi.org/10.1063/1.3382344>.

(11) Hehre, W. J.; Lathan, W. A. Self-Consistent Molecular Orbital Methods. XIV. An Extended Gaussian-Type Basis for Molecular Orbital Studies of Organic Molecules. Inclusion of Second Row Elements. *J Chem Phys* **1972**, *56* (11), 5255–5257. <https://doi.org/10.1063/1.1677028>.